THE ROLE OF GRAVITY WAVES IN THE SEVERE CONVECTIVE OUTBREAK OF 3-4 APRIL, 1974

by

Dennis Alan Miller

B. S., State University of New York at Albany

(1975)

Submitted in partial fulfillment of the
requirements for the degree of
MASTER OF SCIENCE
at the
MASSACHUSETTS INSTITUTE OF TECHNOLOGY
June, 1978

Signature of Author. . . . . Department of Meteorology, 24 May 1978

Certified by . . . . . Thesis Supervisor

Accepted by . . . . . Chairman, Departmental Committee

THE ROLE OF GRAVITY WAVES IN THE SEVERE CONVECTIVE OUTBREAK OF 3-4 APRIL, 1974

By

Dennis Alan Miller

Submitted to the Department of Meteorology on
May 24, 1978 in partial fulfillment of the
requirements for the degree of
Master of Science.

ABSTRACT

A thorough investigation of the mesoscale pressure fields which accompanied the severe convective outbreak of 3-4 April, 1974 is undertaken. Surface weather records, rawinsonde observations, and radar photographs, from scores of stations, are utilized. Although tornado producing thunderstorms occurred throughout a vast area of the Midwest and South, propagating mesoscale pressure waves, organized into discrete lines, are found to have occurred primarily in the northern portion of this region, where a lower level, stable layer existed. Four major waves are delineated, with wavelengths ranging from 60 to 150 km, periods generally about 90 minutes, phase speeds ranging from near zero to 28 M/sec, and amplitudes as high as .15" hg (5 mb). Some of these waves are associated with convective squall lines, while others are not, and in one case in particular, a wave without accompanying precipitation is seen to develop suddenly into a squall line. The fields of wind and, where present, precipitation, are generally consistent with the divergence patterns of a gravity wave. However, when the atmosphere is tested in these regions for its ability to support lower level, ducted gravity waves, after the criteria set forth by Lindzen and Tung (1976), good, corroborative results are not attained.

Pressure fields surrounding two squall lines—one in the North and one in the South, are then examined in detail. The Northern squall line is rather coherent and symmetric, and has a pronounced mesoscale pressure structure associated with it. Wave-CISK is thought to likely provide the organization for this line. The Southern squall line, on the other hand, is rather disjointed, and has no wave structure associated with the line as an entity, although pressure oscillations are found along with the individual thunderstorm cells. Wave-CISK is not believed to provide the organization for this convective line. Other possibilities are explored, and inertial instability, and frontogenetic-type circulations are both viewed as likely candidates to produce the ascent necessary to sustain this band of convection.

Thesis Supervisor: Frederick Sanders
Title: Professor of Meteorology

ACKNOWLEDGEMENTS

The author would like to thank Professor Frederick Sanders for suggesting the research topic and supervising the endeavor; Kerry Emanuel and Frank Marks for offering valuable insights and suggestions; Ginny Powell and Patricia Farrell for typing the bulk of the manuscript; and especially, Isabelle Kole for painstakingly drafting the numerous figures.

The research was supported under National Science Foundation Grant No. 74-24405 ATM.

TABLE OF CONTENTS

LIST OF FIGURES

INTRODUCTION

The April 3-4, 1974 tornado outbreak was the worst in recorded history. A total of 148 tornadoes, many extremely destructive, were reported in 13 states in the Midwest and South during the 24-hour period of 1800Z April 3 to 1800Z April 4 (See Fig. I-1). The purpose of this paper is to investigate the role that gravity waves may have played in producing this severe weather.

Gravity waves in the atmosphere are transverse waves caused by a vertical displacement under statically stable conditions. Buoyancy acts as the restoring force. They are often thought of as propagating along a horizontal interface separating two fluids of different density. Actually, what is perceived as the gravity wave is usually a wave packet made up of a Fourier series of components:

$$f(x) = \sum_{m=1}^{\infty} (A_m \sin k_m x + B_m \cos k_m x) \qquad (1)$$

where k is the horizontal wave number
and A and B are the wave component amplitudes

The speed of the packet, or group velocity, will generally differ from the average phase velocity of its components. The energy travels with the wave group. In time, the group generally broadens so that the energy is dispersed (Holton, 1972).

Considerable speculation has arisen amongst meteorologists as to the role gravity waves might play in initiating convection. Squall lines in particular, since they often appear as a wave front and frequently produce an undulation in the barogram trace of a station over which they pass,

have come under close scrutiny. A number of case studies have been undertaken documenting traveling mesoscale pressure perturbations detectable at the surface. A broad range of findings have been yielded on a number of matters, such as the recorded wavelength and propagation velocity; the lateral extent of the wave and the horizontal distance traversed; the relationship between the wave velocity and wind shears, jets, and synoptic features such as cyclones and fronts; the cause of the wave and the vertical structure of the atmosphere through which it travels; the amplitude of the wave and the nature of the signature it produces on a microbarograph trace; and the relationship between the gravity wave and the surface wind field, the vertical motion field, and, when present, the location of convective cells, hail swaths, and tornadoes.

Tepper (1950) studied the case of a squall line with an associated pressure jump. The line was oriented parallel to - and moving away from, at about 53 knots - a cold front located further to the west. The onset of the pressure rise was followed immediately by a strong northwesterly wind and a rain gush. Tepper perceived the squall line as the manifestation of a propagating gravity wave. He proposed that the acceleration of a cold front against a warm air mass containing an inversion causes a sudden rise in the height of the inversion, or pressure jump. Once formed, the pressure jump moves away from the cold front at a speed greater than that of the surface wind. Its speed, relative to the ambient wind field, is a function of the strength and height of the inversion, determined by the formula:

$$c = \sqrt{(1-\frac{\theta_1}{\theta_2})\, g\, h} \qquad (2)$$

where θ_1 is the mean potential temperature from the surface to the base of the inversion,

θ_2 is the mean potential temperature from the top of the inversion to 500 mb,

and h is the height of the middle of the inversion.

Actually, an inversion is not strictly necessary. An isothermal or stable layer separating two adiabatic or quasiadiabatic regions is sufficient for the propagation of a gravity wave. The pressure jump, he suggests, causes squall line conditions by forcing the potentially unstable air above the inversion or stable layer up vigorously.

Wagner (1962) investigated the case of a gravity wave which passed over New England at a speed of 50-85 knots, the direction of travel - northeastward - being normal to the direction of the ambient (northwesterly) winds. The wave was marked by a sharp rise in pressure over a period of 1-2 hours. Yet, despite amplitudes as great as 6 mb/hour, no precipitation, only slight cloudiness, and no surface wind changes were noted in conjunction with the wave passage. The stations which experienced the pronounced pressure rise were characterized by soundings which showed a deep inversion, isothermal or stable layer extending from the surface to over 790 mb. Pressure rises, in fact, were most intense where the inversion was strongest. As to the cause of the gravity wave, the author speculates that a convective outbreak in eastern Texas the previous afternoon was responsible.

Ferguson (1967) studied the case of a gravity wave which propagated eastward across the lower Great Lakes region at about 40 knots; the wave

straddling a warm front. He noted the presence of a strong east-to-westerly wind shear in the lower levels, culminating in a "low-level jet" of 50 knots at 700 mb, near the center of the wave. Soundings revealed the presence of a lower, stable layer capped by an upper adiabatic layer, throughout the region which experienced the perturbation. The gravity wave passage was characterized by a sharp dip and then rise in the pressure trace, the maximum amplitude being 3.3 mb. In this instance, a weak convective line was associated with the wave. The author places the center of the convective line coincident with the minimum pressure, and associates westerly component winds with the pressure fall period preceding the convective line, and gusty, easterly component winds with the rising pressure period following the line, as predicted by Goldie's (1925) equations. However, close scrutiny of his wind and pressure records seems to reveal that the shift to strong easterly winds occurred as the pressure drop began. Finally, the author notes the presence of both an accelerating cold front and some rather severe convective activity further to the west earlier in the day, and postulates that either may have initiated the gravity wave.

Bosart and Cussens (1973) investigated an elongated wavefront which moved east-southeastward in the southeastern United States at about 25 knots, against the lower level winds. Again, the medium of propagation was believed to be an inversion, where low level cold air was capped by warm air overrunning a front to the south. The wave, as recorded on barograph traces, was typified by maybe a slight rise in pressure, followed by a rapid drop of up to 7 mb, which was then followed by a series of small oscillations of period 5-12 minutes. The gravity wave, taken from time of onset of rapid pressure drop to the time of occurrence of lowest pressure,

had an average duration of 65 minutes, and an average amplitude of 3.5 mb. The period of rapid pressure fall was accompanied by gusty east-southeasterly winds of 20-30 knots, whereas after the trough passed, winds were generally light southeasterly, or even reversed to light northwesterly. Bosart and Cussens attribute this to the fact that the convergence field, which they place in advance of the wave trough, resulted in a gusty, ageostrophic wind component which reinforced the surface wind, whereas behind the wave, the ageostrophic wind countered the surface flow. This is a noticeably different result than that obtained in the previous case study by Ferguson based on Goldie's equations, which Bosart and Cussens assert are erroneous. Precipitation is associated with the wave passage, tending to start just at or before the period of rapid pressure fall and terminate shortly after the minimum pressure is attained. The gravity wave is believed to be triggered by thunderstorm activity further to the west.

Jae Kyung Eom (1975) studied a gravity wave occurrence in the Midwest which was quite different from the previously discussed cases in several respects. In this case, the "wave" was confined to a 200 km wide channel, giving it more the character of a mesolow than of a line-type phenomenon. The low moved north-northeastward on a path parallel to, and about 500 km east of, the axis of the 300 mb jet stream, which had maximum winds of about 150 knots. The barograph traces were typified by rather large pressure drops - of up to 14.6 mb (she claims !) - followed by almost equally large pressure rises. The period was typically 3-4 hours, the wavelength 500 km. The surface winds, generally east or northeasterly,

did not change much in direction, but became stronger and gustier with the approach and passage of a mesolow, typically increasing from about 10-15 knots to 50 knots or over. The computed wind deviation field showed almost an exact correlation between the location of the mesolow center and that of the strongest wind component in the direction counter to that of the mesolow propagation, i.e. northeasterly. Although the system produced no precipitation, there was an association of overcast skies with high pressure, and broken cloudiness with low pressure. A schematic view of the gravity wave presented by the author (Fig. I-2) depicts divergence and sinking motion in the region between mesohigh and approaching mesolow, and analogously, convergence and rising motion to the rear of the low. Maximum cloudiness and lightest winds, directed opposite to the direction of the wave, are found in conjunction with the mesohigh, and reduced cloudiness and strongest winds are found with the mesolow. This is a somewhat different picture than that presented by Bosart and Cussens. The soundings that day over the region of gravity wave passage showed a lower layer of nearly isothermal air - full of small inversions - about 200 to 400 mb deep, capped by a nearly adiabatic, nearly saturated layer reaching up to about 200 mb. No conjecture is raised as to the cause of the gravity wave.

Uccellini (1975) studied a case which was similar in many respects to the one discussed above: a gravity wave occurrence in the Midwest in which a number of waves, confined in their lateral dimensions, moved north-northeastward, in the basic direction of the upper level flow and along a surface front. The phase speed was generally 35-45 m/sec, the period two to four hours, the wavelength 300-450 km and the amplitude of the pressure

deviation from the mean synoptic pressure as high as 2.0 mb. In this case, some serious convection developed in association with the gravity waves. Typically, as a mesolow passed and a mesohigh approached, thunderstorm cells were seen to develop or intensify. Thus, rainfall tended to be periodic, with maximum amounts occurring just before, or at the time of arrival of, a ridge. Some severe weather was observed late in the day, in the form of tornadoes and strong wind gusts, generally occurring shortly after the passage of a trough. The cells moved northeastward, but generally at half the wavespeed, so that the waves moved through the cells. Uccellini's depiction of the gravity waves, like Eom's, also portrays maximum rising motion in the lower troposphere occurring midway between the trough and the trailing ridge, with maximum upward parcel displacement coinciding with the ridge. The region of gravity wave propagation was characterized by soundings which showed, again, a lower, moist, stable layer capped by an inversion and topped by a deep layer with a nearly constant lapse rate. A strong wind shear also existed, with upper level (500 mb) winds generally being about 40 m/sec. Not all the stations over which gravity waves passed experienced convective activity, even when the amplitudes were quite large. The author shows that in regions which do experience convective activity, the lifting provided by the gravity wave destabilizes the lapse rate and brings saturated parcels to their level of free convection. In regions which do not experience convection, the lifting is insufficient to overcome the lower-level inversion. As to the cause of the gravity waves, the author notes that they are initiated in the vicinity of a rapidly deepening cyclone. He also notes the existence

of a strong vertical wind shear in the region.

As seen in the above review, gravity waves are observed in a wide variety of situations in the atmosphere. In their summary article on gravity waves for Project Sesame, Einaudi et al. (1977) divided mesoscale gravity waves into two broad categories. One group includes pre-frontal disturbances. The wave will take the form of a line oriented parallel to, and moving away from, a trailing cold front. Usually the feature will be found in the warm sector of a synoptic system. If rather intense convective activity is associated with the line, it is termed a "squall line". The wavelength is typically 100 km or less. Situations such as those described by Tepper and Ferquson fall into this category. The second group includes disturbances which are of rather small lateral dimension, so that the waves take on the appearance of mesohighs and mesolows. These waves travel parallel to the axis of orientation of a surface front - usually right along the front - in the same general direction as the upper level flow, which is typically strong. The wavelength is much longer for this category - characteristically several hundreds of kilometers. The situations studied by Eom and Uccellini fall into this class. Other cases, such as those investigated by Wagner, and Bosart and Cussens, although line-type in nature, fall into neither category.

As to what initiates gravity waves, there appears to be quite a bit of uncertainty. Einaudi et al. envision four probable causes: 1) Active convection, often along a front - the cumulonimbus clouds acting as a source of heat and momentum; 2) Geostrophic adjustment accompanying the frontogenesis process; 3) Some instability of the frontal flow,

as yet unidentified; and 4) Jet streams and vertical wind shears. The first two processes are thought to be associated with pre-frontal disturbances, while the third is viewed in connection with along-the-front propagating waves.

In a number of the above-discussed cases, an inversion, or a sharp zone of discontinuity separating two layers of different density, is hypothesized as the propagating medium for the gravity wave. In fact, there often appears to be a correlation between the strength of the inversion and the amplitude of the gravity wave. Lindzen and Tung (1976), however, dispute this notion. According to them, there are two mechanisms which commonly account for the propagation of gravity waves. One is wave CISK (Conditional Instability of the Second Kind). This is an interactive process between a cumulonimbus cloud and a gravity wave. It occurs when the atmospheric sounding shows a conditionally unstable state through a great depth of the troposphere, with warm and moist air near the surface. The cumulonimbus cloud provides thermal forcing which concentrates the energy of the gravity wave, which in turn organizes the convection, which further forces the wave, etc.

The other mechanism is ducting in a low-level stable layer capped by an unstable layer. The energy of a gravity wave is seen as being confined to a low-level, stable "duct". Without the proper type of upper reflective surface, the energy will quickly be dissipated vertically. Lindzen and Tung show that an inversion is not a good reflective surface. A much better capping surface is a conditionally unstable, moist layer. The greater the ratio of the stability of the lower layer to that of the upper layer, the greater will be the retention of wave energy in the lower

layer. In fact, the Richardson Number (Ri):

$$Ri \equiv \frac{-\frac{g}{\bar{\rho}}\frac{d\rho}{dz}}{\left(\frac{du}{dz}\right)^2}$$

, where g is the gravitational acceleration,
ρ is the density,
u is the horizontal wind velocity,
z is the vertical distance,
and - (the overbar) denotes a mean for the layer.

somewhere in the upper layer should be less than ¼, or nearly so, if the layer is very moist (in which case, the effective stability is some mean of the dry and saturated stabilities). Furthermore, the reflectivity will be greatly enhanced if there is vertical wind shear such that there exists within the capping layer a "steering level" where the wind speed is equal to that of the uncorrected (for mean lower level wind) phase speed of the wave below. Even if such a condition does not exist, reflectivity will still be rather high if the windspeed in the upper level is slightly less than the phase speed of the gravity wave, in which case a steering level may lie above the second, capping layer. On the other hand, if the wind speed in the lower layer is equal anywhere to the wave phase speed, a critical level will exist, and the wave energy will be absorbed (as explained by Hoskins and Bretherton, 1967). Furthermore, in order for a gravity wave to propagate in the lower "duct", the layer must be statically stable, and it must be thick enough to accomodate one quarter of the vertical wavelength corresponding to the ducted wave mode. The vertical wavelength of a mesoscale wave is proportional to the phase speed and inversely proportional to the static stability:

$$Ln = 2\pi C_{d,n}/N_l \quad , \quad \text{where } C_{d,n} \text{ is the corrected phase speed of the } n^{th} \text{ mode}$$

N_l is the Brunt-Väisälä frequency of the lower level.

and Ln is the vertical wavelength (3)

The phase speed of the wave is thus a function of the static stability and the height of the duct:

$$C_{d,n} = \frac{N_l H}{\pi(\frac{1}{2}+n)} \quad \text{where } H \text{ is the height of the lower layer,} \quad (4)$$

and n is the mode of the wave in question; n = 0, 1, 2, ...

The lowest order mode (n=0) has the greatest horizontal phase speed and the longest vertical wavelength. Other, higher order modes dissipate readily due to friction, and are of little interest.

Of the two above-described mechanisms for maintaining gravity waves, wave CISK is thought of in association with more severe convection. In fact, wave CISK is a possible explanation for a problem raised by Einaudi et al: how do gravity waves maintain themselves in the face of the disruption caused by the convection which they may initiate? The violent vertical motions of a severe thunderstorm create pulsations in the pressure field which may be of an entirely different period than that of the gravity wave which produced the convection, and thus distort or destroy it.

However, the wave CISK view, as presented by Raymond (1975) attempts to solve this dilemma by envisioning the squall line as being itself a packet of forced internal gravity waves. A sort of coupling exists between the mesoscale and convective scale motions. The wave or wave

packet generates regions of low-level convergence and divergence. This creates concentrated regions of updrafts and downdrafts, which in turn drive the gravity wave. The amplitude of the wave is a function of the driving force (see Fig. I-3).

The wavelength is on the order of tens of kilometers. He speculates that a severe storm may be generated by the growth of a random, small-amplitude distribution of eigenmodes, the dominant eigenmode being the most unstable, or by a large amplitude perturbation arising from, say, the action of a cold front or cyclogenesis. The gravity wave is thus portrayed as initiating, and then being sustained by, the squall line; the squall line therefore being the manifestation of a self-perpetuating gravity wave.

The general school of thought on gravity waves and convection presented thus far is adopted, a priori, as the basis for the analysis of the convective activity of 3-4 April, 1974, which ensues. That is, the existence of pressure perturbations, wind fluctuations, etc., in the surface weather records are taken, under the proper circumstances (i.e. not when a synoptic warm or cold front, for example, is involved) as evidence of the presence of gravity waves. Mechanisms believed responsible for the generation of, and conditions believed conducive to the propagation of, gravity waves are explored. The wave CISK view - that a squall line is a consequence of the convergence field provided by a gravity wave under potentially unstable conditions - is originally accepted. Through the course of the investigation, the validity of this assumption is explored for various cases. In some instances, it will be found to be more tenable

than in others. In the later chapters, mechanisms other than gravity waves which may have contributed to the initiation and organization of convection - such as inertial instability and frontogenesis - are investigated.

CHAPTER I

SYNOPTIC OVERVIEW

The synoptic analyses for the surface, 850 mb, 700 mb, and 500 mb levels at 0000Z April 3, 1200Z April 3 and 0000Z April 4, in addition to the surface analyses at 1500Z, 1800Z, and 2100Z April 3, 1974 are shown in Figures 1.1-1.15 (after Hoxit and Chappell, 1975). In the upper levels (i.e. 500 mb), a sharp, negatively tilted trough centered over the eastern Rockies at 0000Z April 3 moved to eastern Nebraska-western Iowa by 0000Z April 4, where it had a closed contour of 540 dm. The matching surface low, located in southeastern Colorado with a central pressure of 983 mb at 0000Z April 3, advanced to southeastern Iowa, with a central pressure of 987 mb, by 0000Z April 4. Two cold fronts, the first marking the leading edge of maritime polar air and the second marking the forward boundary of continental polar air, moved eastward, south of the low pressure center, while a stationary front extended northeastward from the low center to Lake Michigan, and then eastward across the Great Lakes. A warm front, located through southern Tennessee at 0000Z April 3, and marking the northern boundary of maritime tropical air, advanced to the central Indiana-Ohio region by 0000Z April 4 (important note: the analyses of mesoscale troughs, highs and lows seen in Figures 1.8-1.12, adopted from Hoxit and Chappell, do not necessarily correspond to those presented in this paper in chapters to follow). For a more thorough description and analysis of the synoptic situation on 3-4 April, 1974, the reader is referred to Hoxit and Chappell, 1975.

CHAPTER II

MESOSCALE PRESSURE FIELDS

A. Goals and Methods of Analysis

The purpose of this chapter is to gain some insight into the scope, intensity, and character of the mesoscale pressure activity which occurred before, during, and after the period of severe convection on 3-4 April, 1974. The primary focus is on traveling pressure perturbations or gravity waves, and the relationship of weather events (i.e. thunderstorms and tornadoes) and wind fields to the hourly pressure change fields.

To accomplish this, a series of cross sections was constructed through the Midwest and South, covering the vast area which experienced severe convection on that afternoon. These slices were oriented to coincide with the mean direction of motion of the numerous observed tornadoes - i.e. towards 55° - so that the tornadoes could be tracked explicitly along the cross sections. The section lines were not perpendicular to the squall lines, which were generally oriented from north-northeast to south-southwest. Thus, the tornadoes, and their accompanying parent thunderstorm cells, generally moved north-northeastward along the squall lines as the lines propagated east-southeastward, as will be seen in later chapters. A total of twelve cross-sectional analyses were performed (see Fig. 2.1); all the surface recording stations which were subjectively determined to contain complete and reasonable data were dropped to the nearest cross section, along a line parallel to the mean orientation of the squall lines (which were assumed to be slab-symmetric) - i.e. NNE-SSW.

Thus, considering that pressure waves were generally oriented parallel to the squall lines, each station was assumed to be in the correct position relative to the pressure wave or convective line at any given time. As will be seen in Chapter III, a NNE-SSW orientation of the pressure wavefronts was not always observed, so that the above assumption was not necessarily correct. Thus, the distances from stations to squall lines may at times have been misrepresented; nevertheless, it was the most reasonable assumption which could be made in constructing the cross-sectional lines, considering the vast amount of convective and pressure perturbation activity which was present that day.

The hourly pressure changes were taken as a measure of the mesoscale pressure fields in these cross sections. While this actually represents the absolute pressure change field and the synoptic pressure change field has not been filtered out, the mesoscale tendency can be discerned as an increased or decreased rate of hourly pressure change compared to the mean change seen during the surrounding period. Taking the hourly pressure change field filters out, to some extent, the very short term, sharp pressure jumps and falls associated with convective cells. The units of measure are hundredths of inches of mercury (hg), used because of the availability of altimeter setting records at many stations, which do provide conventional observations of pressure reduced to sea level (note: a change in altimeter setting of .03" hg is approximately equal to a barometric pressure change of 1 mb). Usually the period of pressure change was taken between consecutive standard hourly observations, although, when available, inter-hourly measurements were used to help decipher the field.

Three cross sections, specifically II, V, and IX, chosen because they best highlight the findings of the analyses, are displayed, in two parts each, in Figures 2.2-2.4. In each figure, part 'a' reveals the relationship between the hourly pressure change field and the wind field, while part 'b' displays the relationship between precipitation and pressure tendency. Additionally, the tracks of tornadoes, determined from Fujita's analysis of locations (Fig. 1), with the aid of the April, June and December "Storm Data" publications (1974) to fix the tornadoes in time, are superimposed on parts 'b' of the cross sections.

B. Morning Wave Activity

1. Description

The first noteworthy featured encountered in these analyses is an early morning series of oscillations, seen, for example in Section II (Fig. 2.2) beginning at 0700Z. The feature is more evident in the northern cross sections than in the southern ones. It is a continuous feature, observed from Missouri and Arkansas through Pennsylvania and western New York. The signature of the major, discernable wave is a pressure rise followed by a sharp fall (although at quite a few stations additional rises and falls are seen in succession). The amplitude of the major rise is +.032" hg/hr; and of the fall, -.070" hg/hr, as averaged over all the stations along Sections II-V which experienced the wave. The largest observed amplitudes of pressure change are +.10" hg/hr at LRF at 0945Z and -.20" hg/hr at STL at 1130Z (the matter of the phase speed and wavelength of this and other waves observed later will be deferred till the next

chapter, since the measured values of these parameters on the cross sections may be unrepresentative, due to the fact that the waves cross the section lines at as yet undetermined angles). Considerable thunderstorm activity is associated with this wave, as seen in Cross Sections II and V (Figs. 2.2b and 2.3b). The activity generally spans the later period of pressure ascent and the early period of pressure descent; that is, it is centered over the mesoscale pressure maximum. The surface winds are generally south-southeasterly throughout the vast area affected by this pressure perturbation. However, a consistent pattern of wind shifts towards the east accompanying falling and low pressure, and wind shifts towards the west accompanying rising and high pressure, is observed as the wave passes. Notice, for example, stations VIH, STL, ALN, DEC, CMI, SBN, and BTL on Cross Section II (Fig. 2.2a).

2. Discussion

The above described interrelationship of the mesoscale fields of pressure, wind and precipitation fits the view (held by Eom, Uccellini, and others) of sinking motion being correlated with falling pressure, and ascending motion with rising pressure, during the passage of a gravity wave. The corresponding surface level divergence field results in strong easterly component winds in association with the mesotrough, and weak easterly, or westerly, component winds in conjunction with the mesoridge. Strong, short period pressure fluctuations of thunderstorm scale are generally not associated with this wave. Furthermore, the band of convection associated with the wave is rather continuous and slab-symmetric (see Fig. 2.5). Thus, it would certainly not seem unreasonable to view

this propagating pressure perturbation as a gravity wave with superimposed convection, sustained by wave-CISK forcing.

C. Afternoon Wave Activity - Northern Sections

1. Description

After a lull of a few hours, mesoscale pressure perturbation activity picks up considerably in the afternoon and evening, beginning at around 1800Z. The character of the activity, though, differs from region to region. Along the northern cross sections, covering Illinois, Indiana, Michigan, and northwestern Ohio, continuous, sustained pressure undulations of significant amplitude are in evidence. Some apparently continuous waves are observed to cover distances of hundreds of kilometers (e.g. see Figures 2.2a and 2.3a). The average amplitude of the afternoon waves encountered in Sections I, II, and III is +.063" hg/hr for the rise periods and -.076" hg/hr for the fall periods (the 'average' being that of the one-hour periods for which the greatest rate of pressure rise or fall is observed); the largest observed amplitudes are ± .130" hg/hr. The multiple nature of perturbation activity in the northern regions is revealed in Cross Section II (Fig. 2.2a), where a sequence of three successive (relative) fall-rise undulations marches from western Missouri to southern Michigan. The wind patterns are generally as seen previously: westerly winds associated with high mesoscale pressure and easterly winds associated with low mesoscale pressure. Precipitation is not associated with all of the waves in the sequence, but when it does occur, it again tends to be centered about the pressure peaks (the matter of causality between pressure perturbations and convective bands is explored in later

chapters). A number of tornadoes are observed with these oscillations, generally occurring during a period of pressure rise or coinciding with a pressure peak (see Fig. 2.2b).

D. Afternoon Wave Activity - Central Sections

1. Description

Along the central cross sections - through Kentucky, Tennessee, southern Ohio, West Virginia and western New York - significant afternoon wave activity is also observed, though generally not as pronounced as in the northern sections. The average amplitude of the perturbations seen in Cross Sections V - VIII is + .025" hg/hr for the rise periods and -.059" hg/hr for the fall periods. Again, coherent waves are observed over distances of hundreds of kilometers. For example, in Cross Section V (Fig. 2.3a) a wave is in evidence from PUK to JHW, a span of 870 km. This wave is of particular interest because with it are associated some of the fiercest tornadoes of the day, including the one which devastated Xenia, Ohio. The maximum observed hourly pressure change is -.10" hg. However, in the region along the Ohio River Valley, from about Ft. Knox, Ky. (FTK) to Columbus, Ohio (CMH) (a line which actually falls along Cross Section VI - not displayed), where some of the most severe thunderstorm activity of the afternoon occurred (e.g. 65,000 foot tops of convective cells) between 2000Z April 3 and 0000Z April 4, very large amplitude pressure changes are observed over varying periods shorter than an hour (i.e. a fall of .20" hg in 44 minutes at CVG; a rise of .14" hg in 8 minutes at SDF). Meanwhile, in relating the convective activity to the mesoscale

pressure pattern, the precipitation is again centered approximately over the ridge, but the tornadoes, by and large, appear to occur during a period of rapid pressure fall, or coinciding with mesoscale low pressure.

2. Discussion

In the region along the Ohio River Valley where convection was so severe, large amplitude pressure perturbations were occurring on many different scales, ranging from thunderstorm scale through mesoscale. At station OSU in northwestern Columbus, Ohio, for example, the following sequence of events was recorded: beginning at 2129Z April 3, the wind backed from east at 12 knots to north at 25 knots to northwest at 45 gusting to 60 knots and finally west at 30 gusting to 45 knots, during a span of 21 minutes. The pressure dropped .05" hg in the preceding 24 minutes, then rose .08" hg during the 21 minute span. Concurrently, an obscured sky with lightning, heavy rain and 3/4" hail was observed. The station is directly in line with the path of the tornado which destroyed Xenia, Ohio - about 55 miles to the southwest - at around 2030Z, although no tornado or funnel cloud was observed at OSU. But the above observations are most likely indicative of an intermediate scale "tornado cyclone" passing just to the southeast of OSU. A similar sequence of events was recorded shortly thereafter at station CMH in Columbus - about 16 km to the southeast of station OSU, only at CMH the evolution of the wind field was indicative of a sharp mesolow passing to the northwest. The likelihood, then, that the severe tornadoes in the Ohio Valley region were embedded in tornado cyclones, which are of large enough scale to appear as small mesolows, may account for the observed association of tornadoes with low

mesoscale pressure in the analyses of Cross Sections V and VI.

The above evidence again brings up the subject of the interaction between gravity waves and convective lines. In the face of such intense convection as that seen around the Cincinnati area, it would seem likely that the strong, short period pressure pulsations would seriously disrupt any organizational capabilities of a gravity wave (and, as will be seen in the next chapter, there is considerable evidence that this squall line was initiated by a gravity wave). Indeed, the Cincinnati (CVG) radar, during the height of strom activity, reveals not a continuous line of echoes but rather a broken band of "super-cell" thunderstorms (see Fig. 2.6). It would thus seem unlikely that a wave-CISK mechanism is operating here over any extended distance along the axis of the "squall line". On the other hand, the presence of a noteworthy amount of intense mesoscale pressure perturbation activity could well be indicative of a wave-CISK type mechanism operating in association with the individual supercells which roughly constitute this squall line (indeed, in his model, Raymond (1975) found that wave-CISK could account for the propagation of "super-cell" thunderstorms in a continuous fashion).

E. Afternoon Wave Activity - Southern Sections

1. Description

Through the southern cross sections, covering Mississippi, Alabama, eastern Tennessee, western North Carolina and Virginia, mesoscale activity is not nearly as evident as it is across the central and northern sections. Some fairly large amplitude hour-to-hour pressure undulations may be viewed

at certain stations, but the features are rarely continuous from one station to the next (though station separation distances are generally greater in the South than they are in the North). The largest observed hourly pressure change is only +.07" hg (at Chatanooga, Tenn. at 0300Z). And yet some monstrous thunderstorms and devastating tornadoes are also observed in these regions. Cross Section IX (Fig. 2.4) is presented because it covers a swath which also experienced some of the most severe weather of 3-4 April 1974, including the infamous Guin tornado. In Fig. 2.4a, only a modest amount of pressure perturbation activity is observed, even during the time when most of the heavy convective activity was occurring. Some of the tornadoes are observed during periods of rising or high pressure, others during periods of falling or low pressure, and still others while the pressure pattern is quite steady, in the area covered by Cross Sections IX through XII (see Fig. 2.4b).

2. Discussion

The relative mildness of mesoscale pressure activity in the South stands in marked contrast to the situation further north, and will be investigated more closely in Chapters VI and VII.

For the entire series of cross sections, in relating the convective activity to the mesoscale pressure fields, a good correlation is found between thunderstorm precipitation and high pressure. There is found to be some association between tornadoes and rising or high mesoscale pressure; however, many tornadoes are also observed with falling or low mesoscale pressure, or with little pressure change. Other than those instances previously noted, in which tornadoes are embedded in tornado

cyclones or small mesolows, the absence of the expected strong relationship between tornadoes and rising mesoscale pressure (where the convergence field is the strongest) is quite likely a consequence of the analysis technique which was employed. Squall lines, as the result of differential growth and movement of convective cells, are not symmetric laterally. Such, however, was assumed when the tornado tracks were superimposed as distinct events on the nearest cross sections. Furthermore, tornadoes are primarily related to thunderstorm cells, and can be considered as being secondarily related to the larger, mesoscale pressure field. Illustratively, see Fig. 2.7. This matter of the interrelationship between pressure fields and convective events will be examined in greater detail in Chapters VI and VII.

CHAPTER III

DELINEATION OF GRAVITY WAVES AND SQUALL LINES

A. Goals and Methods of Analysis

The purpose of this chapter is to delineate the life histories, and characteristics of, the major individual pressure perturbations.

Toward this end, the pressure records of over 150 stations were analyzed for evidence of wave-like undulations. Then the events at neighboring stations were compared in an attempt to discern coherent, traveling pressure waves. The waves at each station were considered to be a sequence of relative high, then low, then high pressure. Each wave's amplitude was taken as the difference between the computed pressure along a straight line drawn from the preceding to the following ridges at the time of occurrence of the trough, and the actual pressure at the trough. If P_1 is the pressure at the first ridge at time t_1, P_2 the pressure at the trough at time t_2, and P_3 the pressure at the second ridge at time t_3, the amplitude (h) of the wave, in hundredths of inches of mercury, is thus given by the formula:

$$h = \frac{P_1(t_3-t_2) + P_3(t_2-t_1)}{t_3-t_1} - P_2 \qquad (5)$$

Since the data available were surface station observations and not barogram traces, it was sometimes difficult to resolve the waves exactly, especially since the stations often reported only once an hour on the hour. Thus, there will often be some uncertainty in the locations of the troughs and in the determination of wavelengths and periods. Furthermore, the ampli-

tudes were likely to be underestimated, since the points used in determining the amplitudes did not necessarily correspond to the actual (relative) pressure ridges and troughs. However, many stations did report between the hours if an important weather event - including a significant pressure change - occurred. In fact, one of the problems that had to be dealt with was that when convection became very severe, the pressure records often became extremely chaotic. When this occurred, an attempt was made to connect one mesoscale pressure event with each squall line.

Four major, long-lived pressure pulsations were revealed from the analysis. The hourly positions of the wave troughs, as well as the amplitudes and the weather recorded at stations which each wave passed, are presented in Figures 3.1-3.4. Due to the aforementioned uncertainty in determining the precise time of occurrence of minimum pressure at many stations, minor lateral variations in the wave front locations were neglected, and the trough lines were drawn as smoothly as reasonable. In fact, leeway of up to one hour was allowed from the time when a station may have recorded its lowest (mesoscale) pressure to that time when the wave trough in question was designated as passing that particular location, particularly when the station reported pressure only once an hour. A fairly constant, or at least slowly varying, wave velocity was assumed. "Average" periods of the waves were determined by averaging the time differences between mesoscale pressure ridges recorded at stations through which each wave passed. Wavelengths (λ) were then calculated from the knowledge of the velocities (V) and periods (p) via the simple formula:

$$\lambda = p \cdot V \qquad (6)$$

B. Wave Histories

1. Wave No. 1

The first significant wave apparently originates in central Missouri and Arkansas very early in the morning - around 0800Z - and travels all the way to western New York, Pennsylvania, Maryland and Virginia by 2100Z (see Fig. 3.1)(due to an absence of data west of Missouri and Arkansas, it cannot be determined with certainty whether this wave may have originated even earlier than the above-mentioned time). The wavefront is generally oriented from NNW to SSE throughout its journey. The distance covered - about 1300 km in 13 hours - gives the wave an average speed of 28 m/sec. The average recorded period of the perturbation is about 90 minutes, and the wavelength is thus ~ 150 km. Precipitation - occurring in conjunction with the trailing pressure ridge - is generally associated with the wave for its entire journey, except for along the southern fringes. Some rather severe convective activity (i.e. heavy thundershowers, with hail) is reported at several stations, though it is generally not of the extreme variety seen with later squall lines. Amplitudes (as defined above) are typically .02-.04" hg, the largest value being .093" hg, recorded at DTW (Detroit).

2. Wave No. 2

The second pulsation also originates in Missouri and Arkansas during the early morning (as best as could be determined, considering, as previously mentioned, the absence of data farther west), following on the heels of the first wave. Some evidence of it is seen as early as 0800Z

in the western parts of these states. This perturbation is very interesting because if provides an excellent illustration of apparent gravity wave initiation of a squall line. The wave becomes pronounced in central Missouri at about 1100Z. In the next few hours, stations throughout eastern Missouri, southeastern Iowa and Illinois experience large amplitude pressure pulsations with no associated precipitation (see Fig. 3.2). In this region, amplitudes of greater than .06" hg are common, with the maximum observed value being .13" hg at STL at 1200Z. Winds are typically seen to back towards the east with the approach and passage of the pressure trough - a characteristic feature of a gravity wave (as previously explained). For instance, the wind at St. Louis shifts from 180° at 9 kts at 1100Z, coinciding with the advance pressure ridge, to 120° at 18 gusting to 24 kts at 1200Z, coinciding with the trough. The weather correlated with the trailing pressure ridge ranges from only scattered clouds to overcast skies at the various stations in this region. During this phase of its journey, the wave's velocity is about 19 m/sec, its period ~90 minutes, and its wavelength ~100 km.

Then, following right in sequence, convection suddenly breaks out in central Indiana at about 1800Z, along a line from EVV to GUS. Within an hour, the convection is severe, with IND reporting heavy rain, thunder, hail, and obscured sky. In the ensuing hours, this squall line gives birth to scores of devastating tornados in southeastern Indiana, southwestern Ohio and central Kentucky (discussed in Chapter II) and even into Tennessee and northern Alabama, as the line grows southward. The propagation velocity of this squall line is about 13 m/sec from 1700Z to 2200Z - when severe convection just about reaches its peak. Wave amplitudes

along the Ohio River Valley at this time are the highest observed during the day - up to .15" hg. The average recorded period is now about 80 minutes and the wavelength - considerably shortened - about 60 km.

At around 2200Z, this squall line begins to undergo an interesting transformation. As seen from the radar at Nashville (BNA) (Fig. 3.5), some of the cells which comprise the line become stationary along an axis running from southwestern Ohio through east-central Mississippi, while another group of cells continues to advance east-southeastward. At first, the leading band of cells is more powerful, but later, the stationary line becomes the dominant one, producing severe weather for several more hours. The advancing line, evident as a wave in the surface pressure records, eventually reaches central New York through western South Carolina, traveling, between 2200Z and 0400Z, at an average speed of ~20 m/sec. Convection, some of it severe, is associated with this "phase" of the wave at most stations which evidence it, except far in the South. Amplitudes, though, are generally only .01-.04" hg. The average measured speed of the wave during this stage is 1 hr, 55 min and the wavelength is ~ 140 km.

3. Wave No. 3

A third major squall line originates in central Illinois along an axis oriented from NNE to SSW between 1700Z and 1800Z (see Fig. 3.3). Unlike the previous squall line, no pre-existing gravity wave without associated convection is seen to have possibly triggered this one. It moves eastward and is responsible for numerous tornadoes in eastern Illinois, northern Indiana, southern Michigan, and northwestern Ohio. In the southern regions of Illinois, Indiana, Ohio, and into Kentucky, a pressure

perturbation is observed but generally with no accompanying precipitation. The speed of the wave through central Indiana is about 16 m/sec. After 2300Z, the northern portion of the line continues to move at about the same speed while the southern portion stalls, so that the squall line's orientation becomes more NE to SW as it advances through Ohio and Kentucky. The average recorded period is about 85 minutes and the wavelength ~ 80 km. Amplitudes of .05" hg or greater are common, with maximum values (up to .101" hg) being recorded in northern Indiana.

4. Wave No. 4

A fourth pressure pulsation of some significance is first observed in western Illinois at 1900Z. Oriented along an axis running from NNW to SSE, it proceeds east-northeastward - following the previous squall line but at an angle to it - reaching eastern Michigan by 0400Z April 4. Laterally, the area of influence extends from northern Illinois and later central Michigan at its northern edge to central Illinois and Indiana, and northwestern Ohio, at its southern edge (see Fig. 3.4). Only sporadic convective activity is associated with this pressure perturbation. Through southern Michigan in particular, a large amplitude (up to .085" hg at AZO) perturbation is experienced, with accompanying easterly and then westerly wind shifts (typical of a gravity wave passage) but with only partly cloudy to overcast skies observed along with it at the trailing pressure ridge. The average speed of this wave is about 22.5 m/sec, the period 85 minutes and the wavelength ~115 km.

A number of other apparent instances of pressure pulsations passing sequentially from station to station in a generally west-to-easterly

direction were observed. These may have been gravity waves or may, in some cases, have been a fortuitous consequence of the analysis method. In any event, these 'waves' were shorter-lived, and of lesser amplitude, than the ones discussed above and are not displayed.

C. Discussion

The fact that continuously propagating pressure perturbations, often of large amplitude and with associated wind shifts but no associated convection, were observed on at least a couple of occasions would seem to indicate that significant gravity wave activity was occurring in conjunction with the severe storms of 3-4 April, 1974. In the case of "Wave No. 2", a gravity wave apparently initiates, or develops directly into, a squall line. This, and the evidence that mesoscale "waves" were observed which had convection associated with them in some locations but none in others (for example: "Wave 4"; "Wave 2" in central Ohio) would tend to support the view which has been adopted thus far: that a squall line is the manifestation of a self-perpetuating gravity wave or wave package, sustained by wave-CISK. Such a view may be reasonable in explaining the propagation of some of the squall lines, such as the first, which was rather slab-symmetric and relatively mild. However, in other cases, such as that of the second 'squall line' at its peak - which was more a loose conglomeration of intense, individual "supercells" than it was a continuous squall line - it is somewhat difficult to think of wave-CISK in association with the line as a whole (as discussed in Chapter II). Perhaps it is more reasonable to consider CISK in association with each individual supercell. But then one is left to consider what might organize the cells - even if

loosely - into a line. In later chapters, other possible explanations for the organization of these convective lines and associated mesoscale pressure fields are explored.

Chapter IV

ORIGIN AND PROPAGATION OF GRAVITY WAVES

A. Goals

In this chapter, the synoptic situation and the vertical structure of the troposphere on 3-4 April, 1974 are examined in an attempt to discern the conditions which may have been responsible for the generation and propagation of the gravity waves and squall lines delineated in the previous chapter. The original viewpoint — that all the major propagating pressure perturbations are gravity waves — is again adopted initially.

B. Source of Gravity Waves

First, speculation is raised as to the source of the waves which originated (apparently) in Missouri and Arkansas during the early morning — at around 0800Z April 3. Inspection of the sequence of synoptic charts (refer to Chapter I) reveals that during the 18-or-so hour period preceding the initiation of these waves, the situation developed from one of ill-defined low pressure in the central Rocky Mountain region (note: the 1200Z April 2 maps are not displayed) to one which exhibited a strong surface cyclone to the lee of the Rockies, with closed contours to at least 700 mb and a considerably sharpened trough aloft. Furthermore, in the hours just prior to the onset of the gravity waves, a considerable amount of thunderstorm activity was already occurring in Oklahoma, Kansas, Missouri and Arkansas. Thus, cyclogenesis (as sited by Uccellini in his case study), or preexisting convection (as sited by Ferguson, Wagner, Bosart and Cussens

in theirs), could have triggered these pressure pulsations.

As for the waves which were spawned in northwest Illinois after 1800Z, examination of the synoptic maps again reveals a number of mechanisms which may have been responsible for their initiation. Figures 1.8-1.12 reveal that between the hours of 1200Z and 2100Z, the isotherms behind the major, trailing cold front — through Okalahoma, Kansas and later, western Missouri— became much more closely packed. Thus, frontogenesis was occurring during this period. The rapid development of a front has been shown theoretically (Ley & Peltier, 1978) to be able to produce, via the geostrophic adjustment process, a wavepacket of mesoscale internal gravity waves travelling away from the cold front in the warm sector of a synoptic system. Another possible causative mechanism is also revealed in Figures 1.8-1.12. Between 1500Z and 2100Z, the original surface cyclonic center gives way to a secondary circulation center, located approximately 200 km to the northeast, at the occlusion point, in southeastern Iowa. During the period 1200Z April 3 to 0000Z April 4, the 850 mb low center deepens by about 4 dm (see Figs. 1.7-1.15), although the 700 mb and 500 mb centers weaken somewhat during this time span (Figures 1.5, 1.6, 1.13 & 1.14). Thus, geostrophic adjustment accompanying lower-level cyclogenesis could also have initiated these gravity waves. Indeed, the position of the newly developing cyclone at 1800Z corresponds very well with the focus of the waves which originated in northwestern Illinois short by thereafter, as seen in comparing Figures 3.3 and 3.4 with Figure 1.10.

Another phenomenon which may have been significant in initiating both the earlier and later sets of pressure pulsations is the action of vertical wind shears and jet streams. This matter will be investigated

from a more physically rigorous standpoint as an aside in the forthcoming discussion.

C. Propagation of Gravity Waves

In comparing once again Figures 2.2-2.4 and Figures 3.1-3.4, with the surface analyses (Figures 1.8-1.12), it is seen that most of the significant amplitude mesoscale pressure oscillation activity—both in association with independent of the major squall lines—was confined to the region bounded by the primary cold front to the west, the stationary front to the north, and the position of the warm front at 1200Z April 3 to the south. In order to gain some insight into the vertical structure of the atmosphere in this and other regions experiencing convection, a number of soundings, revealing temperature, humidity and wind profiles, were now drawn up. (See Figure 4.1).

At 1200Z April 3, soundings in the South (covering the Mississippi, Alabama, Georgia, Tennessee region) reveal a conditionally unstable, extremely moist layer near the surface, reaching up to heights ranging from 3,000 feet (890 mb) at Jackson (JAN) to 7,400 feet (750 mb) at Nashville, (BNA), topped by a sharp inversion of 3°F-5°F, and then capped by a deep, nearly absolutely unstable layer reaching to about 200 mb, which is also very dry, for the most part, except for possibly at the upper levels. (See Figures 4.2 & 4.3). Winds are generally southerly in lower levels, and southwesterly—veering to west-southwesterly—in upper levels. These constitute classic conditions for severe convection from stability considerations. In fact, lifted indices throughout Alabama, western Mississippi and western Tennessee were less than -8 at this time (Hoxit &

& Chappell, 1975), denoting extremely unstable conditions in this region where some of the most severe convection was later observed. Soundings with a sharp inversion separating two nearly adiabatic layers—such as these—were also sited classically (e.g. Tepper's formula for gravity wave-speed) as being conducive to gravity wave propagation, but have not been observed in conjunction with gravity waves in most of the documented studies. And, as seen in the previous two chapters, pressure perturbation activity in the Southern region on 3-4 April, 1974 was rather mild and unorganized.

In the Indiana-Illinois-Missouri area at 1200Z—a time when pressure perturbation activity was quite pronounced—soundings reveal a low level inversion reaching up a little over 2,000 feet—to 900 mb or slightly above—topping by a layer which is conditionally unstable through some levels and nearly so through others, reaching up to the tropopause. The atmosphere is quite moist through most of its depth. (See Figures 4.4-4.6). This type of vertical structure is generally considered to be one which could well support gravity waves (Uccellini, Eom, Ferguson, Wagner), in addition to being one which could support deep convection if the necessary forcing—be it dynamically induced cooling at mid levels, or gravity wave induced uplift (as demonstrated by Eom and Uccellini)—were provided.

Surface layer winds in this region were from the southeast at this time, veering towards the southwest with height. Curiously, a rather pronounced wind maximum of order 45 knots from the SSW is observed at Salem and Peoria at about 3,000 feet. This made for some rather strong wind shears in the boundary layer—of up to 21 kts/1,000 ft. from 192° at Peoria and 27 kts/1,000 ft. from 213° at Salem. (Wind shears in the

boundary layer were generally less than 12 kts/1,000 ft. in regions outside of the western and northern Midwest at this time, except for at Jackson, Mississippi, where the computed wind shear was 18 kts/1,000 ft. from 221°) This observation of the presence of strong wind shear inspired the computation of Richardson numbers for these soundings, as well as others. The Richardson number is the ratio of the Brunt-Vaisala frequency squared (a measure of the static stability, given by $N^2 = \frac{-g}{\bar{\rho}} \frac{d\rho}{dZ}$ for an inviscid fluid, or, equivalently, $N^2 = \frac{g}{\bar{\theta}} \frac{d\theta}{dZ}$ for a Boussinesq atmosphere) to the wind shear squared, $(\frac{dU}{dZ})^2$. Computations were done through selected layers, usually 1,000 - 2,000 feet thick, using the finite difference approximation:

$$Ri = \frac{\frac{g}{\bar{\theta}} \frac{\Delta\theta}{\Delta Z}}{(\frac{\Delta U}{\Delta Z})^2} \qquad (7)$$

where θ is potential temperature, and other symbols are as explained previously.

If $Ri < \frac{1}{4}$, kinetic energy from the mean wind shear may be converted to perturbation kinetic energy, resulting in an oscillatory deformation of surfaces of constant density and hence, a gravity wave known as a Kelvin-Helmholtz wave. (Booker & Bretherton, 1967). Once formed, though, the wave requires a stable layer in order to propagate over any considerable distance. The direction of propagation is parallel to the shear.

The values of Ri in the boundary layer at this time ranged from .26 to .52 in Illinois (PIA and SLO) and Missouri (UMN). Though not less than .25, these values are very close to being so, and it is not unlikely that necessarily small values of Ri for the production of Kelvin-Helmholtz waves were attained at various places in the Missouri-Illinois region around 1200Z. It is doubtful, though, that this mechanism could account for

the pressure pulsation, previously identified as "Wave No. 2", which passed through eastern Missouri and Illinois from west to east at about that time. That wave, as could best be discerned, was oriented from 350° to 170° at PIA and from 10° to 190° at SLO (Refer to Figure 3.2). Thus, its direction of propagation was displaced about 65° to the right of the direction of the lower-level shear. Furthermore, Kelvin-Helmholtz waves in this situation (contained within a very shallow layer near the surface) would be confined to a rather limited area, and "Wave No. 2" was quite large in its horizontal extent. In time as well, these Kelvin-Helmholtz wave would be of a considerably shorter period than those mesoscale waves which were discerned through analysis of the hourly pressure change fields. Thus, some larger scale forcing mechanism, as previously suggested, was probably responsible for the generation of "Wave No. 2", (as well as the other major waves delineated in the previous chapter). However, instabilities due to the action of the strong wind shear may have been responsible for the amplification of "Wave No. 2" at certain specific locations (e.g: St. Louis at 1200Z).

The central and northern Midwest (Ohio and Michigan) also experienced a significant amount of pressure oscillation activity, some of the perturbations being accompanied by convective activity and others not. The 1200Z sounding at Dayton, Ohio (see Figure 4.7) reveals an inversion near the surface extending 2,100 feet upwards, topped by a layer which is marginally stable/unstable extending to about 700 mb and capping finally by a layer which is conditionally unstable—or nearly so—to the tropopause. The atmosphere is fairly dry in the lower few thousand feet, quite dry at mid levels, and moist from about 600 mb upward. Similar to the Illinois soundings, the Dayton sounding reveals a pronounced lower-level wind

maximum—of 30 knots from 195° at 2,000 feet—with strong shears in the boundary layer below—24 kts/1,000 ft. from 199°— and a Richardson number of .26. Thus, this sounding appears also to be one which could support gravity wave activity (as well as deep convection), and by 1600Z, the first pressure wave—with accompanying thundershower activity—was passing through southwestern Ohio.

The 1200Z April 3 sounding at Flint shows a structure somewhat similar to that seen at Dayton at the same time, except that the surface-level inversion is very shallow—only 700 feet deep. By 0000Z April 4, however, the Flint sounding (Figure 4.8) reveals a stable layer about 2,400 feet deep near the surface, topped by an atmosphere which is conditionally unstable, or nearly so, up to the tropopause at 200 mb and which is even absolutely unstable through some layers. A pronounced wind maximum—of 41 knots from 165°—now exists at 3,000 feet elevation, and strong wind shears—16 kts/1,000 ft. from 169° with a corresponding Richardson number of .43,—are seen in the stable layer below. Thus this 0000Z April 4 Flint, Mich. sounding is very similar to ones observed earlier in the day at Peoria, Salem and Dayton, where pressure perturbation activity was occurring, and indeed, some of the most pronounced mesoscale pressure oscillations (without accompanying precipitation) observed during the early hours of April 4, 1974 were found right in the vicinity of Flint.

Elsewhere at 0000Z April 4, east of the position of the surface-level cold front, which at that time extended through central Illinois and then southward along the Mississippi River Valley, soundings generally reveal an atmosphere which was very warm at the surface (70°-80°F), with a nearly adiabatic lapse rate extending all the way up to the tropopause.

Generally the air is quite moist through most of this depth. (See 0000Z soundings for Dayton, Huntington, W. Va., Montgomery Ala., and Jackson, Miss., Figures 4.9-4.12). These atmospheric conditions were in accordance with the severe and widespread convection which was occurring at this time. Such a structured atmosphere could only support gravity wave activity through a CISK-type interactive forcing between the wave and the convection. Speculation as to whether or not this mechanism was responsible for the propagation of the observed squall lines has previously been raised, and, in order to possibly shed more light on this matter, the mesoscale pressure fields in the vicinity of various squall lines will be examined more closely in Chapters VI and VII.

Chapter V

LINDZEN & TUNG'S THEORY ON DUCTED GRAVITY WAVES

A. Theory

The theory advanced by Lindzen and Tung for the propagation of a gravity wave in a lower level duct, discussed previously, is now tested at selected stations in the regions which experienced apparant gravity wave activity. Summarizing, the major criteria which should be met are:

i) The presence of a lower-level, stable "duct" thick enough to accommodate one-quarter of the vertical wavelength corresponding to the ducted wave mode.

ii) The non-existence of a level within the stable layer at which the wind speed equals the wave phase speed.

iii) The presence of a capping, upper layer of low stability in which the Richardson number is less than .25. If the layer is moist, so that the stability is effectively some mean of the dry and saturated stabilities, the Richardson number (referred to the dry-adiabatic lapse rate) may be slightly greater than .25.

iv) The existence of a 'steering' level within the capping layer, where the wind speed is equal to the phase speed of the wave below, or is nearly so, in which case:

v) A 'steering' level may exist above the capping layer.

B. Methods

The observed mesoscale waves for which these criteria are tested are considered to be modes of order zero. The measured phase speeds (c) are first

corrected for the mean wind in the lower level in the direction of wave propagation (U_l) by means of the formula:

$$C_d = c - U_l \qquad (8)$$

where C_d is the wave phase speed relative to the mean wind.

U_l is calculated by first computing the component of wind speed in the direction of wave propagation at each height level for which a wind observation is given in the sounding being utilized, and then height-weighting these values through the depth of the lower level and taking the mean. This is considered to be an excellent approximation to a pressure weighted mean wind through a layer which is relatively shallow.

Brunt - Vaisala frequencies (N_l) are computed in the stable layer by using the finite-difference approximation:

$$N_l = \left(\frac{g}{\overline{\theta}} \frac{\Delta\theta}{\Delta Z}\right)^{\frac{1}{2}} \qquad (9)$$

where g is the gravitational acceleration.

$\overline{\theta}$ is the mean potential temperature.

$\Delta\theta$ is the difference in potential temperature from the top of the layer to the bottom.

and ΔZ is the depth of the layer.

The vertical wavelength is then computed from equation (3), with $n=0$ and $C_{d',n} = C_d$, or in other words:

$$L = 2\pi C_d / N_l \qquad (10)$$

where L is the vertical wavelength

The minimum required height of the duct to support the observed wave is thus given by

$H = \frac{1}{4}L$ where H is the minimum required height of the duct. (11)

In the upper layer, Richardson numbers are computed from the finite difference approximation (7), through layers which are 1,000 - 2,000 feet thick, where 'U' now refers to the component of wind in the direction of wave propagation. The possible presence of steering levels within and above the capping layer is investigated by simple computation of the observed wind components in the direction of wave propagation.

C. Cases

1. Peoria, 1200Z April 3.

First the 1200Z April 3 sounding at Peoria (Fig. 4.4) is examined with regard to the trough which passed the station between 1300Z and 1400Z. Although the amplitude of the wave at Peoria was only .014" hg, at surrounding stations the amplitude was typically around .090" hg. No precipitation, it should be recalled, occurred with this wave. The measured phase velocity (c) of the wave through Peoria was 19 M/sec, directed toward 80°.

Initially the lower level duct is considered to be the 670 M thick layer between the surface and 900 mb (Refer to Figure 4.4). The value of U_1 computed in this layer is -3 M/sec, so that from (8), C_d = 22 M/sec. Nowhere within the duct is the wind speed equal to the phase velocity. The lapse rate of temperature is fairly constant in the lower level, and, from (9), $N_1 = 2.36 \times 10^{-2}$/sec. From (10), the vertical wavelength is thus 5851 M, and, from (11), the minimum required thickness of the duct is:

$H = 1463$ M

Since the depth of the obviously stable lower layer is only 670 M, this layer could not have supported sustained gravity wave activity, according to Lindzen & Tung's theory.

So, from inspection of the sounding, a new layer, extending up to 760 mb, is now considered to be the lower 'duct' - a layer approximately 2200 M deep. Although this layer is not ideally "stable", it is more so than the region above, in which the lapse rate is nearly dry adiabatic (and the air fairly moist). In their own presentation, Lindzen and Tung (1976) used a similar, rather small magnitude kink in the lapse rate of a sounding to distinguish between their 'upper' and 'lower' layers.

In order to determine the stability of this new lower layer, a mean lapse rate is taken through it. This is the significance of the straight, dash-dot line observed in the lower part of the temperature sounding at PIA at 1200Z (Fig. 4.4). With this mean lapse rate, the Brunt-Vaisala frequency is now $N_1 = 1.22X10^{-2}$/sec; the mean wind is this lower level $U_1 = 5$ M/sec; the corrected phase velocity $C_d = 12$ M/sec; the vertical wavelength L = 6180 M; and the minimum required duct thickness is:

$$H = 1545 \text{ M}$$

Since this new lower layer is 2200 M deep, it is sufficiently thick to accommodate the observed gravity wave.

The upper, capping layer is taken to extend from 746 mb (2200 M elevation) to 549 mb (4560 M elevation), where a small inversion exists and above which height the lapse rate lessens. The Richardson number is calculated where the strongest shear is observed, which is between 7,000 and 8,000 feet—right above the ducted layer (actually, this zone extends slightly into the lower layer). From Eq. 7, Ri = .70. Although this

result is larger than the required value for wave-energy reflection of .25, it should be noted that with a static stability as small as that which is observed here, only slight changes in the lapse rate — or slight uncertainties in its measurement — can lead to significant differences in the calculated value of Ri.

Finally, the capping layer is examined for the presence of a steering level, whereat the wind is equal to the uncorrected phase velocity of the wave below. Such a level, however, is not found, as the winds throughout this layer are typically from the SSW at 20-25 M/sec. Only at 21,000 feet elevation — about 6,000 feet above the capping layer — is such a steering level encountered.

2. Dayton, 1200Z April 3.

Next the 1200Z April 3 sounding at Dayton, Ohio is examined with regard to its ability to support the pressure perturbation which passed through the region between 1500Z and 1600Z. The phase velocity of the wave was 28 M/sec towards 70°. Convection was associated with this perturbation at many stations in the vicinity of Dayton, in which case CISK would likely be thought of as providing the necessary forcing to sustain the wave in the lower levels. However, at other nearby stations, no associated convection was observed, and so the conditions for ducting are examined.

The obviously stable layer from the surface to 900 mb is again found to be insufficiently thick to act as a duct, so the lower "stable" layer is chosen to extend to 700 mb (3030 M elevation), where the lapse rate steepens. (See Fig. 4.7). Again a mean lapse rate is taken through the layer, (given by the dash-dot line in the figure) for which $N_1 = 1.31 \times 10^{-2}$/sec.

The mean wind (U_1) through this layer towards 70° is 8 M/sec, and from (8), C_d = 20 M/sec. Then, from Equs. 10 & 11, L = 9593 M, and

$$H \simeq 2400 \text{ M}$$

Since the 'duct' is now 3030 M thick, it is of sufficient depth to support the wave. Furthermore, at no point within the duct does the wind velocity equal the wave-phase speed.

The capping, conditionally unstable, layer is chosen to extend from 700 mb to 300 mb, where the lapse rate finally lessens. Immediately above the ducted layer, from 10,000 to 12,000 feet, strong wind shears and small static stability are observed. The Richardson number computed here is Ri = .32. A steering level, where the velocity towards 70° is 28 M/sec, is found to exist within the unstable layer at 21,000 feet.

3. Flint, 0000Z April 4.

Finally, the 0000Z April 4 sounding at Flint, Michigan, which, as previously mentioned, had a structure similar to that observed earlier at Peoria and Dayton, is examined. Actually, the next pressure "wave" which passed through the area — between 0100Z and 0200Z — was definitely of squall line character, so that CISK may have provided the forcing. Then, a perturbation of .041" hg amplitude — without associated convection — passed through Flint between 0300Z and 0400Z. However, by that time the structure of the sounding may have been altered by the previous precipitation. Nevertheless, the atmosphere is tested for its ability to support ducted waves.

As before, if the obviously stable layer extending from the surface (967 mb) to 878 mb is considered to be the stable duct, it is much too shallow to supoort $\frac{1}{4}$ of the vertical wavelength corresponding to the

horizontal mode. So, the "stable" surface layer is considered to extend to a height of 778 mb (~1830 M deep), which is reasonable in view of the sounding (See Fig. 4.8). The velocity of the perturbation - (c) - is about 16 M/sec toward 105°, and the mean velocity of the wind in the lower level - (U_1) - is -7 M/sec, so that C_d = 23 M/sec. The other important parameters are then $N_1 = 1.32 \times 10^{-2}$/sec, L = 10,986 M, and

$$H = 2746 \text{ M}$$

Since the surface layer is only 1830 M deep, it is not of sufficient thickness to support the wave. At no point within the layer, though, is the wind speed equal to the wave-phase speed.

A sharp unstable layer exists above the duct — between 772 and 700 mb. Although wind shears are not large through this layer, the lapse rate is virtually dry adiabatic, so that the Richardson number is zero. Actually, a value of Ri of less than .11 will provide for over reflection of the ducted wave's energy. A steering level where U = c is found considerably above the capping layer — at about 14,500 feet elevation. Nowhere within the capping layer itself is U-c small, however.

D. Discussion

The application of Lindzen & Tung's theory to soundings which apparently are supporting gravity wave activity yields mixed results. A definitely stable layer does exist near the surface, extending to over 2,000 feet, but this is not found to be thick enough to act as a duct. A sufficiently thick surface layer can be found in two of the three tested cases if that layer is considered to extend to a height over which it is considerably less stable, though still more stable than the layer which lies

above. At no point within the lower level is the windspeed ever found to be equal to the phase speed, so that no absorption of the waves' energy would occur. A capping layer of very small static stability is seen in all cases, although the wind shear is not sufficiently large to assure a value of Ri of less than .25. A steering level where the wind speed equals the wave phase speed is observed in all examples, though at a considerable height either within or above the capping layer. Particularly, at Peoria, at the precise time when a large amplitude pressure perturbation without associated convection passes through the region, so that good results from the application of Lindzen & Tung's criteria would be most expected, the atmosphere does not appear to be able to support a ducted mode for any significant duration. The smallest value of Ri observed there in the capping layer is only .70, and the closest the wind speed comes to the wave phase speed is 10.5 M/sec less than it, which can hardly be considered a small difference — a necessary condition in order for a steering level lying above the capping layer to be effective. This leaves us with the dilemma of whether the observed pressure phenomena are gravity waves, and Lindzen & Tung's theory has its shortcomings, or Lindzen & Tung's theory is valid and the observed mesoscale perturbations are not gravity waves.

E. Emanuel's "Inertial Instability" theory

Another possible explanation for the pressure perturbations and squall lines is that they are due to the phenomenon of "Inertial Instability", as recently suggested by Emanuel (1978). It arises due to an unstable distribution of angular momentum in a fluid, or, in this case, the atmosphere. A favored region for inertial instability is one in which there is strong

vertical wind shear, small static stability, and anticyclonic horizontal shear. The resulting circulations occur as roll vortices along sloping isentropic surfaces, and are aligned parallel to the vertical shear. Strong convergence in the boundary layer beneath the upward branch of the circulation is believed capable of producing convection if sufficient heat and moisture are available in the lower levels.

Inertial circulations display many characteristics heretofore identified in association with mesoscale gravity waves. The typical wavelength is on the order of 100 km; the descent region is associated with low surface pressure and the ascent region with high surface pressure. Some of the differences in their characters are that inertial instabilities are preferred in regions of low static stability and gravity waves in regions of high stability (unless forcing is provided by CISK) and inertial instabilities tend to propagate little with respect to the synoptic-scale features which force the symmetric circulations (at least in those cases studied by Emanuel thus far), whereas gravity waves propagate as a function of the stability of the atmosphere.

Emanuel employs an "Inertia-Stability Index":

$$\frac{\eta}{f} \text{ Ri} \quad ,$$

where η is the absolute vorticity = $\zeta + f$
f is the coriolis force
ζ is the relative, shear vorticity
and Ri is the Richardson Number

to determine where inertial instabilities are most likely to occur. In regions where the Index is small (i.e: less than 1), an instability and a squall line may result. Emanuel calculates the field of this index along a vertical cross section through the northern Midwest at 0000Z April 4 and finds that the powerful squall line which was located through Ohio at the

time lay in a region where the index was less than one from near the surface to about 750 mb. This squall line, as previously mentioned, remained fairly stationary from approximately 2200Z April 3 to 0400Z April 4. Thus the evidence seems to support that this squall line may have been a consequence of inertial instability. Another squall line, located in Indiana at this time, however, was in a region of cyclonic horizontal shear, with higher values of the Index (~2), and was propagating at about 16 M/sec. Thus it seems less likely that inertial instability can account for this line. A closer look is taken at this particular squall line in the next chapter.

CHAPTER VI

PRESSURE STRUCTURE OF ILLINOIS - INDIANA SQUALL LINE

A. Goals and Methods of Analysis

Previously it has been shown that a considerably greater amount of pressure perturbation activity was observed in the northern regions than in the southern regions, despite the widespread occurrence of convection in both areas. In this and the following chapter, a closer look is taken at the mesoscale and thunderstorm scale pressure structure associated with squall lines in both the North and South.

First the squall line (previously identified as "Wave No. 3", which developed in central Illinois beginning at about 1700Z April 3)is investigated. The line was tracked by the WSR 57 Radar at Marseilles, Illinois (MMO), which is located approximately 50 miles southwest of Chicago (see Fig. 4.1). It was a very cohesive line, oriented from about 205° to 25°, and it built northeastward as it moved toward the ESE at about 14 m/sec. All of the surface stations located within the 125 nautical mile radius of MMO were plotted in a series of six successive radarscope photographs, taken at each hour from 1800Z to 2300Z April 3 (actually, the photographs used were those taken at 5 minutes before each hour - done so to correspond with the time when most of the surface stations reported their hourly, "record" weather observations). Two cross section lines were taken through the squall line, one north of MMO, from RFD (Rockford) to SBN (South Bend), the other south of MMO, from SPI (Springfield) to GUS (Grissom AFB) (see Fig. 6.1). The position of the echo band on each

of the two sectional lines was marked at each hour, and then the echo band was laid off in time and in space on the two cross sectional diagrams. Each cross sectional analysis is presented in two parts, one revealing the hourly pressure tendency with relation to the position of the radar echo line, the other actual pressure, as well as the trough and ridge locations, with respect, again, to the radar echo line (Figures 6.2a&b, 6.3a&b).

Since the actual pressure field was now of direct interest, the errors in the altimeter settings first had to be corrected by reference to a mean synoptic base pressure pattern. This was done by first computing and plotting the mean altimeter settings and wind vectors for the stations within the range of the MMO radar for the six successive hours of 1800Z to 2300Z. Then the mean synoptic-scale pressure field was drawn through the region in a manner so as to minimize the total error in plotted station pressure values (each error being the amount by which the computed station value differed from the value of the pressure field within which it was located). Then, each of these errors was corrected to the nearest .01" hg, by adding or subtracting whatever amount was necessary to bring the mean station pressure into accord with the synoptic field value of pressure at that location.

B. Description: Cross Sections

From Figure 6.2a, it is seen that by 1800Z, the echo line (shaded region) has reached northward to Chicago. Shortly thereafter, a mesoscale pressure fall center of -.08" hg/hr is observed approximately 100 km in advance of the leading edge of the radar echo. A rise center is soon seen

to develop within the active convective band, and by 2230Z, the strength of this rise is .08" hg/hr. Another sharp fall zone is observed just to the rear of the echo region, which by 2330Z also has a magnitude of -.08" hg/hr.

A similar pattern is observed through the central parts of Illinois and Indiana, in Fig. 6.3a. By 1830Z, a mesoscale fall center of -.10" hg/hr is found in advance of the leading edge of the radar echo. A pressure rise center is again observed within the radar echo region, building in intensity with time and reaching a maximum strength of +.13" hg/hr at 2230Z at LAF. A mesoscale fall center of -.06" hg/hr is seen just behind the squall line in the early stages, but diminishes in strength with time.

In Fig. 6.2b, a mesotrough is observed within the leading edge of the radar echo through the RFD-SBN cross section. The strength of the trough is seen to increase (i.e. the pressure decreases) with time. Following closely behind the trough (28-40 km) is a ridge. Between the trough and the ridge, a wind shift - from southeast to southwest or northwest - is observed, thus marking the position of the gust front. Another, less pronounced trough-ridge couplet is seen along the rear edge of the radar echo. Again, the winds shift toward the east as the trough approaches and then veer behind it. A third, rather strong pressure minimum is observed, trailing the radar echo by a considerable time span - 2 hours at DPA, decreasing later to 40 minutes at SBN - in a largely echo-free region.

Across the SPI-GUS cross section (Fig. 6.3b), an advance mesotrough is also observed, but here it is located just ahead of the radar echo line. The trough reaches its maximum intensity at 2100Z, then weakens

slightly with time thereafter. A ridge is again observed a few tens of kilometers back, within the radar echo region, with a gust front located between the two features. As is the case across the RFD-SBN section, a secondary trough-ridge pair is observed along the rear part of the squall line through most of the stations which it passes, and even a tertiary pair is seen at SPI, in advance of a small, trailing echo. Again, another marked pressure trough in an echo-free region is observed trailing the rear edge of the squall line - by about 2 hours at SPI, decreasing later to only a few minutes at GUS.

C. Hourly Radarscope Pressure Analyses

1. Methods of Analysis

Next, a series of pressure maps was constructed, superimposed on the radarscope photographs, taken at (five minutes before) each hour from 1800Z to 2300Z April 3 (Figures 6.4-6.9). This was done both by using the plotted station pressure and wind observations and by matching the coinciding features (i.e. troughs and ridges) seen on each of the two cross sectional lines at each time. Along these troughs and ridges in Figures 6.4-6.9, the pressure values, as discerned by interpolation between the observed pressures at each of the cross sectional intersection points, were marked and used as an aid in drawing the isobars. Tornado tracks, as discerned from the April and December 1974 "Storm Data" publications, were carefully plotted on each appropriate diagram, the times of initiation and termination being noted.

2. Description

From these diagrams, the squall line is observed to build north-northeastward and move towards the east-southeast - very slowly at first, then more rapidly (~ 14 m/sec). The first three levels of radar echo intensity are shown in the diagrams (higher intensity levels did exist but are not presented, in order to best retain clarity in the figures). The primary trough-ridge couplet is seen to develop and intensify, the ridge generally trailing the trough by 28-40 km. By 2000Z, a closed mesolow is seen just ahead of the squall line in an echo-free region around CMI. The pressure gradient between trough and ridge increases considerably between 1900Z and 2000Z. By 2100Z, the secondary trough-ridge set has become more pronounced. The mesolow, which measures about 100 km along the trough and 50 km along the cross-trough axis, has moved northeastward, and is still observed just ahead of the radar echo. At this time, an intense convective cell - complete with hook echo - about 40-50 km in diameter, is seen to have developed just to the east of CMI - centered about 25 km directly behind (to the west of) the center of the mesolow. In the ensuing hours, this cell is observed to move out in front of the squall line and traverse northeastward along the line - following the path of the mesolow center (note: this supercell is not as easily discerned in the sequence of figures presented as it was in the original radarscope pictures from which the diagrams were adopted. In Fig. 6.6, it is centered 80 nautical miles from MMO at 190° from north; in Fig. 6.7, it is found 85 nautical miles from MMO at 160°; and in Fig. 6.8, 85 nautical miles from MMO at 120°. In Fig. 6.9, because the convective line is

now located at the outer periphery of the radar scope, it is difficult to determine with precision the position of the major cell - if indeed, it still stands out as a distinct feature at this time). This intense cell spawns numerous tornadoes, including the long-lasting (2150Z-2320Z) Monticello tornado (seen in Figures 6.8 and 6.9). Other tornadoes are observed at scattered locations. Meanwhile, well to the rear of the squall line, the aforementioned, largely echo-free pressure trough is seen. This is "Wave No. 4", previously identified in Chapter III. This trailing trough is oriented from NNW to SSE, and is travelling faster than the squall line, so that by 2300Z, the perturbation almost meets the southern edge of the squall line. Further to the rear is observed the surface low pressure center or centers, and southward extending cold front. These features are particularly visible at 2200Z and 2300Z. Some rather strong radar echoes, but no real severe events, are associated with the low center(s), and the northern portion of the cold front.

D. Discussion

1. Mesoscale pressure pattern

As previously mentioned, no pre-existing pressure wave was seen which may have initiated this squall line. Yet shortly after the line developed, a rather pronounced mesoscale pressure perturbation, consisting primarily of a trough - with an embedded low - just in advance of the radar echo line, and a ridge within the echo region, was observed (the second trough-ridge pair, denoted in the diagrams, was of minor amplitude compared to the first and was actually not always observed, but the fea-

tures were drawn through for continuity). Thus, apparently, the mesoscale pressure perturbations developed in response to some dynamic or hydrodynamic forcing mechanism provided by the convective line). Neither inertial instability nor CISK appears to be operating, at least at the very initial stages.

The mesohigh behind a gust front is commonly thought to be a consequence of "rain gush" precipitation, causing evaporative cooling in the subcloud layers. This, as well as the water loading, produces increased density and increased pressure (after Fujita, 1959). As for the advance mesolow, different theories exist. In a previous study of the April 3-4, 1974 case, Hoxit, Chappell and Fritsch (1976) also observed the presence of the aforementioned mesolow. They assert that this and other large scale ($>$ 20 km diameter) mesolows seen ahead of vigorous squall lines are caused by subsidence warming in the upper troposphere and lower stratosphere, resulting in hydrostatic reduction of the surface pressure. The amount of sinking required to produce mesoscale pressure falls on the order of 2-4 mb/hr (.06-.12" hg/hr) is tens of centimeters per second. They propose two processes to account for this subsidence. One is the upper level flow in a sheared environment (with southerly winds near the surface and westerly winds aloft), directing the downdrafts which surround deep convective clouds and concentrating them downstream. The other is the upper-level winds - also in a sheared environment - being forced over the cloud tops of a squall line and then returning downward on the east side, creating a sort of lee wave. If there is a particular concentration of downward momentum in one location, due to either the presence of an especially strong convective cell upwind, or to the chance juxtaposition

of a number of such cells, a mesolow embedded within a trough will likely be observed ahead of a squall line.

The sounding which was probably most representative of the upper level conditions in eastern Illinois and western Indiana as this squall line passed through was that of Peoria at 1200Z April 3 (refer again to Fig. 4.4). Boundary layer winds were from the southeast, and, through a great depth of the troposphere above (from about 900 mb to 200 mb), winds were generally south-southwesterly, varying in direction just slightly. Only at extreme upper levels (48,000 feet) were winds westerly, and even there the velocities were rather weak (i.e. 25 knots from 260° at 48,000 feet). This would suggest that the cumulonimbus anvils most likely blew off to the northeast - along the direction of the squall line, and not out in front of the line towards the east or southeast, as Hoxit et al. propose. The evidence then would seem to discredit their argument.

In their studies of the 14 May, 1970 convective cell storm in Oklahoma - which was not a pre-frontal squall line but rather a line along a cold front - Sanders and Paine (1975) and Sanders and Emanuel (1977) observed the presence of a mesoscale downdraft of magnitude 2-3 m/sec at 400 mb elevation, above the position of the surface front (low pressure trough). This was matched by a mesoscale updraft of similar magnitude located some 30 km back into the convective storm. The downdraft, however, was believed to be driven by strong evaporated cooling of cumulus cloud tops, which would not result in a net warming of the air column and a consequent reduction of the surface pressure.

So, if mesoscale downdrafts ahead of a squall line are not responsible for the presence there of a mesolow or trough, what is? Sanders et

al. believe the trough, in their case, to be in a region of active convection not yet producing enough condensate to produce a visible radar echo. Foote and Fankhauser (1973) also observed a mesolow just ahead of the visible radar echo, in the inflow region of a Colorado hailstorm. They suggest that the low is a consequence of the dynamics of a strong updraft, and not of a hydrostatic process (the rapid release of latent heat in the updraft region is thought to act as a buoyancy source, creating non-hydrostatic pressure forces). Hoxit et al. counter that a non-hydrostatic process could not produce a mesolow of the size observed in the 3-4 April '74 case (~ 100 km diameter). They are probably correct in this assessment, although it remains uncertain as to what the source of the heating required to produce the mesolow is: diabatic, adiabatic, or advective; and at what level in the atmosphere this heating is occurring.

2. Interrelationship between mesolow and supercell

Perhaps the most interesting phenomenon observed in the hourly sequence of pressure maps (Figures 6.4-6.9) is the aforementioned interrelationship between the mesolow and the tornado producing supercell. It appears that the mesolow predates the supercell. Once it forms, this major convective cell advances toward the low, almost as if it were sucked toward it. This would lend credence to the scenario presented by Hoxit et al. They suggest that the presence of a forward mesolow causes acceleration of the gust front coming out of the squall line, forcing the ascent of moist unstable air lifted by the gust front and resulting in the buildup of new convective clouds. The local maximum in convergence of mass and moisture in the vicinity of the mesolow leads to the develop-

ment of intense convection in that region. They further suggest that the upper level subsidence (which they assert created the mesolow) causes a temporary suppression of convection, followed by an explosive release of the convective instability which has built up in the lower levels. Thus, the existence of the mesolow to the east of the squall line could have been responsible for the subsequent development of the intense, tornado-bearing thunderstorm cell to its west-southwest and the movement of that cell eastward with respect to the bulk of the squall line. At least it seems that, in this particular case, the interrelationship between the mesoscale low pressure center and the supercell was not merely coincidental.

3. Secondary Troughs and Ridges

Another feature worthy of mention is the secondary, or even, in some instances, tertiary, trough-ridge pairs seen at most stations through which the squall line passed (as seen in Figures 2.2b and 2.3b). These pressure maxima and minima were not generally of large amplitude, and did not show up on the mesoscale (hourly) pressure tendency analyses (Figures 2.2a and 2.3a), whereas the primary trough and ridge were preceded, respectively, by mesoscale pressure fall and rise centers. Thus these secondary features might represent thunderstorm scale (< 5 km), or small mesoscale phenomena (i.e. dynamically induced surface pressure fields of the type observed by Foote and Fankhauser (1973)).

Another possibility is that these features are just a spurious result of the analysis method. In the case of the SPI-GUS cross section (B), Figures 6.1 and 6.4-6.9 show that, due to the angle at which the section line crosses the squall line, more than one major convective cell

is often intercepted, which may account for the secondary pressure minimum-maximum couplet. On the other hand, the RFD-SPI cross section line (A) intercepts the squall line perpendicularly, and it does not appear that more than one major convective cell is generally traversed. Thus, it is possible that the major mesoscale wave in the pressure field, which the primary trough and ridge constitute, is extended upstream, producing one or more additional trough-ridge pairs.

It is also possible that these additional pressure features are the result of gravity waves, generated by the squall line itself, being radiated westward - as observed in a theoretical study of convection by Gordon (1977). Either of these explanations may account for the small amplitude waves observed by Bosart and Cussens (1973) and others in barogram traces following the passage of a squall line.

CHAPTER VII

PRESSURE STRUCTURE OF MISSISSIPPI - ALABAMA SQUALL LINE

A. Goals and Methods of Analysis

In this chapter, the bands of convection which affected northeastern Mississippi, Alabama, and northwestern Georgia are examined in an effort, again, to discern the interrelationship between convective events and pressure perturbation activity, and to possibly gain some insight into the cause of the major convective line.

The methods of analysis used were almost identical to those employed in the previous chapter. This time, ten radarscope photographs were taken at hourly intervals, beginning (nominally) at 2100Z April 3, from the WSR 57 radar at Centreville, Alabama (CKL), located about 60 miles southwest of Birmingham. The sequence of photographs reveals, basically, discrete thunderstorm cells which were loosely aligned into bands. The cells moved northeastward as the bands remained virtually stationary, drifting only very slowly southeastward. Two cross section lines were again drawn, both perpendicular to the axis of orientation of the convective bands; the northerly one (A) stretching from MSL (Muscle Shoals, Ala.) to FTY (Atlanta, Ga.), and the southerly one (B) from CBM (Columbus, Miss.) to LSF (Lawson Field, Columbus, Ga.) (see Fig. 7.1). The altimeter settings at each of the stations within the 125 nautical mile range of CKL's radar were corrected for the 10 hours of 2100Z April 3 - 0600Z April 4, in the same manner as outlined in Chapter VI. From the noted positions of radar echoes across the sectional lines, the echoes were marked off in

time and space on 2 cross sectional diagrams (Figures 7.2 and 7.3). The field of pressure, with maxima and minima denoted (dot-dashed and dashed lines, respectively), is analyzed in each of these diagrams.

B. Description: Cross Sections

In these figures, it is seen that the synoptic pressure changes very little from 2100Z April 3 to about 0400Z April 4, after which time the pressure generally increases and the pressure gradient relaxes. The echoes (shaded regions) appear as elongated bands, oriented almost vertically, with a slight downward tilt towards the right (eastward) with time. This is because of the nature of the convection and its motion: individual, separated cells intercepting each cross section line and then moving on northeastward. A number of mesoscale oscillations are seen in the pressure field in both Figures 7.2 and 7.3. In some instances only one or two closely spaced stations experience the perturbation, while in others, the wave is seen over a considerable horizontal distance. In these instances, the trough (dashed) or ridge (dot dashed) is usually observed simultaneously, or with only a small time lag, at the various stations - that is, the trough and ridge lines are horizontal, or nearly so, in the cross sectional diagrams. Thus the wave fronts are apparently oriented perpendicular to the convective bands - i.e. along a NW-SE axis (the last four stations in each cross section are actually aligned in more of a west-to-east direction, so that it may be more accurate to say that the wave fronts are oriented along a W-E axis). The surface level winds are generally southerly throughout the period. In some instances, when oscillations are observed

in the pressure fields at individual stations, slight windshifts towards the south-southeast accompanying falling pressure, and towards the south-southwest accompanying rising pressure are seen; in other cases, no such windshifts are noticed (not depicted).

During instances in which thunderstorm cells pass over individual stations, hourly pressure changes are generally moderate (i.e.: +.05" hg/hr at MXF (Fig. 7.3): 2200Z-2300Z; +.06" hg/hr at MSL (Fig. 7.2): 2300Z-0000Z); to light (i.e.: +.03" hg/hr at CBM (Fig. 7.3): 0300Z-0400Z). The sharpest observed, inter-hourly pressure change is only +.04" hg in 12 minutes (at BHM: 2047Z-2059Z). These magnitudes aren't nearly as large as those observed with convection further north, particularly around the Cincinnati area. This could be due in part to the fact that the stations in this southern region are more distantly separated, and by chance, most of the major, tornado-producing thunderstorm cells passed between stations. One noteworthy exception is the cell which produced the "Guin" tornado, which passed directly over station CBM at about 0100Z (approximately one hour before the tornado touched down) but produced only a very mild change of +.03" hg in 48 minutes in the station's pressure reading.

A number of instances also occur in which moderate amplitude pressure oscillations are observed a considerably distance away from any active convective cells. For example, successive periods of hourly pressure fall and then rise (or rise and then fall) of magnitude .02-.05" hg/hr are observed at FTY between 2100Z and 2300Z and again between 0200Z and 0400Z (Fig. 7.2);at CSG and LSF between 0200Z and 0500Z (Fig. 7.3); and at MXF between 0400Z and 0600Z (Fig. 7.3). As previously mentioned, these waves appear to be aligned along a W-E, or NW-SE axis, but it is not yet

clear as to which way they are propagating.

C. Hourly Radarscope Pressure Analyses

1. Methods of Analysis

Next, a series of pressure maps was constructed, superimposed on the ten CKL radarscope photographs, in the same manner as was done in Chapter VI, in an attempt to discern the motion of the convective cells and pressure oscillations (Figures 7.4-7.13). In these figures, the range of the radar is 125 nautical miles (~ 230 km), and the thunderstorm cells are shaded, in some instances with two levels of echo intensity and in some with only one (note: this was done because the CKL radar did not always record precipitation on an intensity-calibrated receiver; this does not mean that the higher levels of echo intensity did not exist). The tornado tracks, determined from the "Storm Data" (1974) accounts, are again superimposed.

2. Description

As seen in this sequence of pictures, a few large cells (~ 25 nautical mile diameter), located northeast of CKL at 2100Z, grow into an extended, quasi-squall line oriented from 210°-30° by 2200Z. In the next couple of hours, the line becomes broken and dissipates as it moves eastward at about 10 knots. While it does so, a number of tornadoes form in large thunderstorm cells to the northeast of CKL, and move northeastward at about 30 knots. In the meanwhile, another conglomeration of large, separate cells, which only loosely constitute a continuous line, are seen to the northwest of CKL, beginning at about 2200Z. In the next 5 hours,

many extremely destructive tornadoes form, often associated with visible "hook" echoes located along the southern flanks of these large thunderstorm cells, and move northeastward. The Guin tornado, for one, forms at 0150Z and moves towards 50° at 54 knots (28 m/sec) - seen in Figures 7.9 and 7.10. Between 2200Z and 0200Z, the band of convection changes its direction of orientation somewhat - from 205°-25° to 225°-45°, but displays very little net movement. At about 0300Z, the cells become aligned into more of what could be considered a squall line, which moves southeastward only about 40 km in the next 6 hours.

Pressure oscillations associated with the convective cells move northeastward with the cells. Those oscillations not associated with convective cells - seen mostly at stations east of CKL after 0000Z, also appear to move northeastward - as ripples along the isobars. Some examples are the trough-ridge couplet which passes through ANB from about 2300Z to 0000Z and then through MGE from 0000Z to 0100Z; the ridge which passes through MXF and MGM from 2300Z to 0000Z and then through BMH and ANB at 0200Z, and the trough which moves from the OZR-BHN region at 0100Z to the vicinity of CSG-LSF at 0300Z. Otherwise, though, there is not too much evidence of continuous pressure perturbation activity from one station to the next. Most of the perturbations, apparently, are either confined to a rather narrow lateral dimension or do not travel over too great a distance. No evidence is found, however, to indicate that the waves may have moved in any direction other than northeastward.

D. Discussion: Mesoscale pressure perturbations

As for the cause of these waves, reference back to the vertical sounding at Montgomery, Alabama (MGM) at 0000Z April 4 (Fig. 4.11) reveals wind shears in the lower levels of 12 kts/1,000 ft from 190° between the surface and 1,000 feet; 11 kts/1,000 ft from 209° between 1,000 and 2,000 feet, and 13 kts/1,000 ft from 251° between 4,000 and 5,000 feet. The corresponding Richardson numbers in these layers are .30, .29, and .26, respectively. These values are very close to those which can produce Kelvin-Helmholtz gravity waves (as discussed in Chapter IV). It is quite likely that at various times, at various places around the Montgomery region (i.e. east of the band of echoes), the value of Ri dropped below .25, resulting in overturning and a disturbance in the local pressure field. The waves, however, would not have traveled very far, due to the absence of a lower level, stable layer to serve as a medium of propagation. Even those apparent cases, delineated above, of northeastward traveling waves may just have been fortuitous.

So, as compared to the squall line in Illnois and Indiana discussed in the previous chapter, this major squall line in NW Alabama displays little symmetry along its lengthwise axis, propagates hardly at all in the traverse direction, and reveals little evidence of symmetric, mesoscale wave structure aligned parallel to the convective band. Wave-CISK does not appear to be associated with the squall line as an entity. So, other mechanisms are now considered to try to account for the existence of this band of convection.

E. Evidence of Frontogenesis

Another interesting phenomenon is observed in scrutiny of the 850 mb level map at 0000Z April 4 (Fig. 1.15). A sharp zone of temperature contrast is seen, centered along an axis running from the southwest corner of Alabama through the northeast corner of the state and then into east-central Tennessee and Kentucky. To the east-southeast of this line there is a tongue of cold air, and to the west-northwest, a tongue of warm air. A matching feature, though not as sharp, is observed at 700 mb (Fig. 1.14) displaced somewhat to the east. No such zone of temperature contrast, however, is seen at the surface. Earlier - at 1200Z April 3 - evidence of the building of this zone of temperature contrast is seen at 850 mb and at 700 mb (Figures 1.7 and 1.6). Thus, it is apparent that a frontogenetic -type process is occurring in the lower levels - even if not evident at the surface - in the hours preceding 0000Z April 4.

The strength of the temperature gradient at 850 mb across Alabama at 0000Z is about 4°C over a distance of approximately 240 km. From thermal wind considerations:

$$\frac{\partial V^g}{\partial p} = \frac{-R}{fp} \; K \times (\nabla T)_p \qquad (12)$$

where V^g is the geostrophic wind velocity;

p is the pressure;

R is the universal gas constant;

f is the Coriolis acceleration;

K is a unit vector in the vertical direction;

and $(\nabla T)_p$ is the horizontal temperature gradient along a surface of constant pressure.

a wind shear along the front of about $\frac{.66 \text{ m/sec}}{10 \text{ mb}}$, or $\frac{1.3 \text{ kts}}{10 \text{ mb}}$, directed toward the SSW, would be required at 850 mb. The sounding at MGM at 0000Z (Fig. 4.11) reveals a wind shear of 7 knots, over a height of 60 mb - between approximately 780 mb and 720 mb (centered at 750 mb) - directed towards 220°. This corresponds to a temperature gradient of about 3°C over a distance of 240 km, centered above Montgomery. This confirms the presence of the front, slanting towards the east-southeast (i.e. - towards the colder air) with height, since Montgomery is situated east of the zone of temperature gradient at 850 mb, and west of the zone at 700 mb.

The generation (and maintenance) of such a zone of sharp temperature contrast and accompanying vertical wind shears along the axis of the zone requires acceleration of the ageostrophic wind component 90° to the right of the temperature gradient vector in lower levels, and 90° to the left of it in upper levels. This in turn requires, from the frictionless horizontal momentum equation:

$$\frac{dV}{dt} = -f\,k \times (V - V^g);$$

where V is the horizontal wind vector
V^g is the geostrophic wind velocity
t is time
f is the Coriolis acceleration
and k is a unit vector in the vertical direction.

an ageostrophic wind component towards the warmer air in lower levels and towards colder aid in upper levels, and, from mass continuity, rising motion in the warm air and descending motion in the cold air (Sanders, 1975). From about 2200Z to 0400Z, the aforementioned squall line was virtually

stationary along a line from east-central Mississippi, through northwestern Alabama, central Tennessee and Kentucky, and into southwestern Ohio. Comparison with Fig. 1.15 reveals that this position corresponds almost exactly with that of the warm sector - or ascending region - of the aforementioned frontal-type structure at 850 mb at 0000Z April 4. Thus it seems quite possible that a frontogenetic mechanism was responsible for the existence of this one particular squall line, of the many which were active on 3-4 April, 1974.

F. Evidence of Symmetric Circulations

Finally, the atmosphere was tested for the possible presence of symmetric circulations caused by inertial instability, in the vicinity of this band of convection. Rearrangement of Emanuel's "Inertia-Stability Index" yields the conditions for growth of an inertial instability:

$$\frac{1}{Ri} - \frac{\eta}{f} > 0 \qquad \text{(the terms are as defined previously)} \qquad (14)$$

Actually, this is a rather simplistic assessment of the situation. The rates of diffusion of heat and momentum - which are difficult to determine - have not been considered, but are implicitly assumed equal in (14). If these rates are unequal, growth of an instability may occur even if the value of $\left(\frac{1}{Ri} - \frac{\eta}{f}\right)$ is small negative (Emanuel, personal communication).

At 0000Z April 4, the squall line lay between Jackson, Mississippi (JAN) and Montgomery, Alabama (MGM). The vertical field of $\left(\frac{1}{Ri} - \frac{\eta}{f}\right)$ was calculated for the region between the two stations as follows. The squall line's orientation at the time was approximately 220°-40°, so the component

of wind toward 40° was computed at stations JAN and MGM through the lower 500 mb of the troposphere from the respective soundings (Figures 4.12 and 4.11). Then, Richardson numbers were computed at each station at various height levels from the finite difference approximation (7), and a mean of these values taken as indicative of conditions near the squall line. Finally, values of the relative shear vorticity (ζ) were determined at these same height levels from the finite difference approximation:

$$\zeta = \frac{\Delta V}{\Delta x} = \frac{V_{MGM} - V_{JAN}}{\Delta x} \qquad (15)$$

where V is the component of wind toward 40°
and Δx is the distance between JAN and MGM $\simeq$ 320 km.

The results show a positive value of $(\frac{1}{Ri} - \frac{\eta}{f})$ in the lower boundary layer - below 2,000 feet (of approximately +3.0), and negative values above (fairly uniformly about -.5) - up to the 500 mb level. According to Emanuel, these conditions are rather favorable for the growth of symmetric circulations, though they are only definitely so in the boundary layer. It had previously been shown by Emanuel - as discussed in Chapter V - that conditions were very favorable for the growth of symmetric circulations in the vicinity of the northern end of this squall line (in Ohio). Thus, this entire band of convection may have resulted from inertial instability.

CONCLUSIONS

Gravity wave activity does appear to play some role in the severe convective outbreak of 3-4 April, 1974. Most noteworthy is a large amplitude pressure perturbation, with no associated convection but with associated surface level windshifts of a nature consistent with the convergence and divergence fields of a gravity wave, which travels eastward through eastern Missouri, Illinois and western Indiana between the hours of 1100Z and 1600Z, April 3 and then, apparently, gives rise to a convective squall line in central Indiana at around 1700Z. Another similar wave passes through northern Illinois and Indiana and southern Michigan between 1900Z and 0600Z April 4, producing convective precipitation at some locations but none at others. Mechanisms commonly thought capable of producing mesoscale gravity waves of significant (>100 KM) lateral dimension—e.g: geostrophic adjustment accompanying frontogenesis or cyclogenesis—are observed at the approximate times of initiation of these waves. A low level "jet" from the south-southwest, often observed in the regions experiencing pressure perturbation activity, could be responsible for the generation of Kelvin-Helmholtz waves in the boundary layer, resulting in some locally observed, large amplitude pressure oscillations, but is not believed to be responsible for the generation of the major, (basically) eastward-travelling mesoscale gravity waves. The vertical structure of the atmosphere in the regions experiencing this pressure perturbation activity is of a type often found in conjuncture with gravity waves—i.e., a lower, stable layer topped by one of lesser stability—albeit that the stable layer is rather shallow (2,000-2,500 feet).

However, Lindzen & Tung's theory on gravity wave propagation in a low-level duct, tested on soundings in these regions, does not bear out this atmosphere as being one which could well support gravity wave activity.

As to the originally held, CISK-type view that the squall lines themselves are a manifestation of a packet of forced internal gravity waves, it appears to be a more reasonable one in some instances than in others, as the "squall lines" of 3-4 April, 1974 display a wide range of character. In the case of the early squall line, which travels from eastern Missouri at 0800Z to western Pennsylvania at 2100Z and which is relatively mild (compared to those which occur later) and rather slab-symmetric, it does not appear unreasonable to view wave-CISK as sustaining the line itself, although no in depth analysis of the mesoscale pressure structure in the vicinity of this line is attempted. The squall line which develops in central Illinois around 1700Z and moves to northwestern Ohio by 0600Z April 4 is also rather symmetric and continuous in the along-the-line axis, and displays a wave structure on the scale of the squall line itself, with a trough observed along or in front of the leading edge of radar echoes and a ridge seen embedded within the echo band. Thus wave-CISK may be providing the organization for this line as well, although no preexisting gravity wave was observed to initiate the line; the pressure structure arising after, or simultaneously with, the development of the echo band. The convective line, which originates in central Indiana around 1700Z, moves to a position stretching from southwestern Ohio to eastern Mississippi by 2200Z and then remains virtually stationary there till about 0400Z April 4, and which produces the most severe convection of the day, is more a loose band of separated thunderstorm cells than it is a cohesive squall line. The mesoscale pressure structure appears to be organized around the individual convective

cells and not the "squall line" as an entity, so that it does not seem as if wave-CISK is providing the organization for the squall line itself.

The (aforementioned) squall line with the associated mesoscale pressure structure which travels from Illinois to Ohio has, embedded within the advance trough, a mesolow whose track precedes that of a severe, tornado producing thunderstorm cell. The local maximum in boundary layer convergence of mass and moisture in the vicinity of the mesolow most likely contributes to the severity of the convection observed just behind it. The mesolow undoubtedly develops in response to a hydrodynamic process; however, the mechanism responsible, proposed by Hoxit, Chappell & Fritsch—upper troposphere and lower stratosphere subsidence provided by downwind organization of downdrafts surrounding the cumulus towers, or by the return, downward flow of eastward travelling air parcels which were forced above the cumulonimbus cloud tops—is not borne out by upper air wind observations.

Other mechanisms may have played a role in organizing the convection of 3-4 April, 1974. Strong vertical windshears, low static stability and strong anticyclonic vorticity in the vicinity of the stationary "squall line" indicate that Emanuels "inertial instability" may account for the mesoscale, vertical circulations necessary to maintain the convection, particularly along the northern end of the line (in Ohio and Kentucky). And the presence of a strong temperature gradient and a thermal wind directed counter to the geostrophic wind, just to the east of the same line, indicates that an ageostrophic, frontal-type circulation may also be responsible for maintaining the convection of that squall line, particularly along its southern end (in Alabama & Mississippi).

The severe convective outbreak in the Midwestern and Southern United States on 3-4 April, 1974 is of particular interest not only because it was the most widespread and devastating one in recorded history to date, but because it featured a wide variety of atmospheric conditions, possible convection-initiating mechanisms, and squall line character-types. Perhaps most noteworthy is the fact that the presence of strong mesoscale pressure perturbation activity was seen to be neither a necessary nor a sufficient condition for the outbreak of tornado-producing thunderstorms, as it was that large mesoscale pressure waves were observed both with and without accompanying severe convection, and severe convection was observed both with and without large accompanying mesoscale pressure waves.

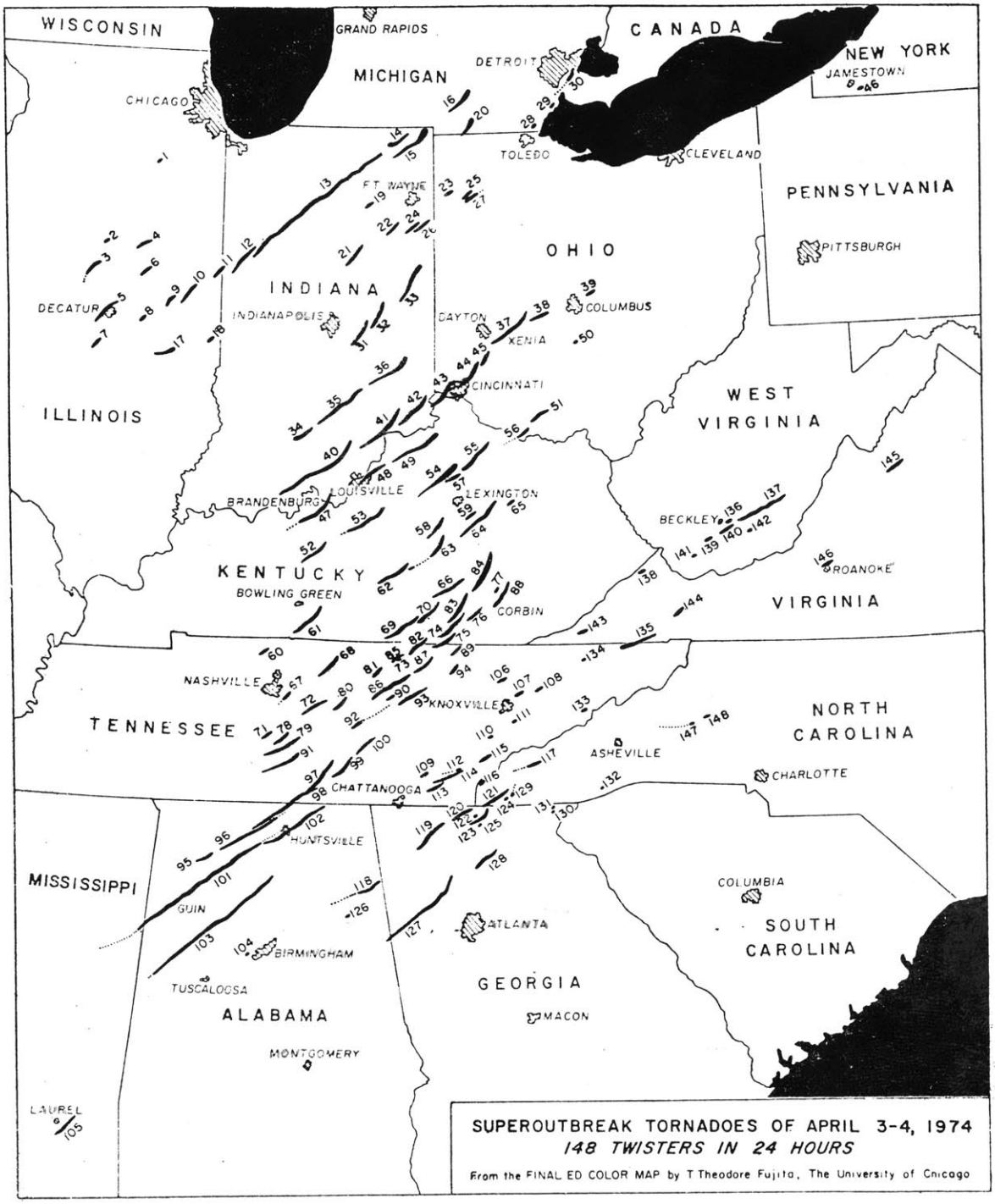

Fig. I-1: Tracks of tornadoes from 1800Z April 3 to 1800Z April, 4, 1974 (After Fujita, 1975, as printed in Hoxit and Chappell, 1975).

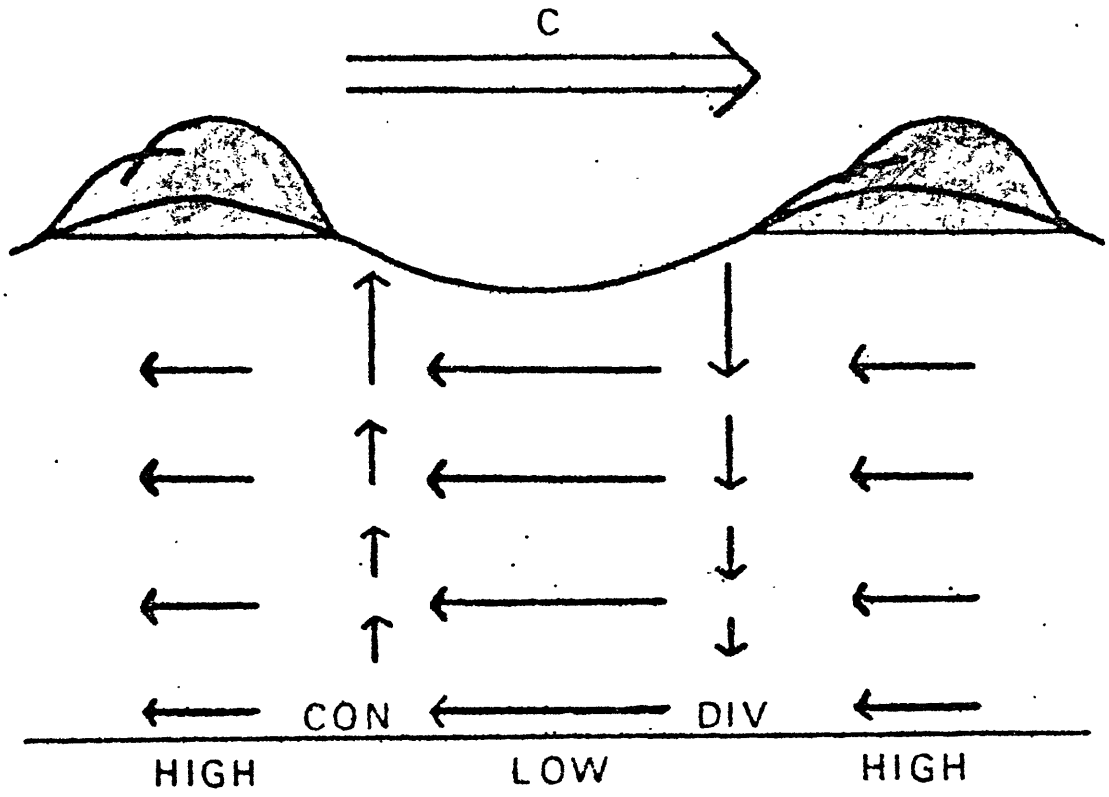

Fig. I-2: Idealized view of gravity wave. Wide arrow on top denotes propagation velocity. Other arrows indicate vertical and horizontal wind velocities. CON = convergence; DIV = divergence. Shaded regions depict clouds. (After Eom, 1975).

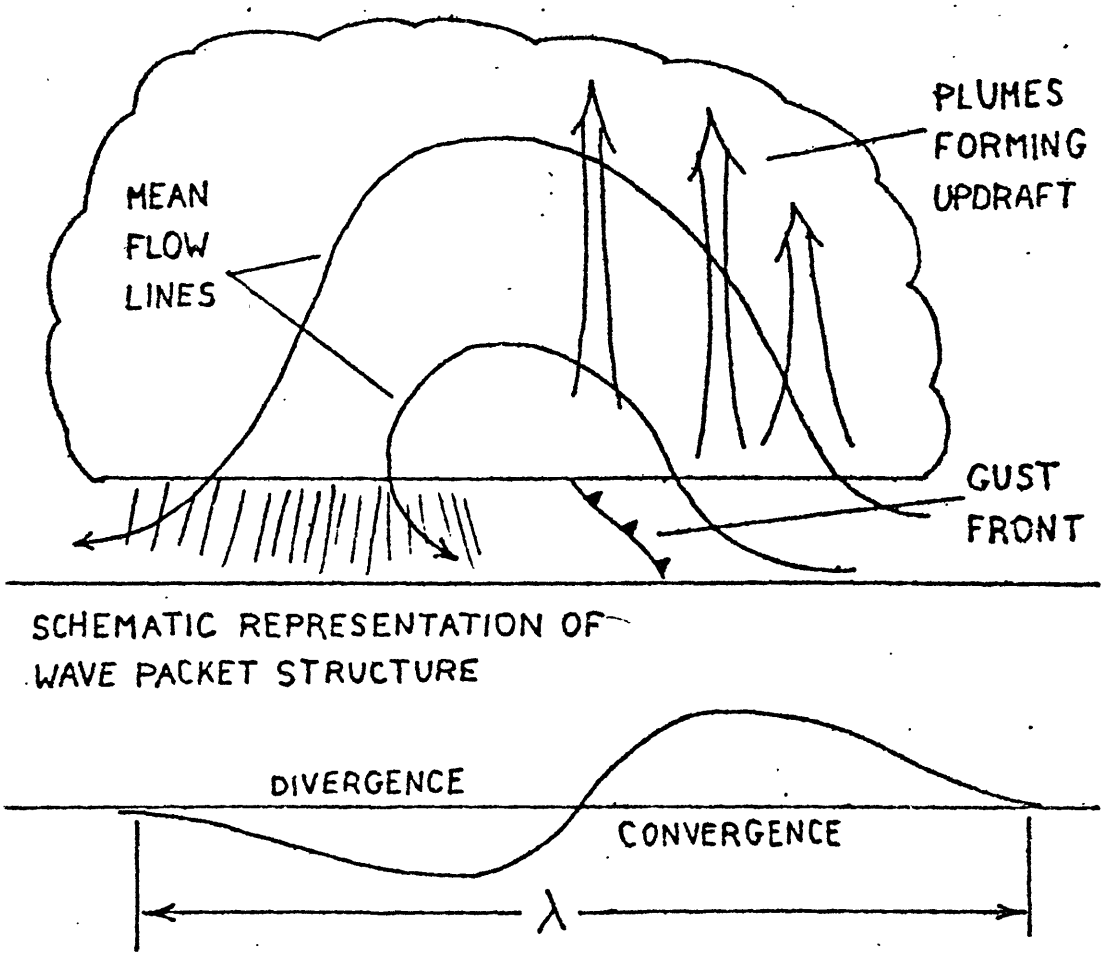

Fig. I-3: Hypothesized view of wave CISK operating in convective storm. $\lambda \equiv$ dominant wavelength gravity wave. Bottom curve indicates strength of divergence or convergence. Wave is travelling towards right (After Raymond, 1975).

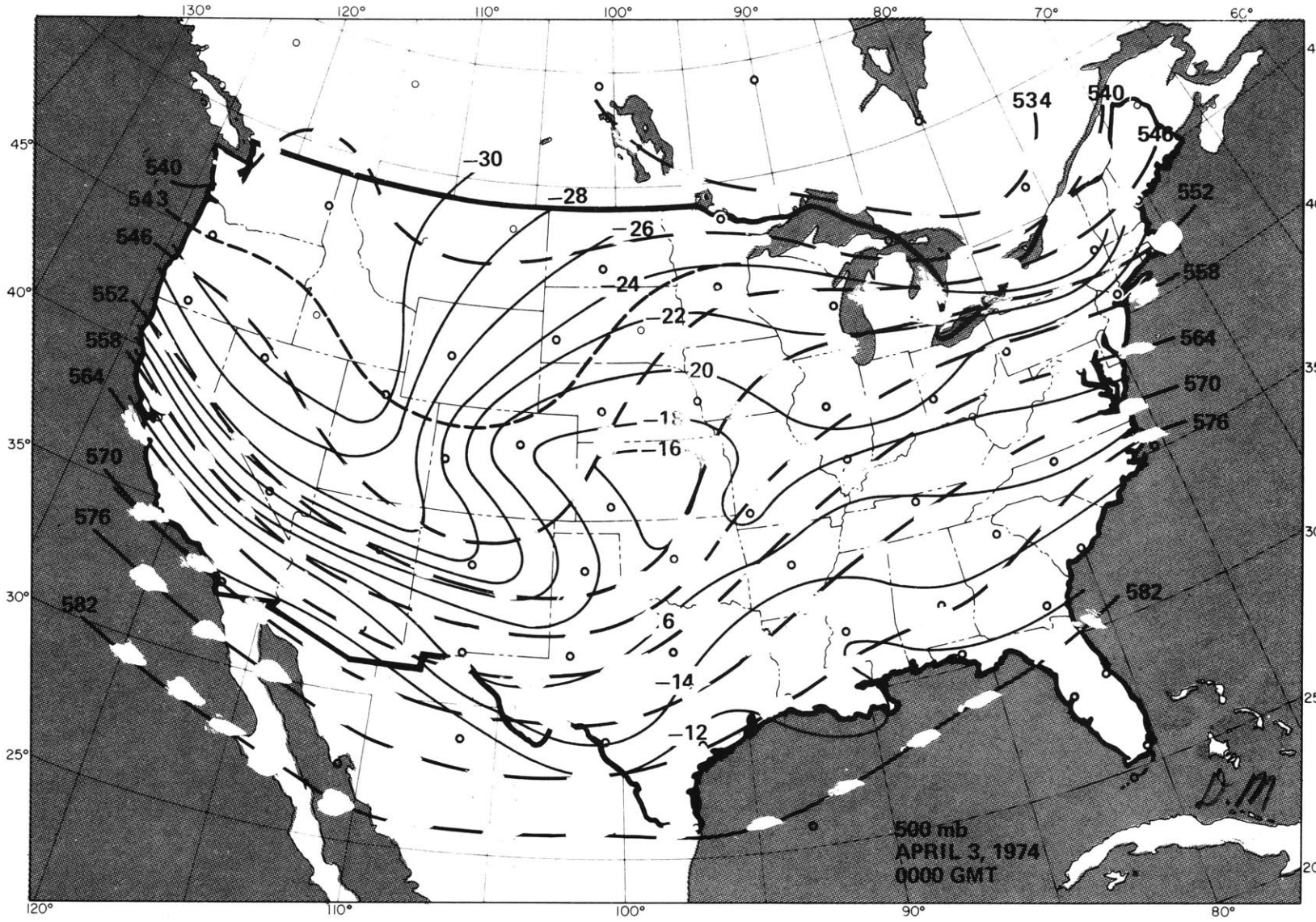

Fig. 1.1: 500mb analysis, 0000Z April 3, 1974. Dashed lines: Height contours at 6 dm intervals; solid lines: Isotherms at 2^{o} C intervals (After Hoxit and Chappell, 1975).

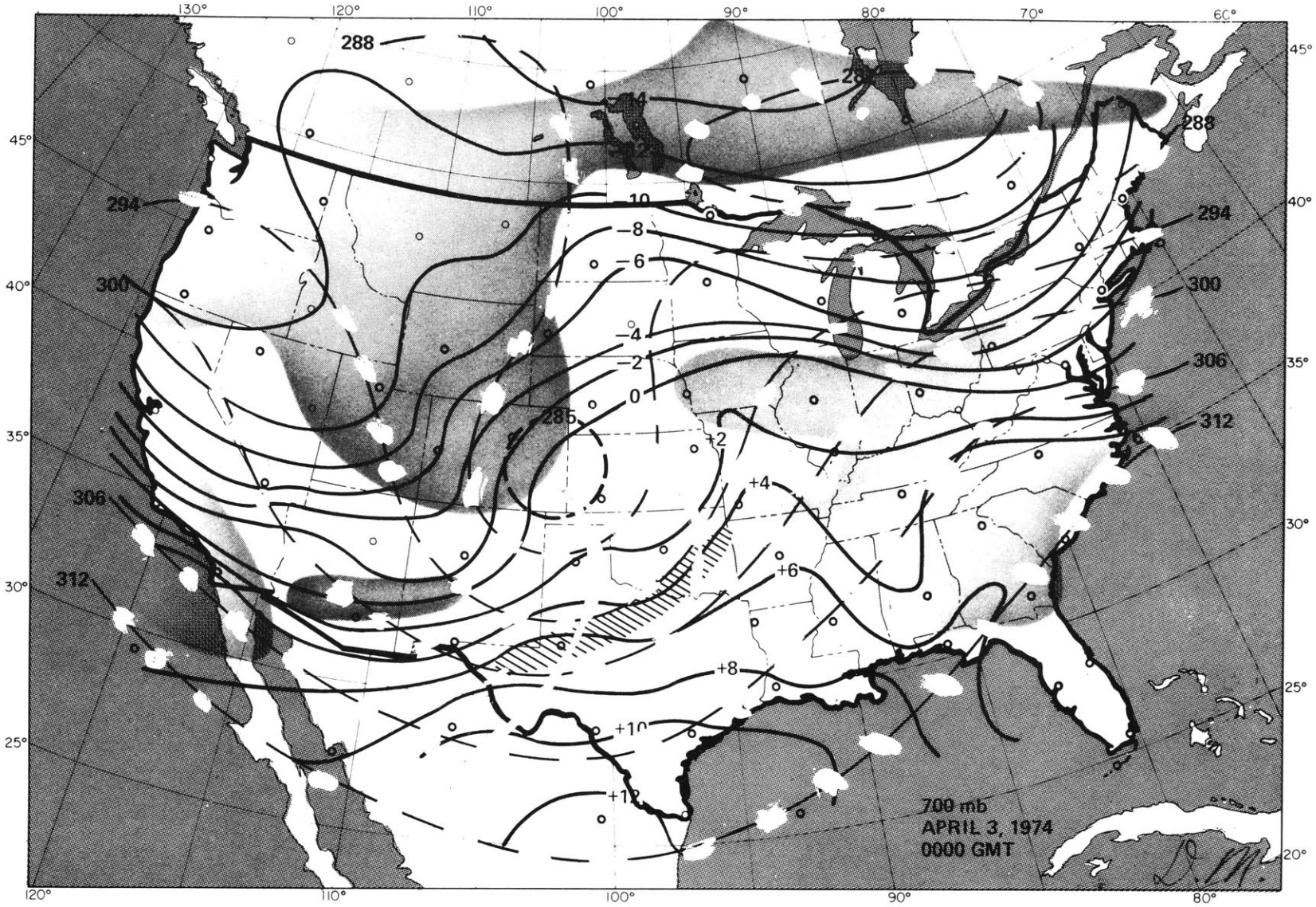

Fig. 1.2. 700 mb analysis, 0000Z April 3, 1974. Dashed lines: height contours at 6 dm intervals; solid lines: isotherms at 2°C intervals; hatched regions: wind speeds $\geq$ 60 knots (After Hoxit and Chappell, 1975).

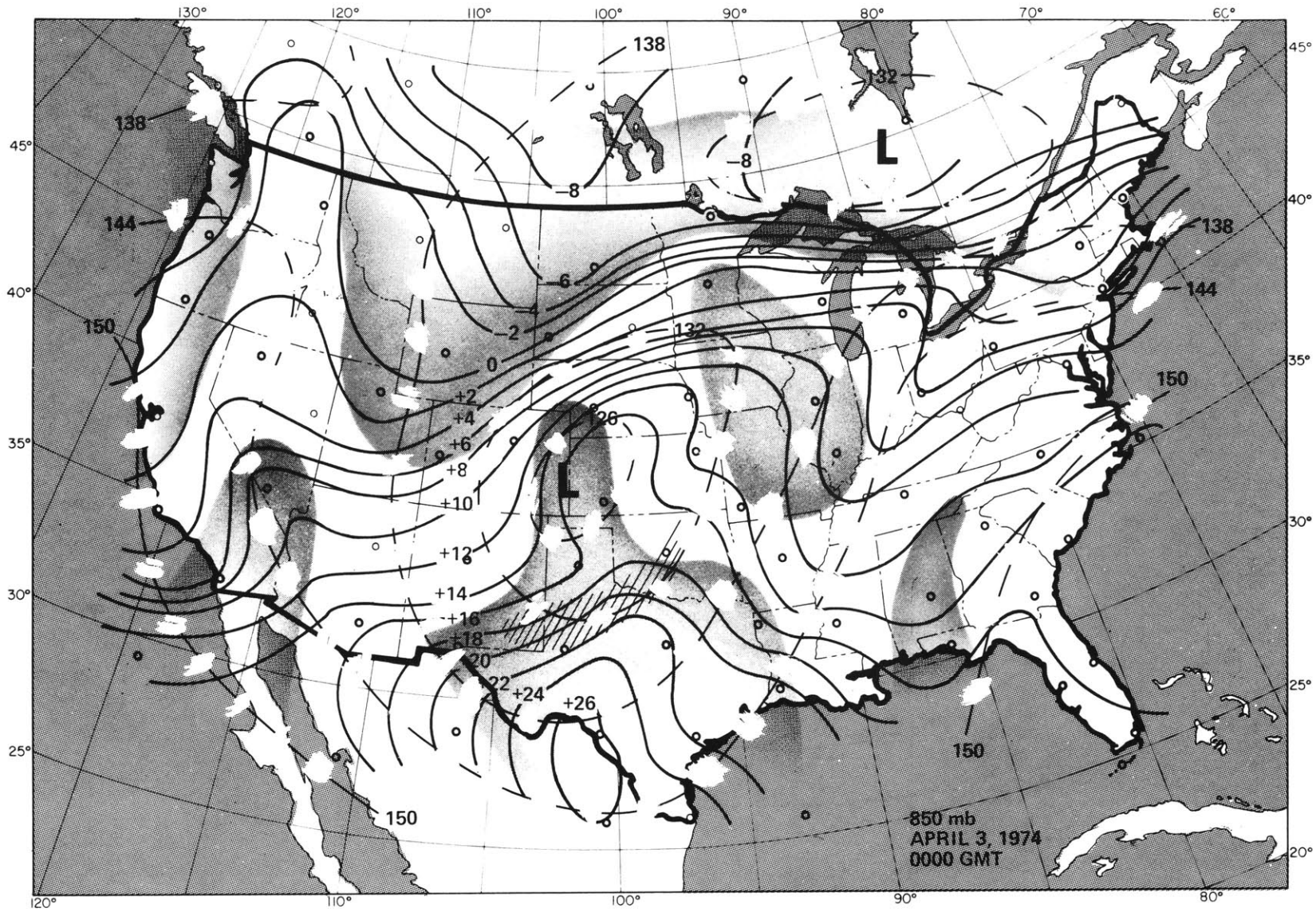

Fig. 1.3. 850 mb analysis, 0000Z April 3, 1974. Dashed lines: height contours at 6 dm intervals; solid lines: isotherms at 2°C intervals; hatched regions: wind speeds $\geq$ 50 knots (After Hoxit and Chappell, 1975).

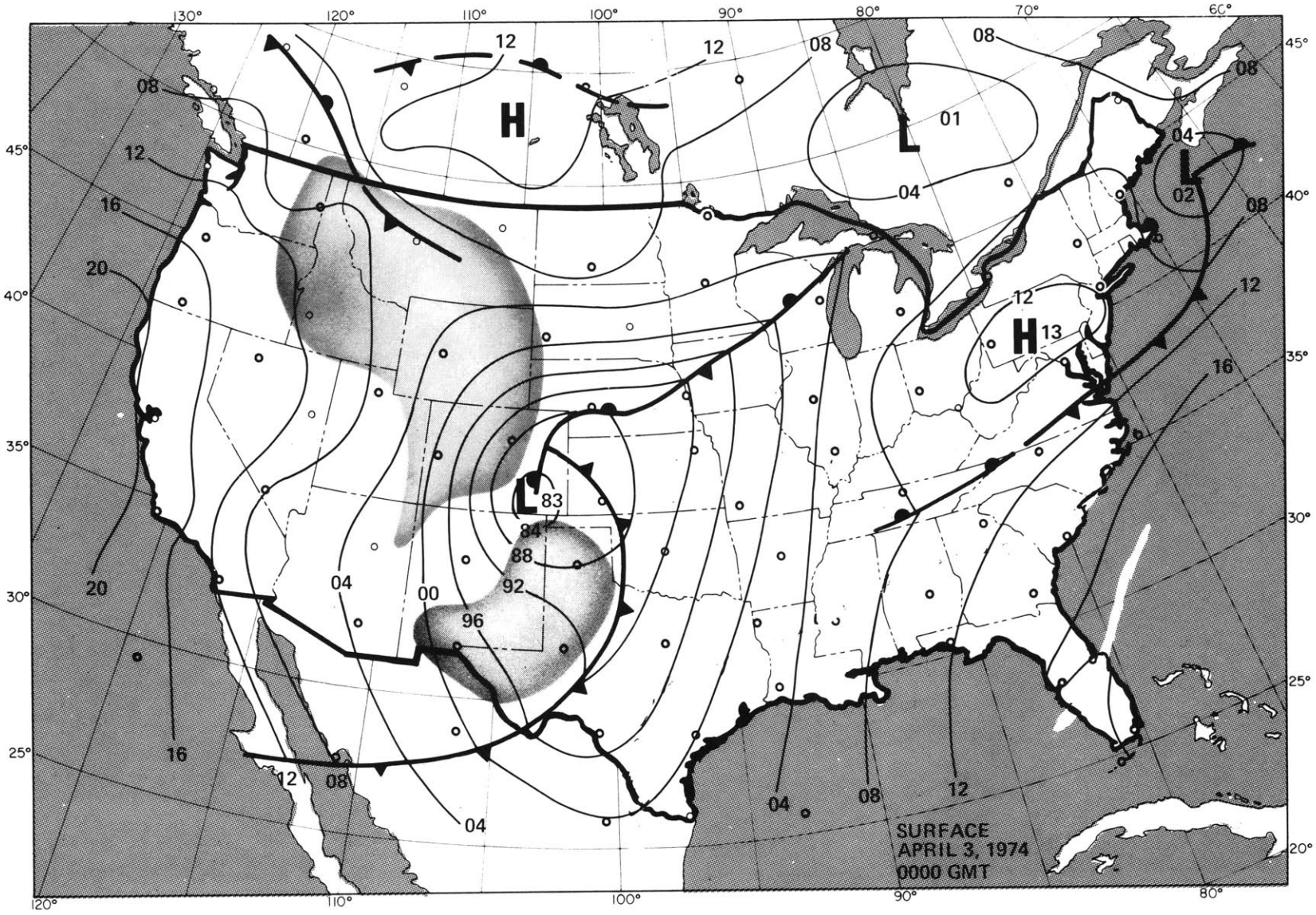

Fig. 1.4. Surface analysis, 1200Z April 3, 1974. Solid lines: isobars at 4mb intervals (After Hoxit and Chappell, 1975).

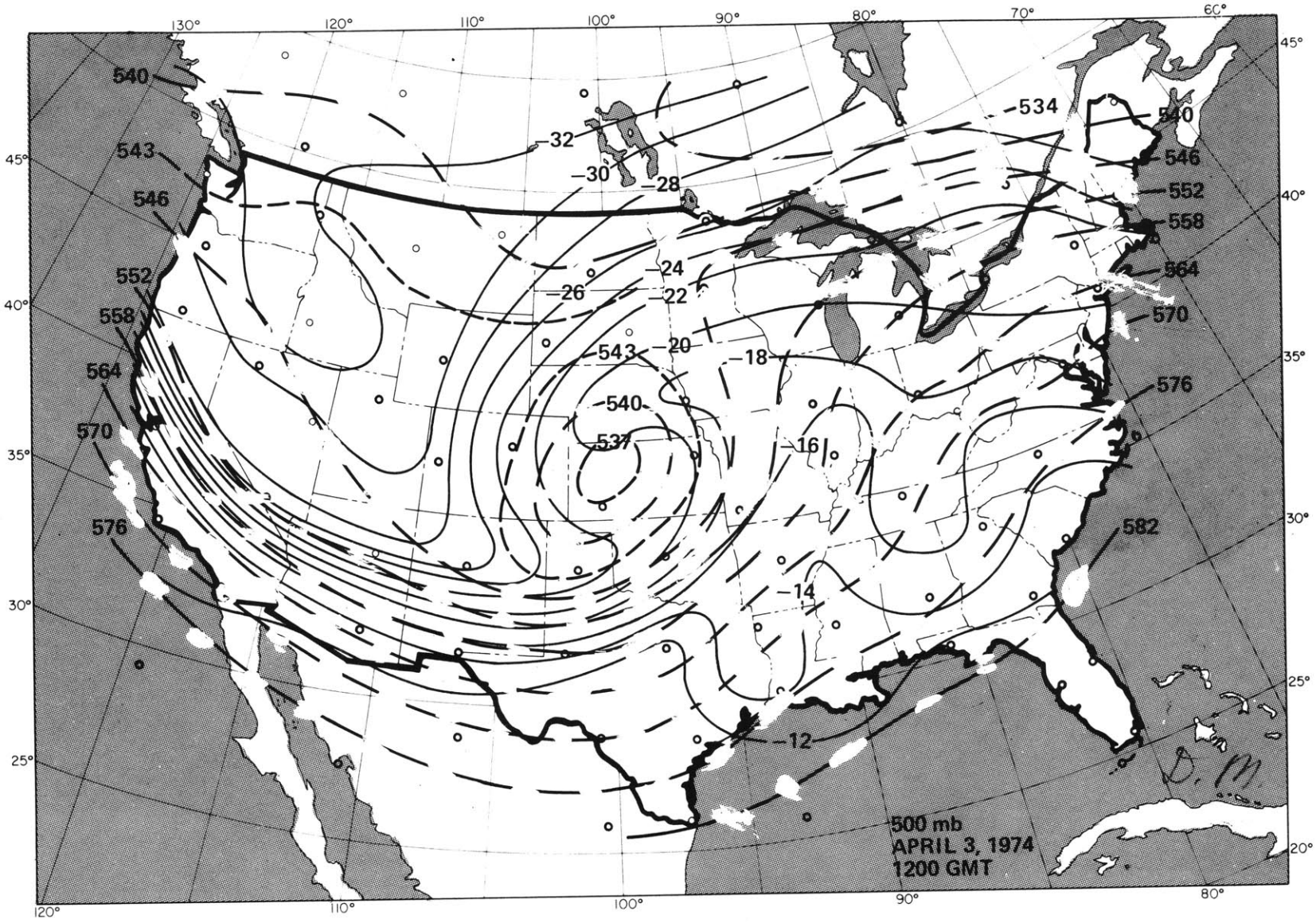

Fig. 1.5. 500mb analysis, 1200Z April 3, 1974. See legend for Fig. 1.1 (After Hoxit and Chappell, 1975).

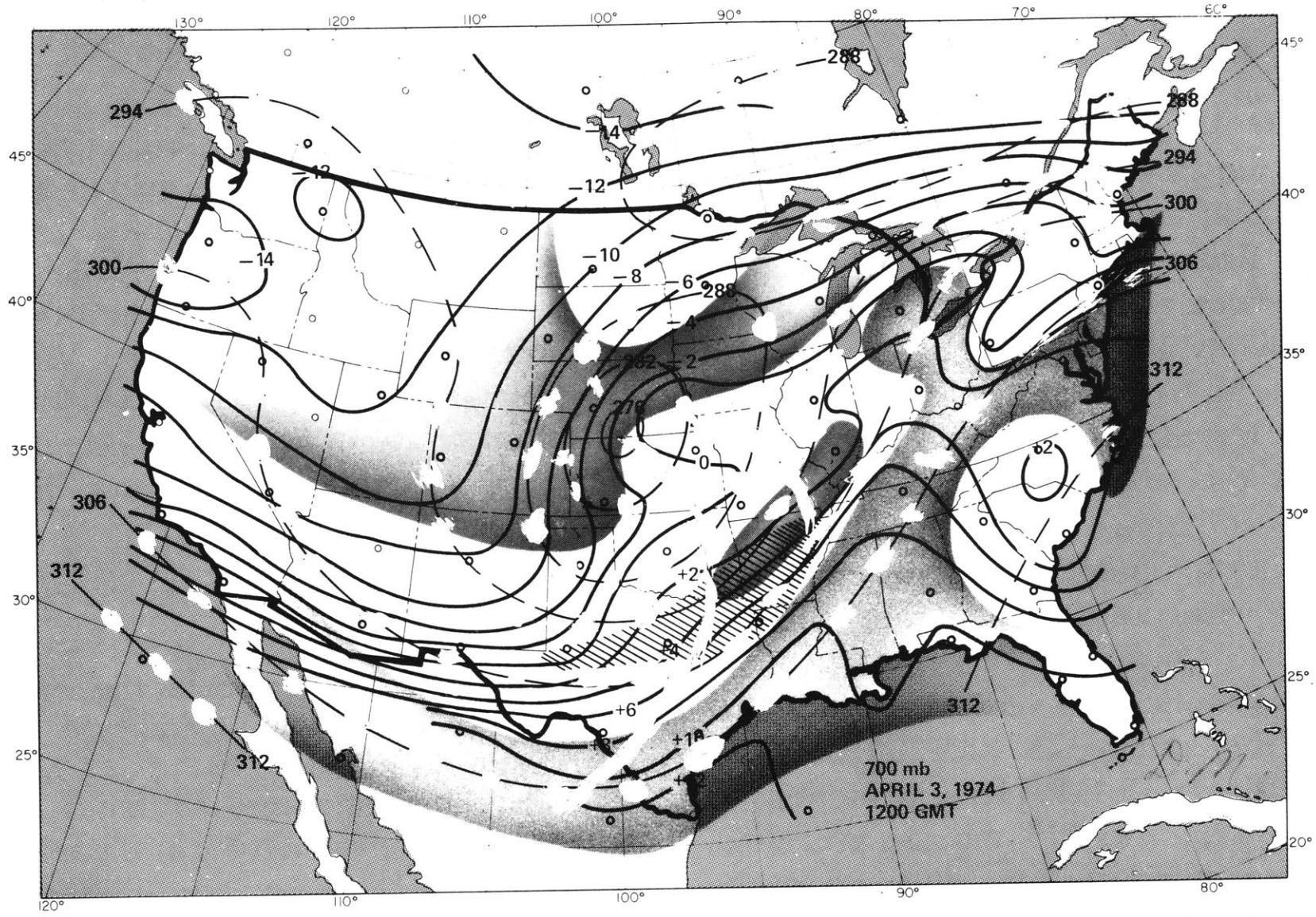

Fig. 1.6. 700mb. Analysis, 1200Z April 3, 1974. See legend for Fig. 1.2. (After Hoxit and Chappell, 1975).

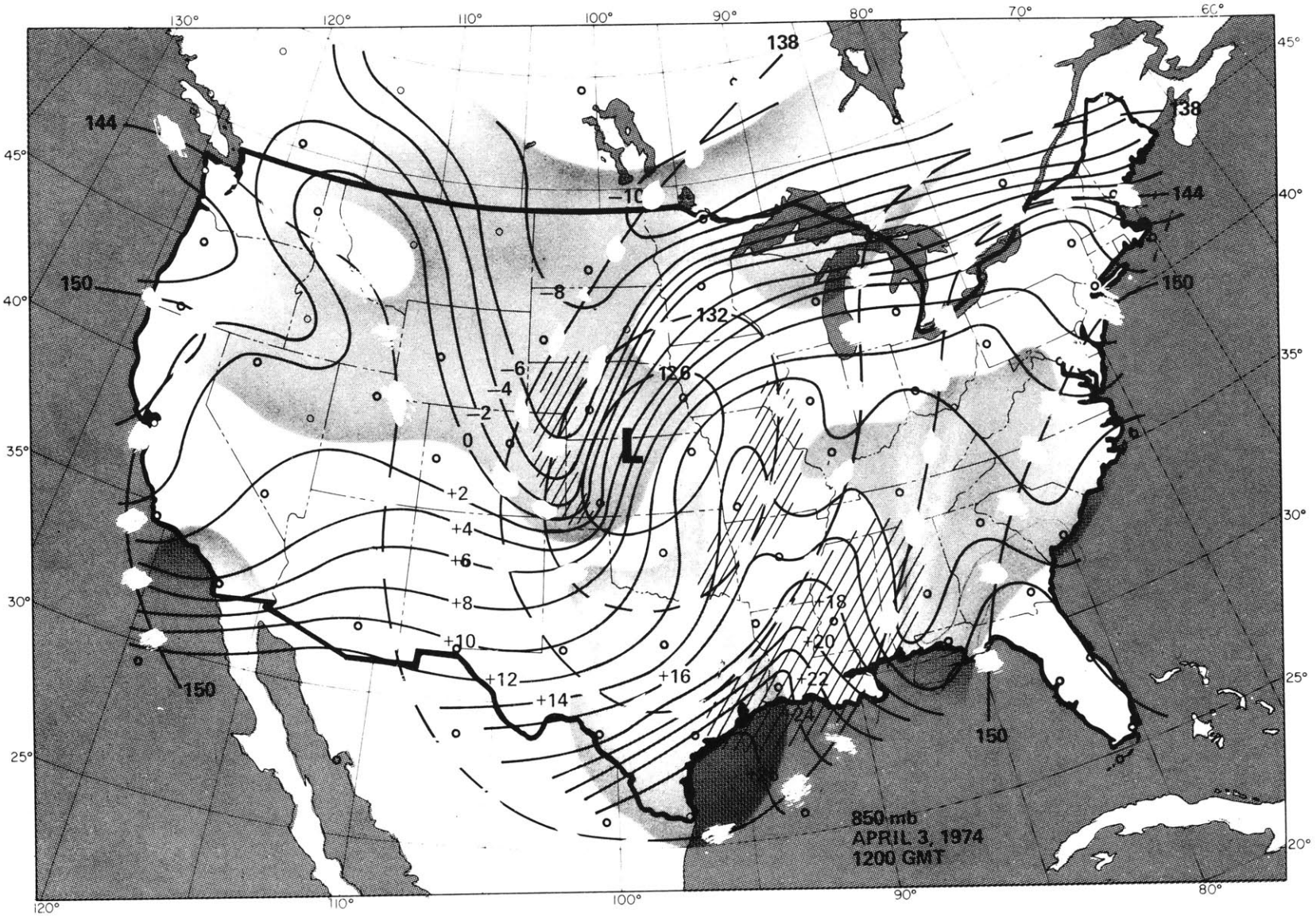

Fig. 1.7. 850 mb analysis, 1200 Z April 3, 1974. See legend for Fig. 1.3 (After Hoxit and Chappell, 1975).

Figs. 1.8 - 1.12 . Surface analyses. Thick lines: pressure (above 29.00 " hg), at intervals of .05 "hg; dotted lines : isotherms , at intervals of 5° F; thick dashed lines: mesoscale pressure troughs; line with hollow, rounded barbs: forward extent of dry tongue (after Hoxit and Chappell, 1975)

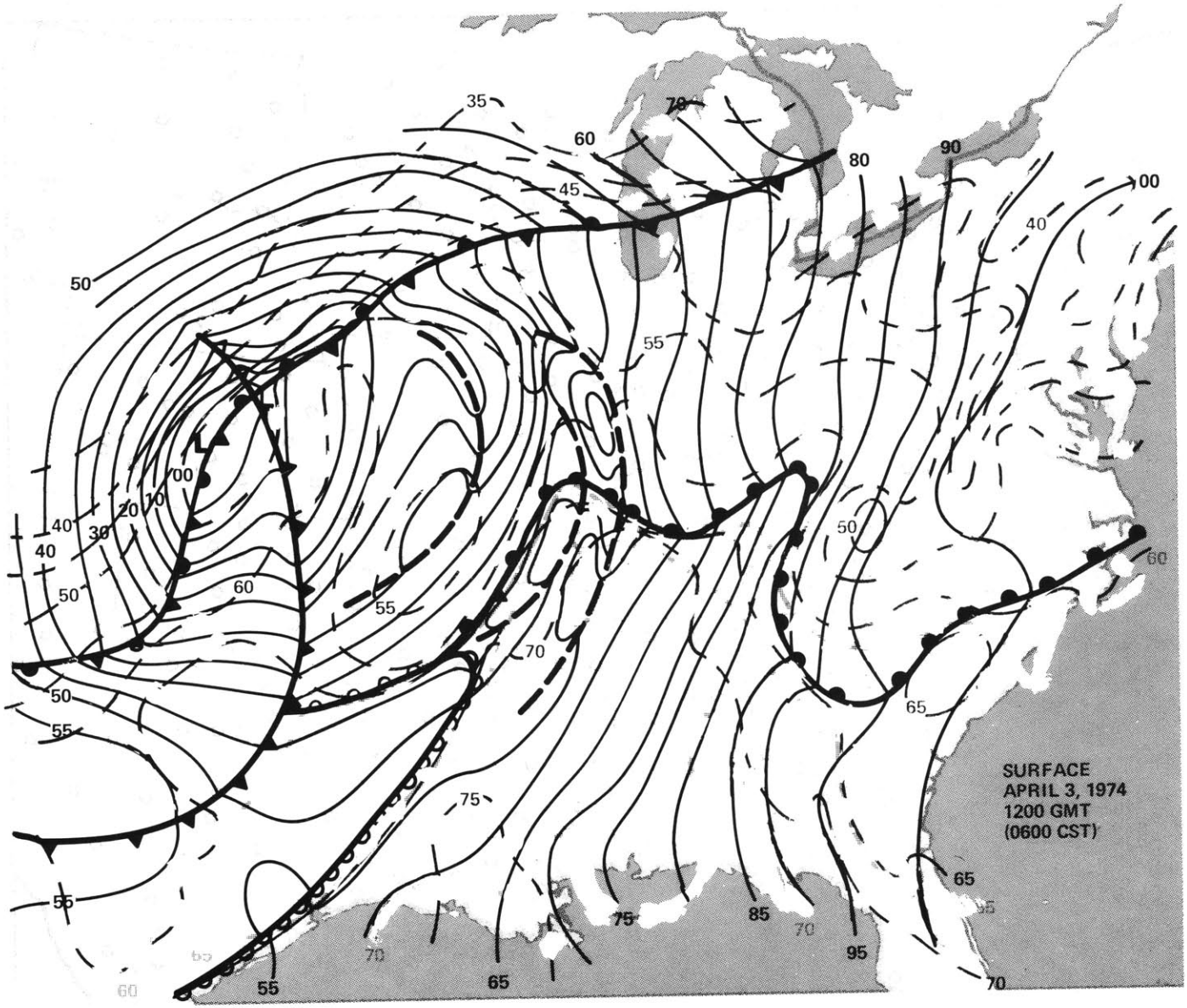

Fig. 1.8. Surface analysis, 1200Z April 3, 1974. See opposite page.

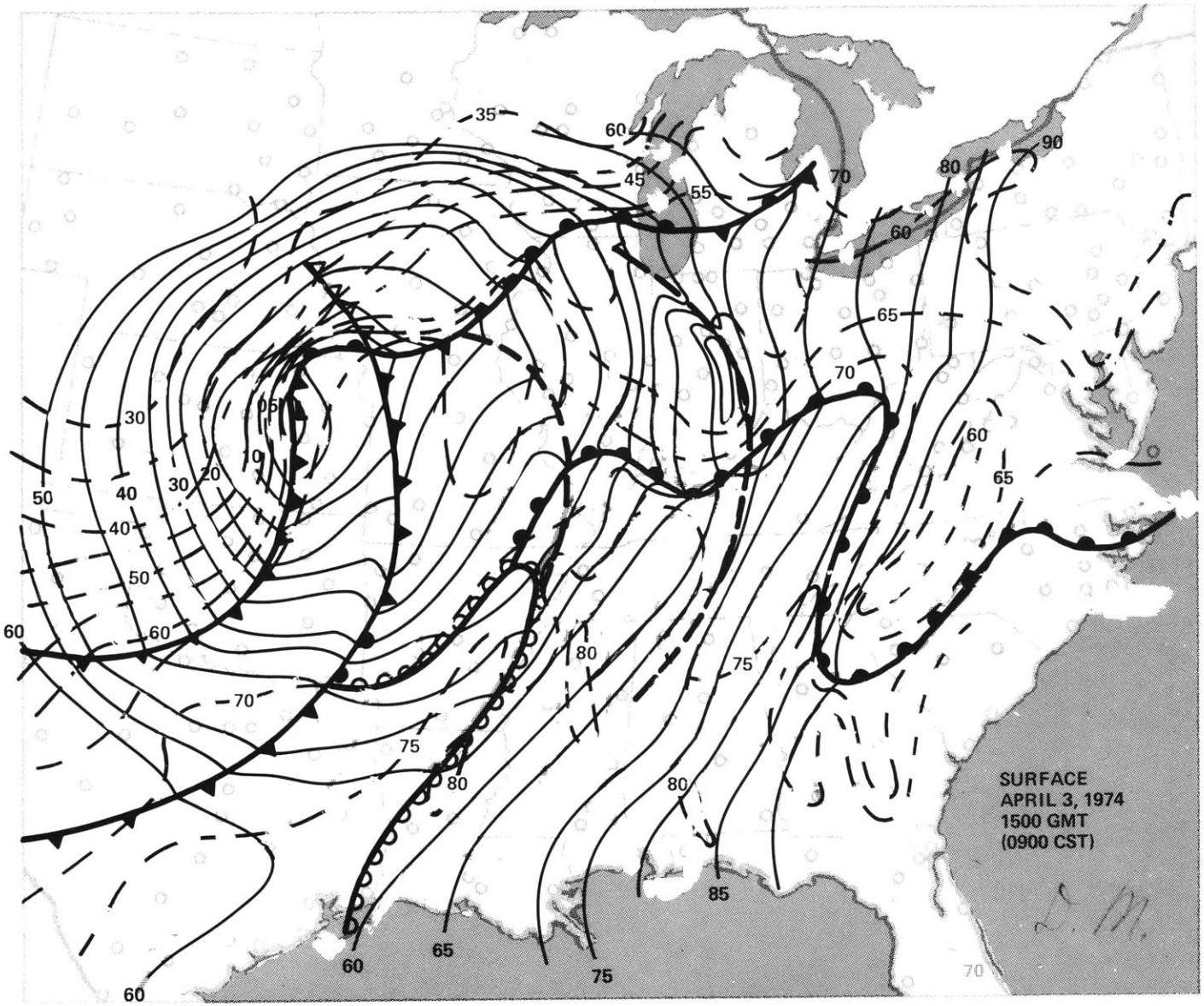

Fig. 1.9. Surface analysis, 1500Z April 3, 1974. See explanation opposite Fig. 1.8.

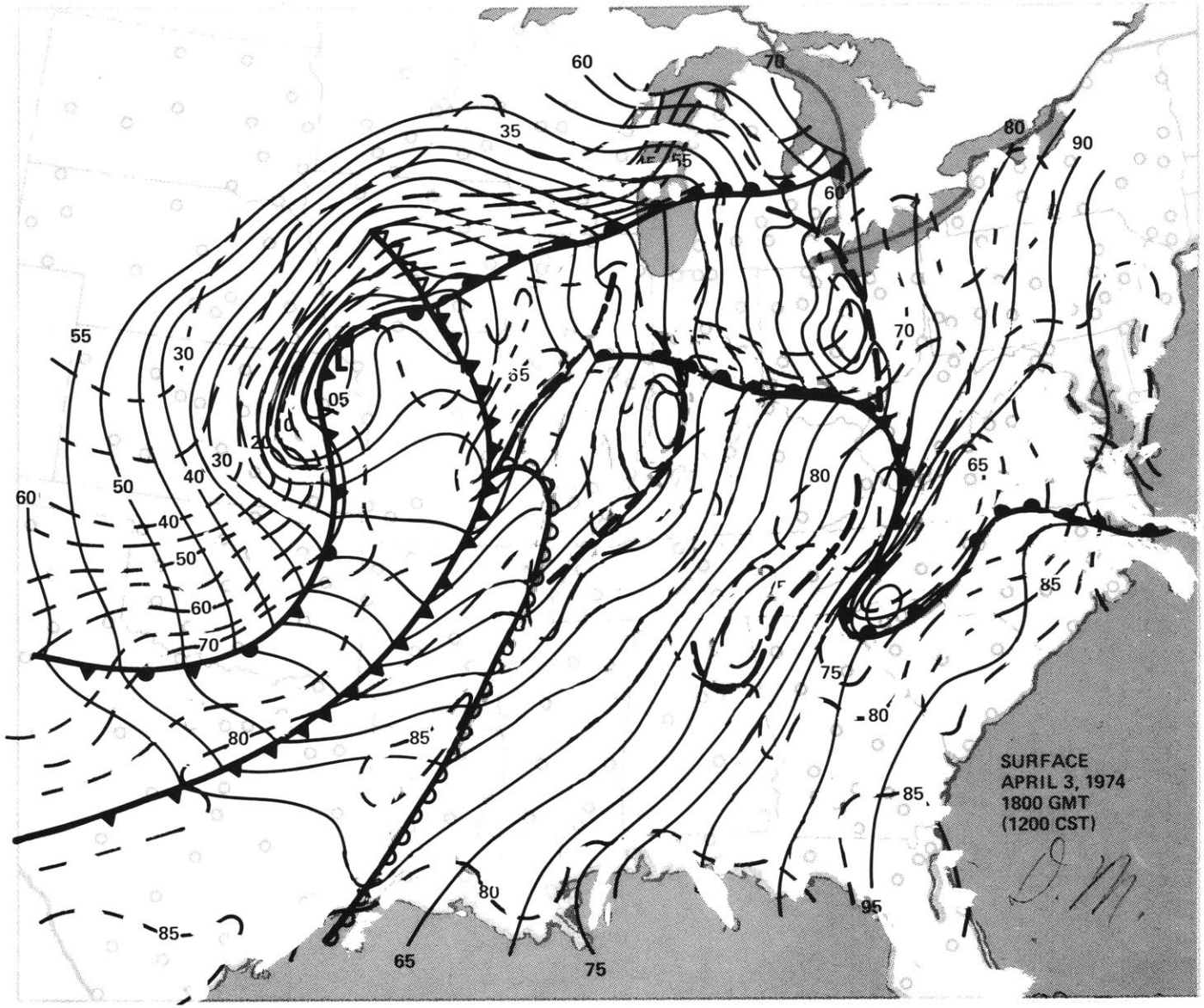

Fig. 1.10. Surface analysis, 1800Z April 3, 1974. See Explanation opposite Fig. 1.8.

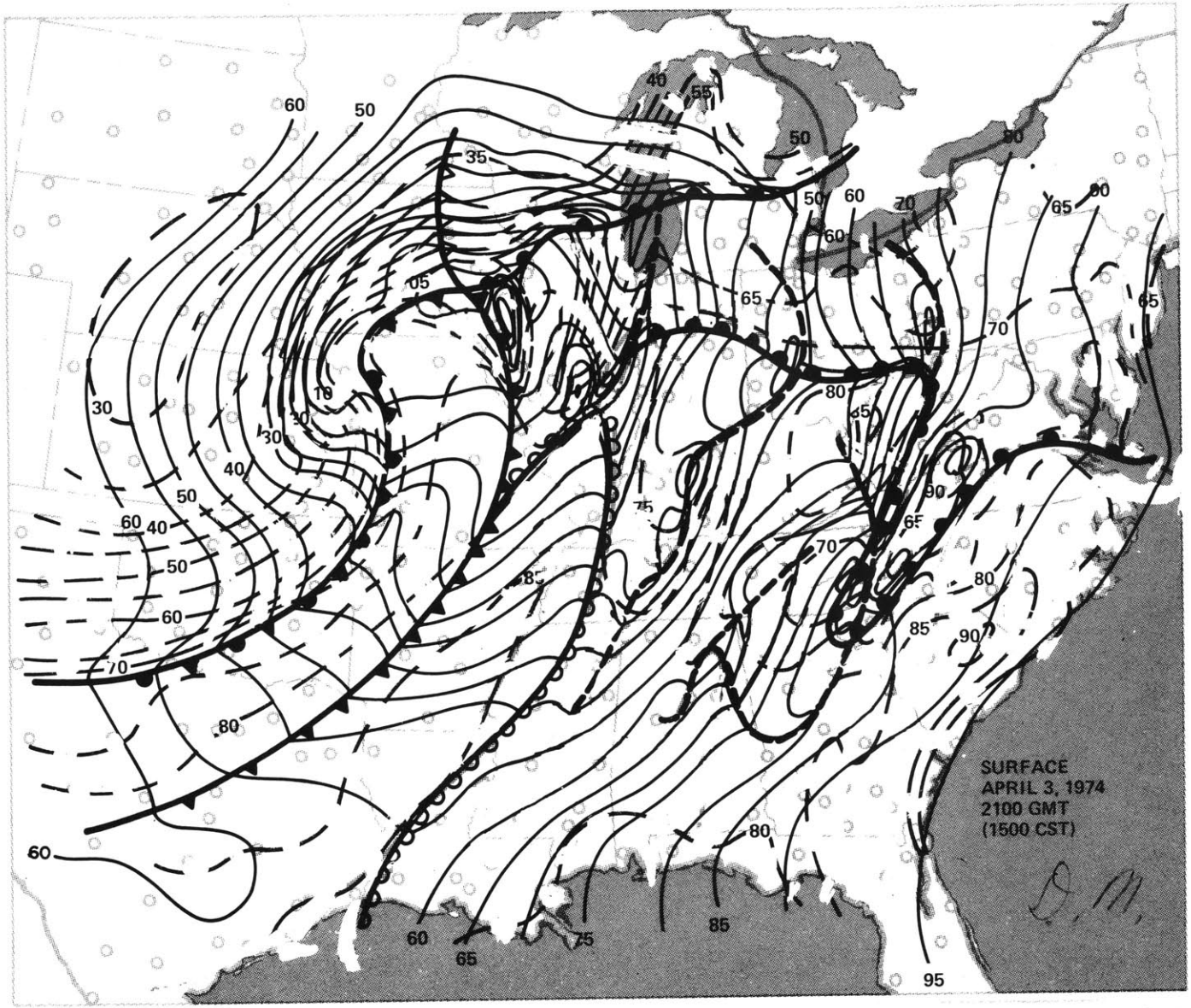

Fig. 1.11. Surface analysis, 2100Z April 3, 1974. See explanation opposite Fig. 1.8.

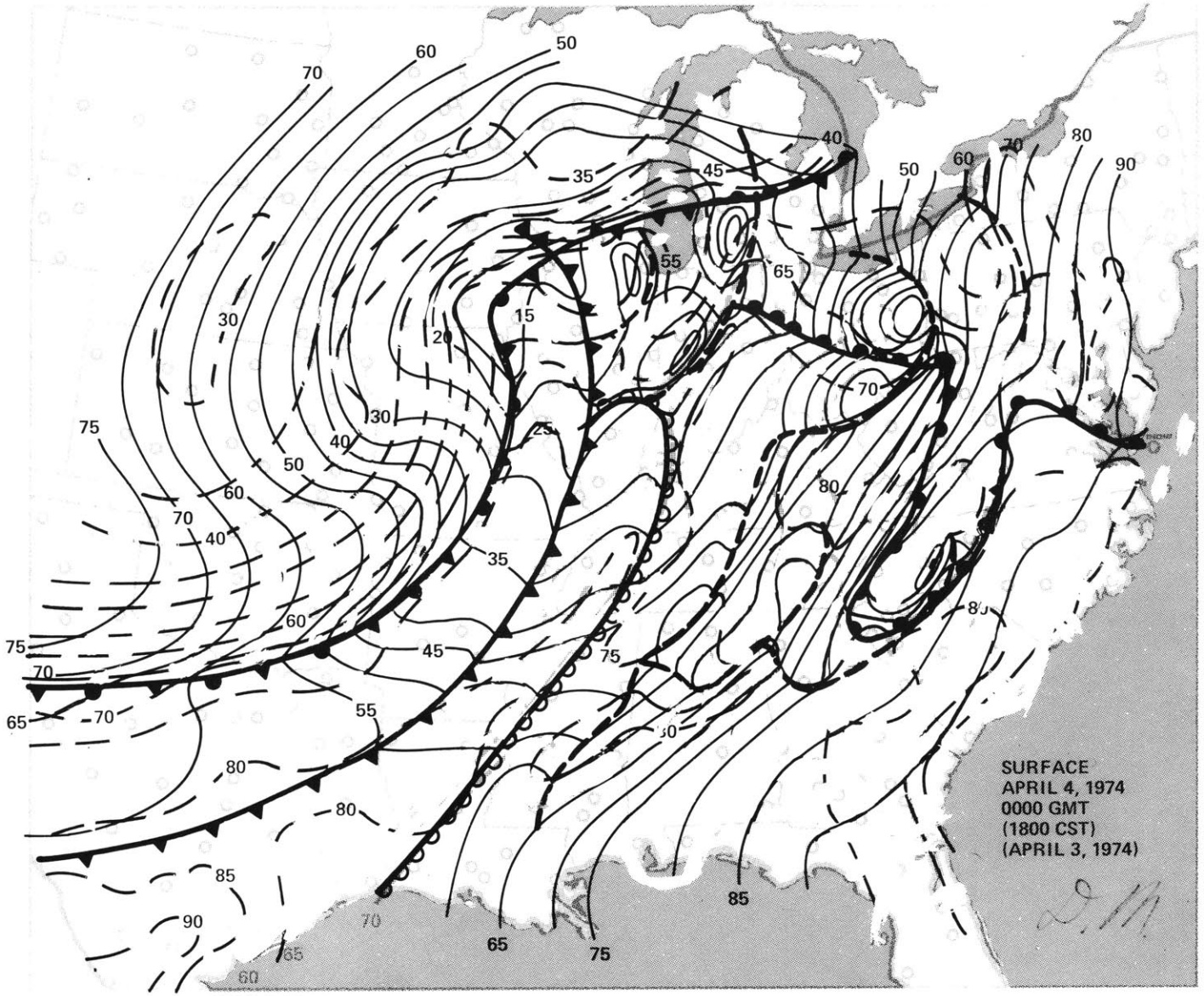

Fig. 1.12. Surface analysis, 0000Z April 4, 1974. See explanation opposite Fig. 1.8.

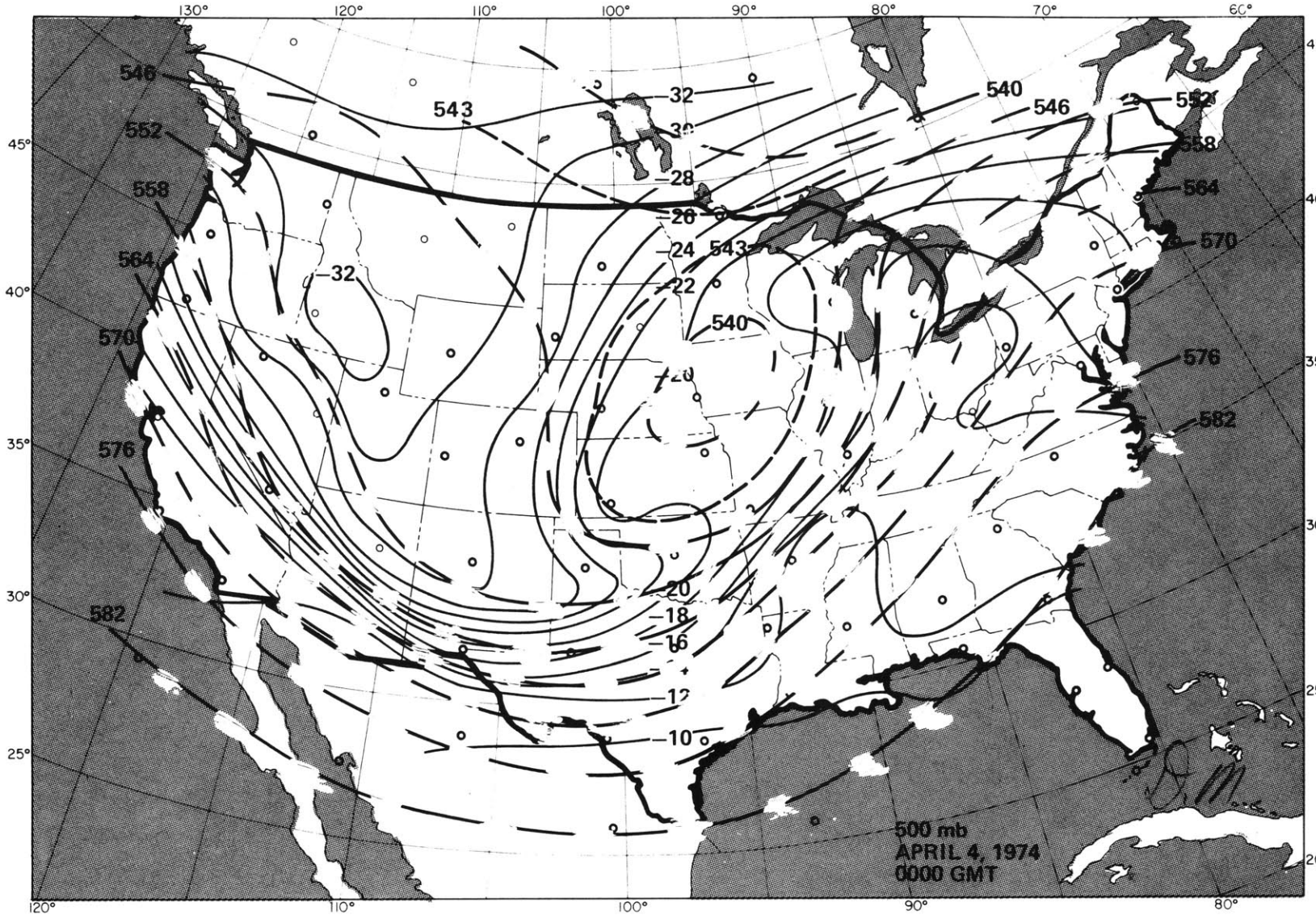

Fig. 1.13. 500mb analysis, 0000Z April 4, 1974. See legend for Fig. 1.1. (After Hoxit and Chappell, 1975).

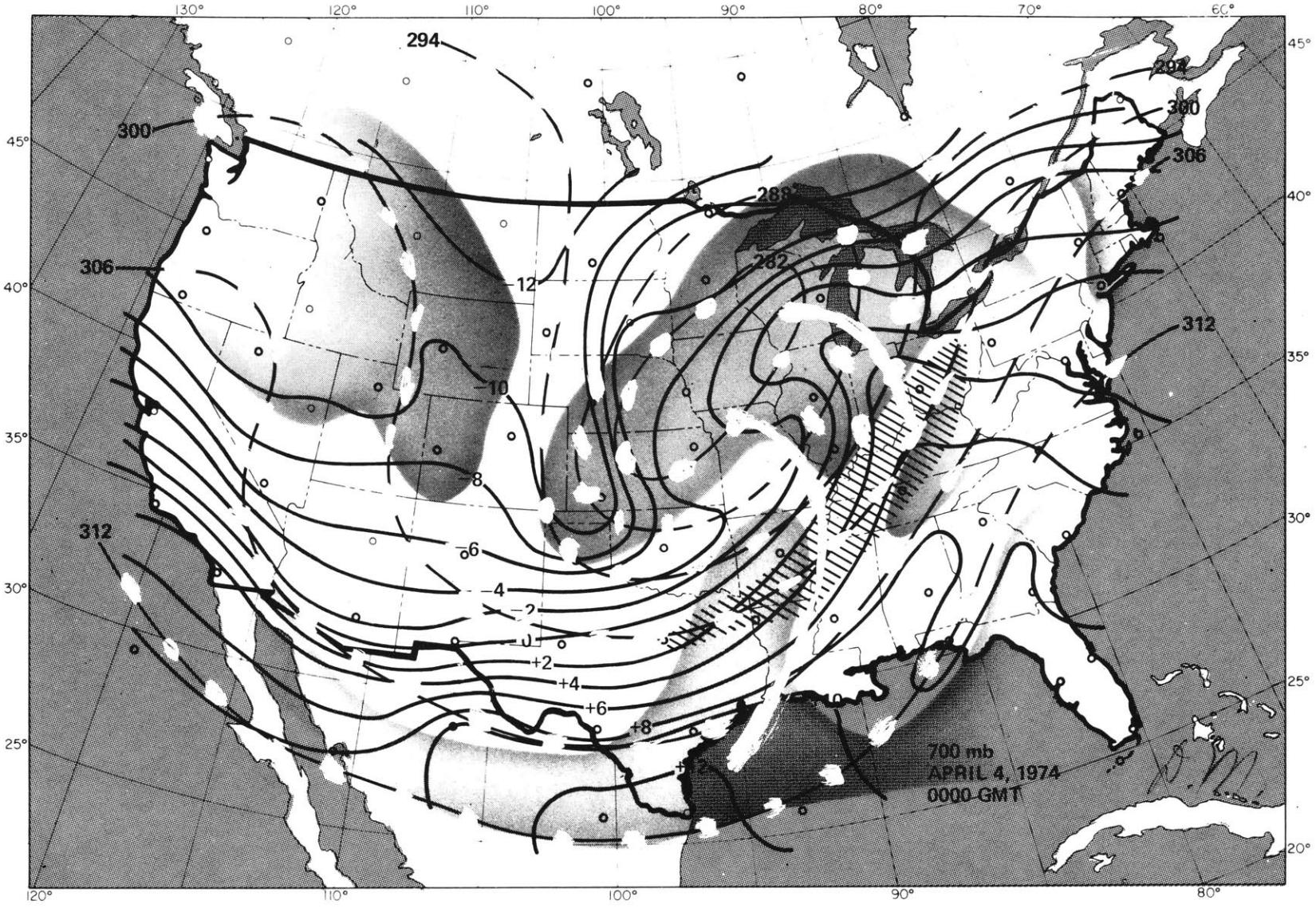

Fig. 1.14. 700mb analysis, 0000Z April 4, 1974. See legend for Fig. 1.2. (After Hoxit and Chappell, 1975).

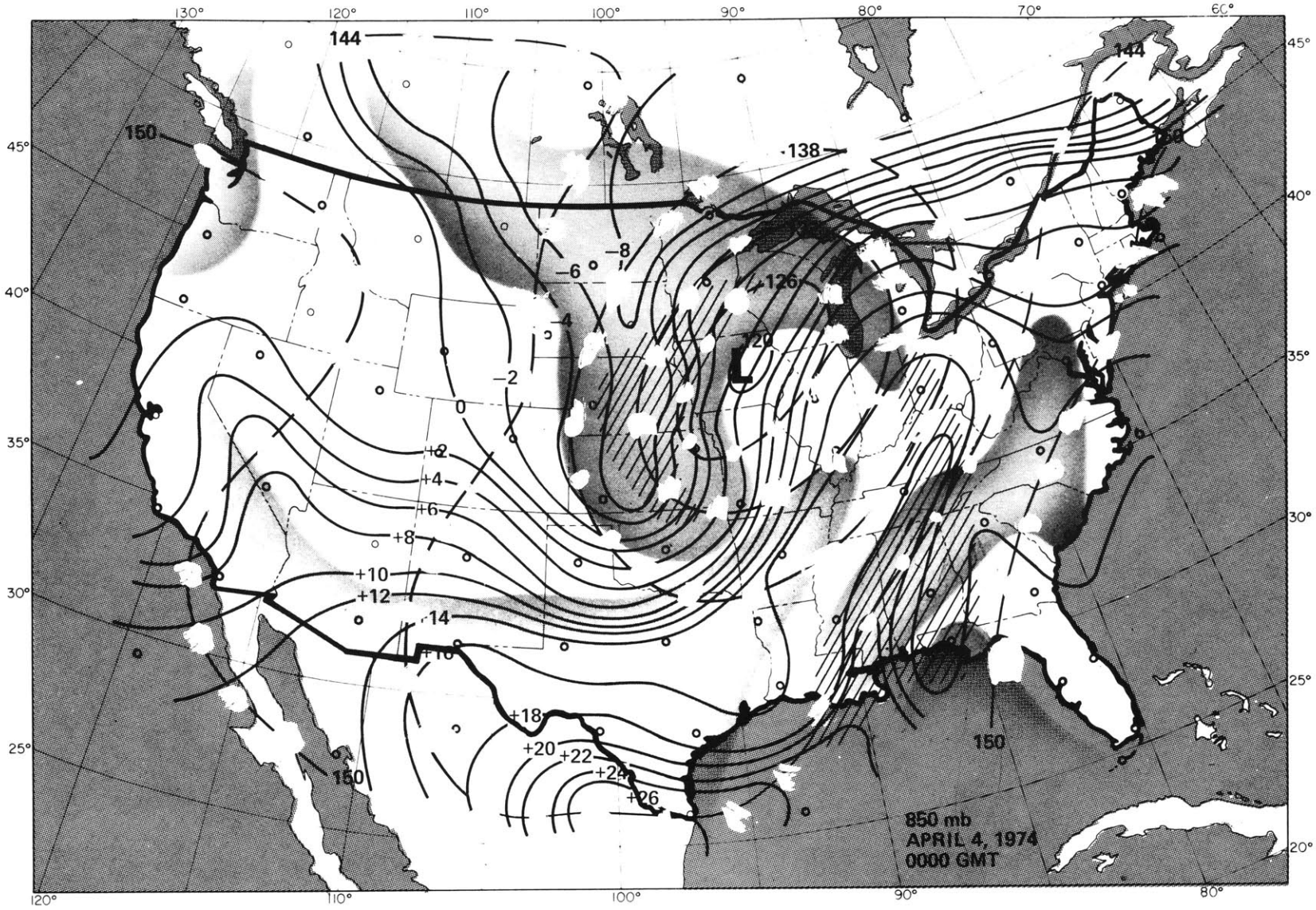

Fig. 1.15. 850mb analysis, 0000Z April 4, 1974. See legend for Fig. 1.3(After Hoxit and Chappell, 1975).

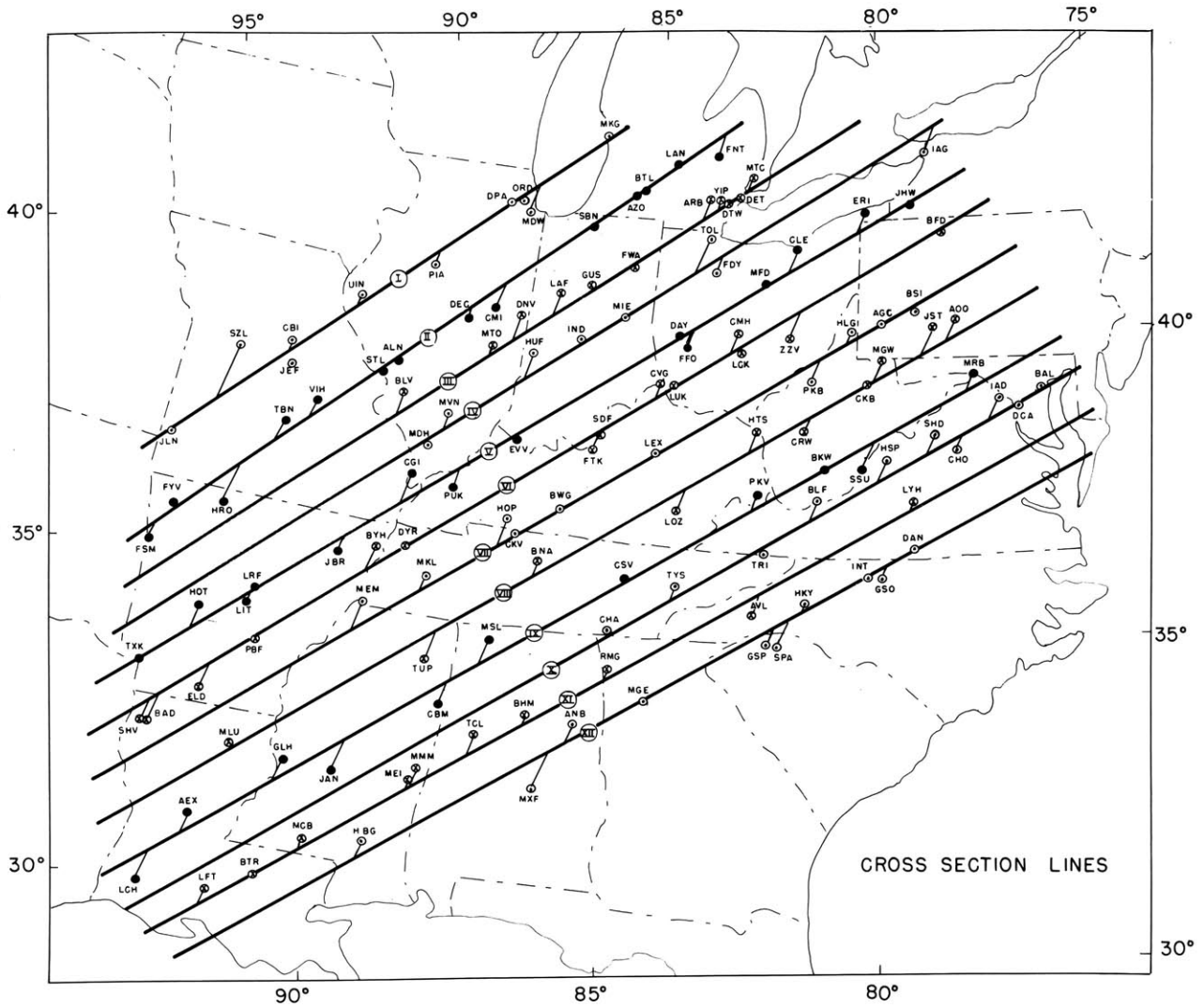

Fig. 2.1. Lines along which cross sections are constructed. Stations used to construct each line coded similarly.

Figs. 2.2a - 2.4a: Time cross sections: hourly pressure tendency and surface wind field, 3-4 April 1974. Pressure changes at intervals of .03 "hg/hr. Thin solid lines: positive tendency; thin dashed lines: negative tendency; thick solid lines: no pressure change. Wind barbs: short lines: 5 knots; longer lines : 10 knots; C ≡ calm. G followed by number is speed, in knots, to which wind is gusting.

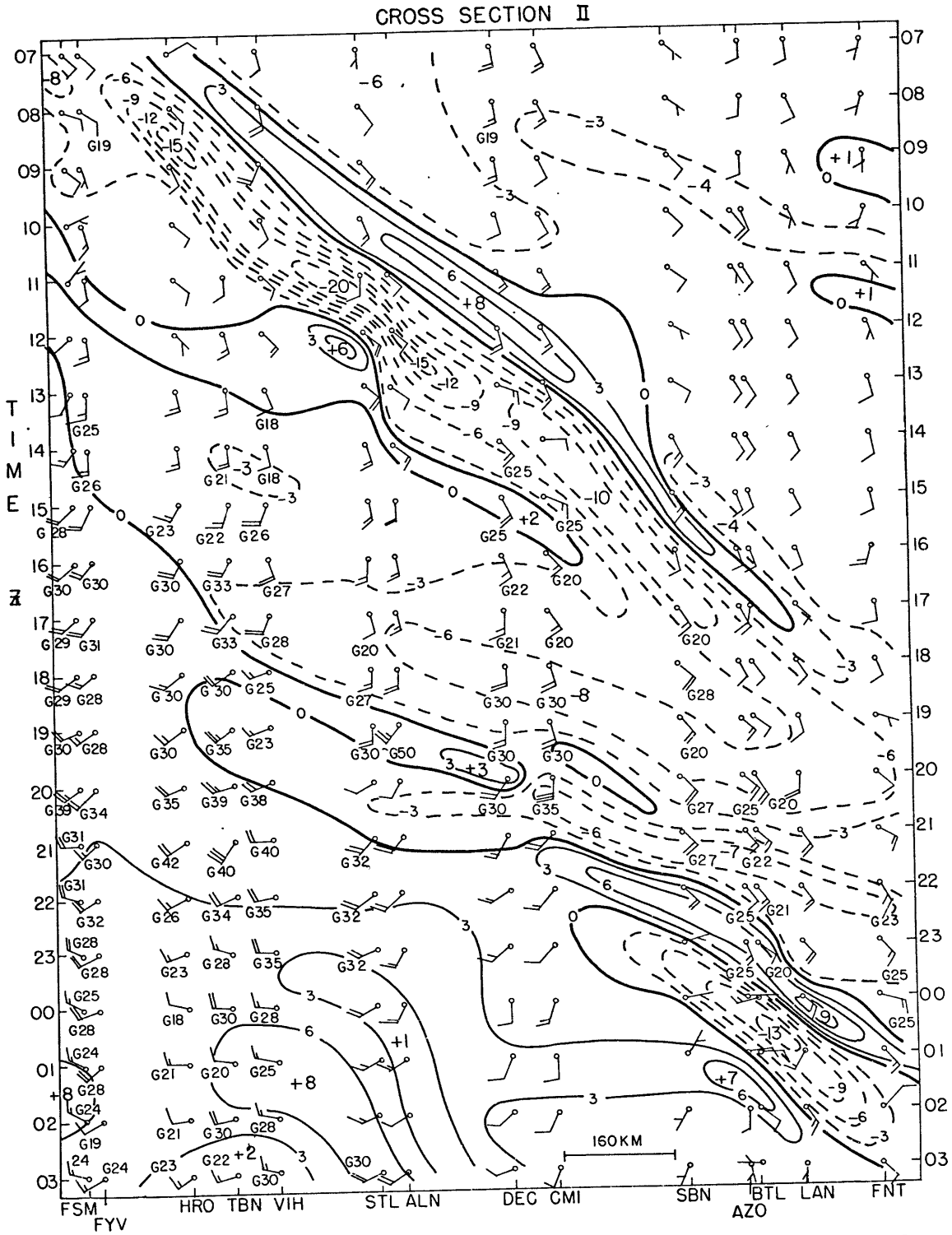

Fig. 2.2a. Time cross section II: hourly pressure tendency and surface wind field, 3-4 April, 1974. See opposite page .

Figs 2.2b - 2.4b: Time cross sections: hourly pressure tendency and surface weather, 3-4 April, 1974. Dot shaded regions: pressure change greater than +.03 "hg/hr; hatched regions: pressure change less than -.03 "hg/hr. Weather events: T ≡ thunder; R ≡ rain; RW ≡ rainshower; A ≡ hail; E preceded by above letters: that weather ends; straight thick diagonal lines: tornado tracks. Intensity: (--) ≡ very light; (-) ≡ light; ( ) ≡ moderate; (+) ≡ heavy.

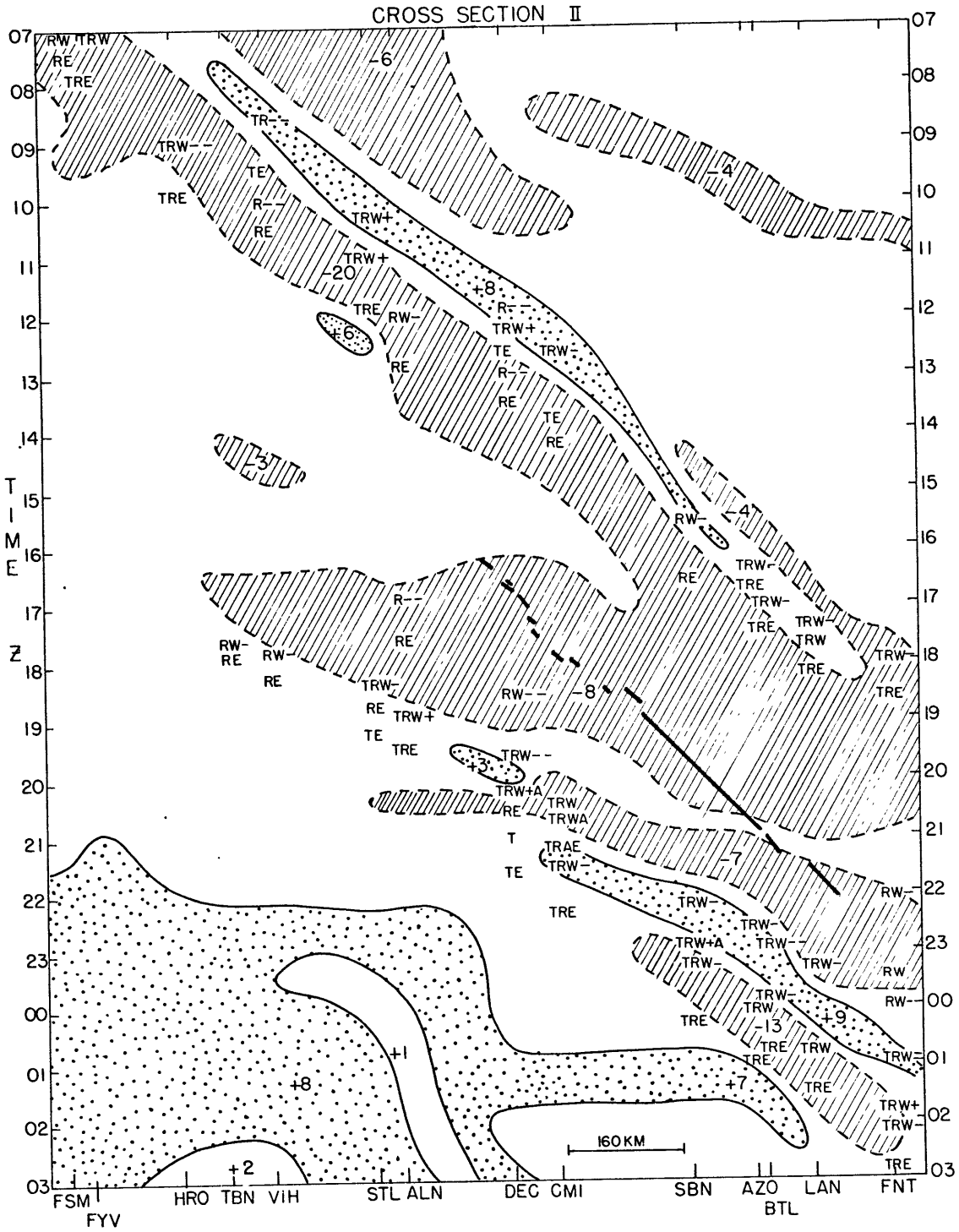

Fig. 2.2b. Time cross section II: hourly pressure tendency and surface weather, 3-4 April, 1974. See opposite page.

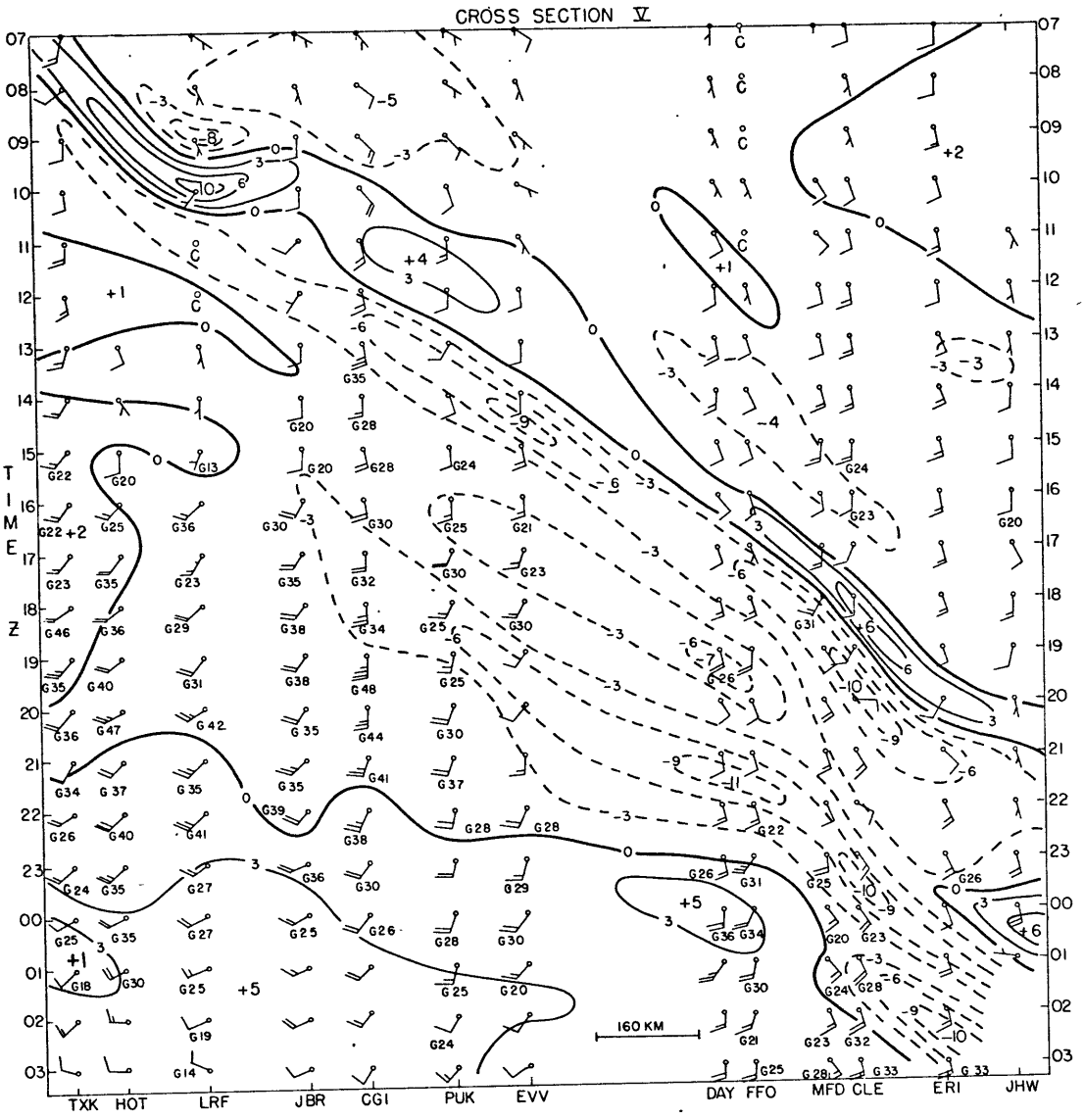

Fig. 2.3a: Time cross sectionV: hourly pressure tendency and surface wind field, 3 - 4 April, 1974. See explanation opposite Fig. 2.2a.

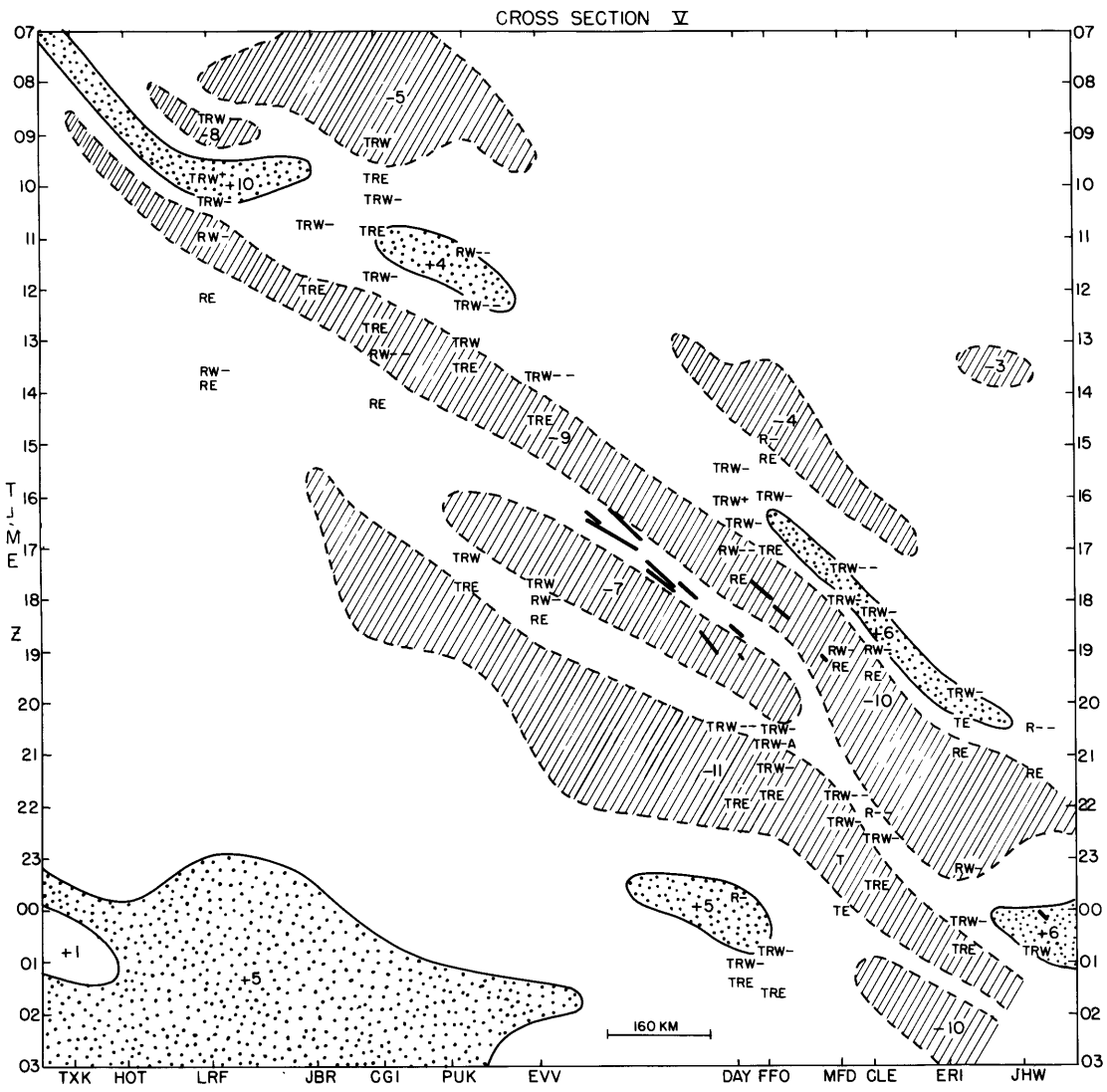

Fig. 2.3b: Time cross section V: hourly pressure tendency and surface weather, 3-4 April, 1974. See explanation opposite Fig. 2.2b.

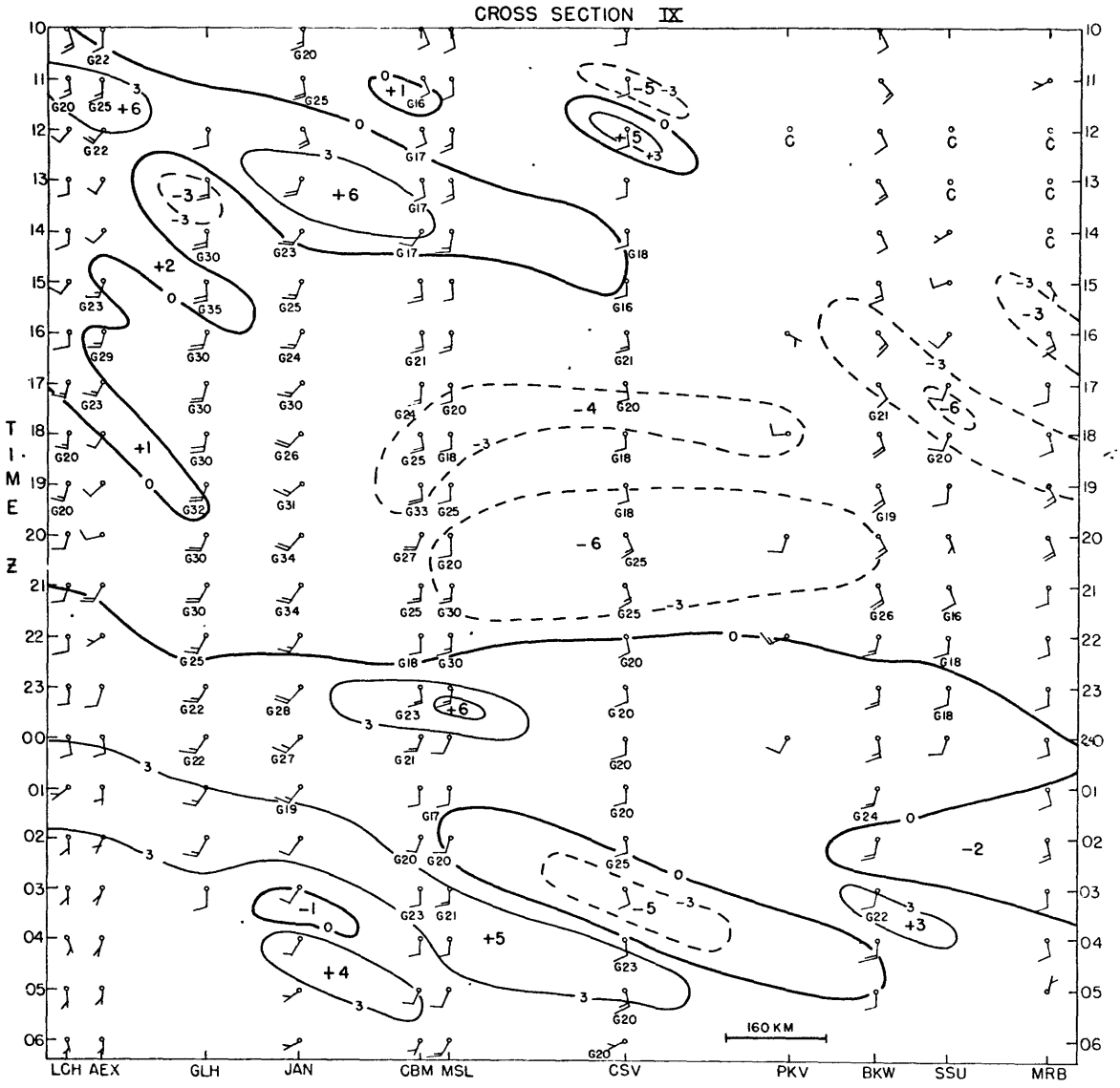

Fig. 2.4a: Time cross section IX: hourly pressure tendency and surface wind field, 3-4 April, 1974. See explanation opposite Fig. 2.2a.

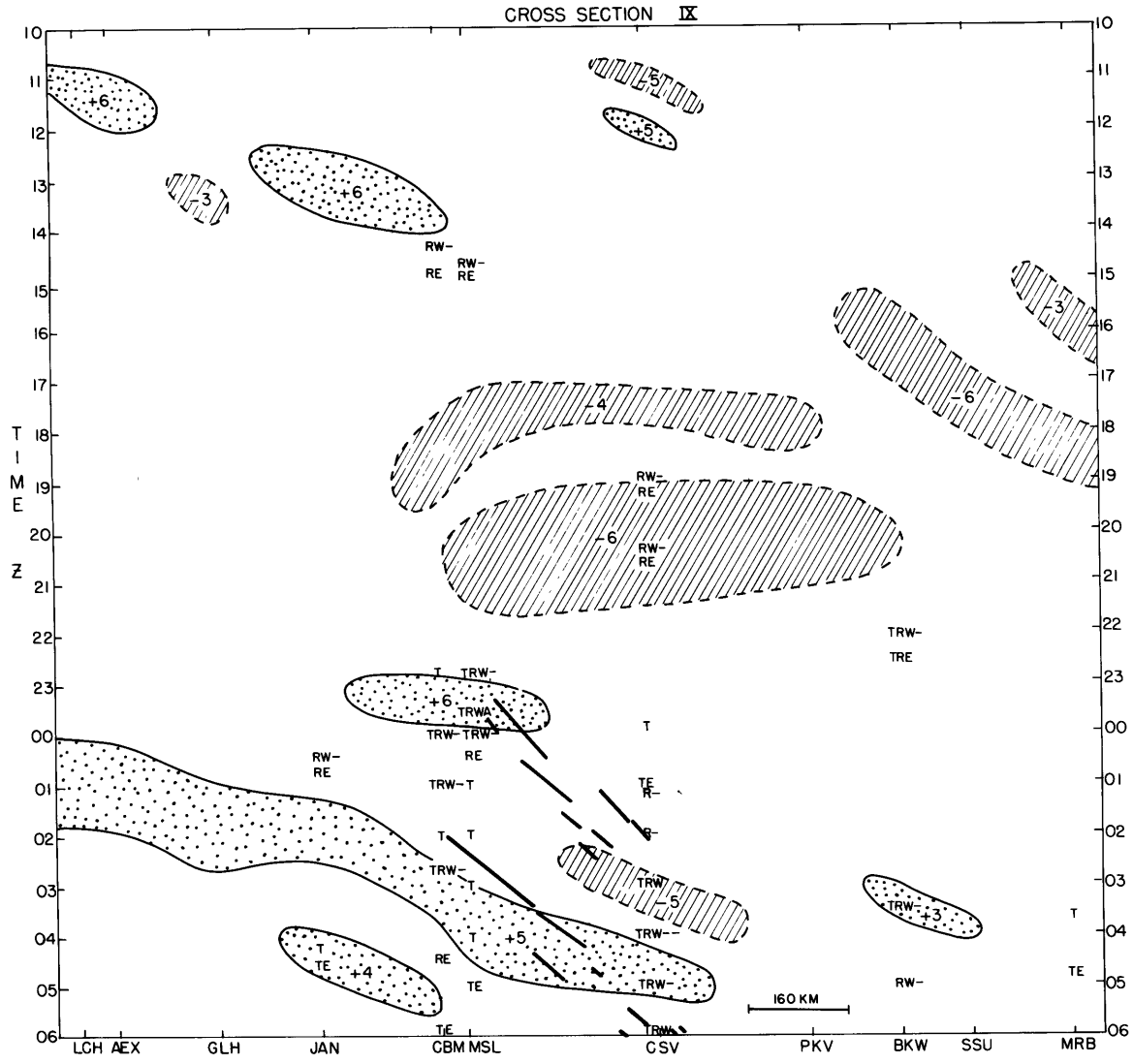

Fig. 2.4b: Time cross section IX: hourly pressure tendency and surface weather, 3-4 April, 1974. See explanation opposite Fig. 2.2b.

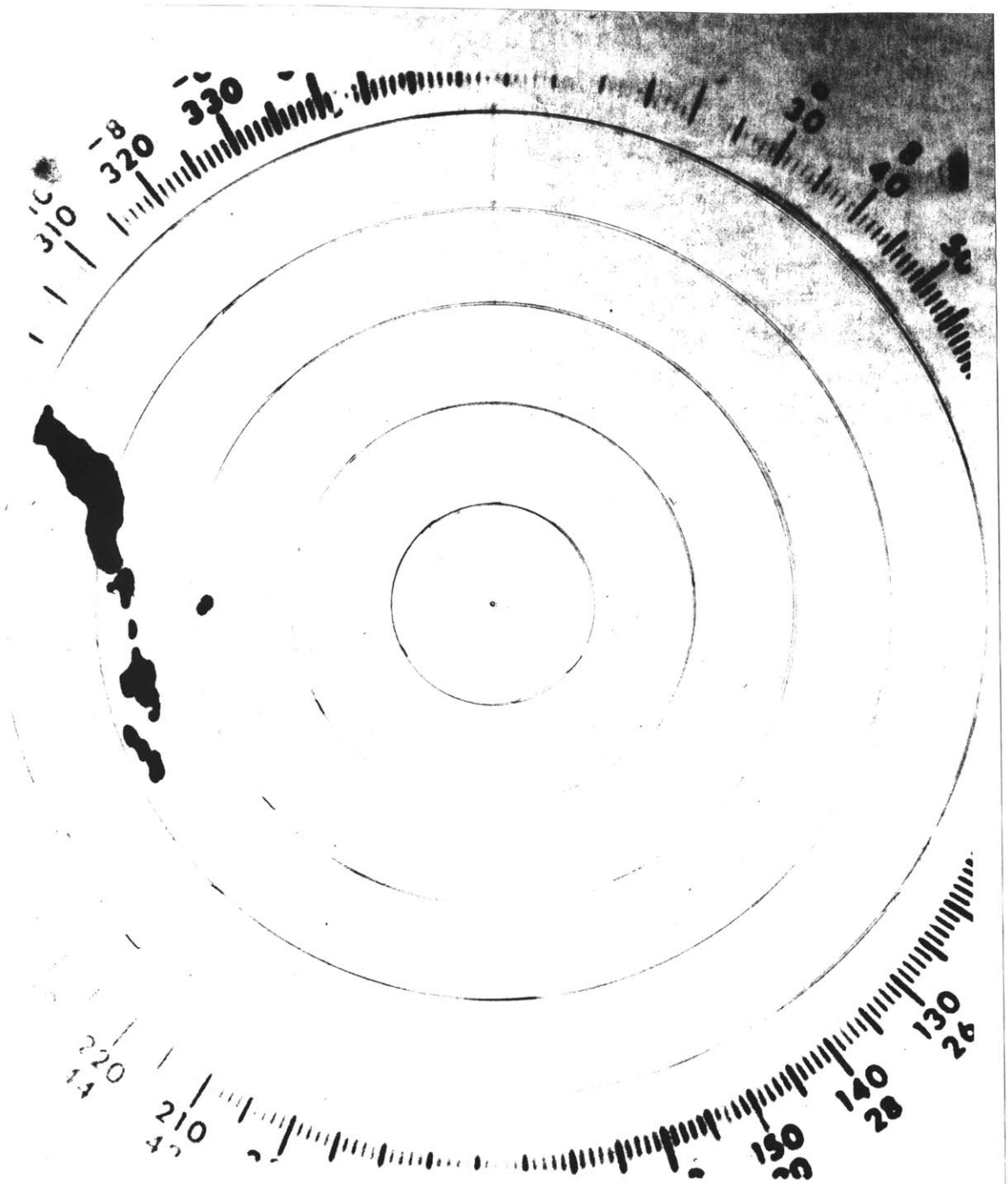

Fig. 2.5: Character of convection in Ohio Valley region associated with the morning pressure perturbation activity, (1325Z), as seen from radar at Cincinnati (CVG). Radar echoes are dark regions. Each ring denotes a 25 n. mile (46km) radius; total radius is 125 n. miles (230 km) .

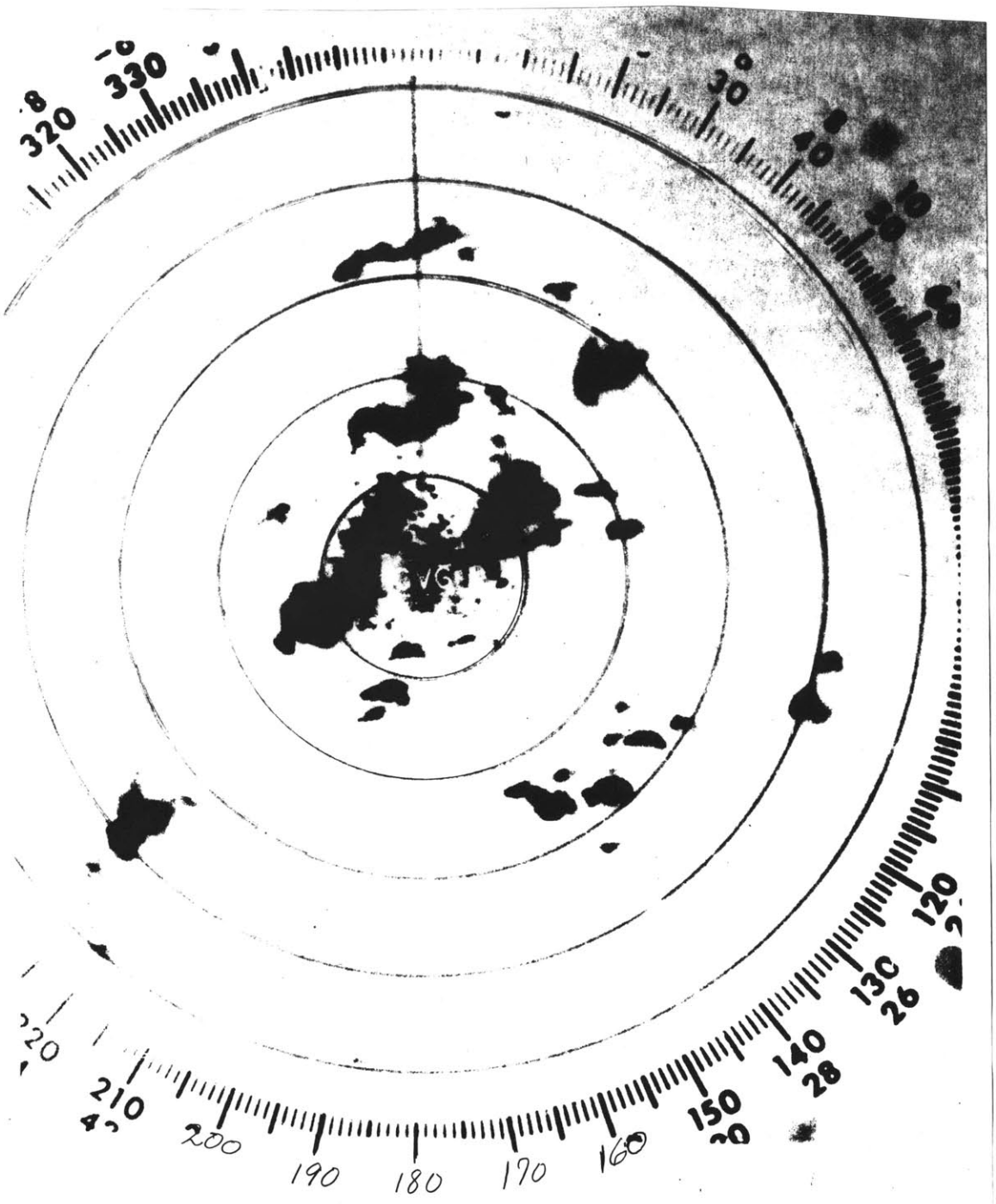

Fig. 2.6. Character of convection in Ohio Valley region at peak of storm activity (2100Z), as seen from radar at Cincinnati (CVG). Radar echoes are dark regions. Each ring denotes a 25 n. mile (46km) radius; total radius is 125 n. miles (230km).

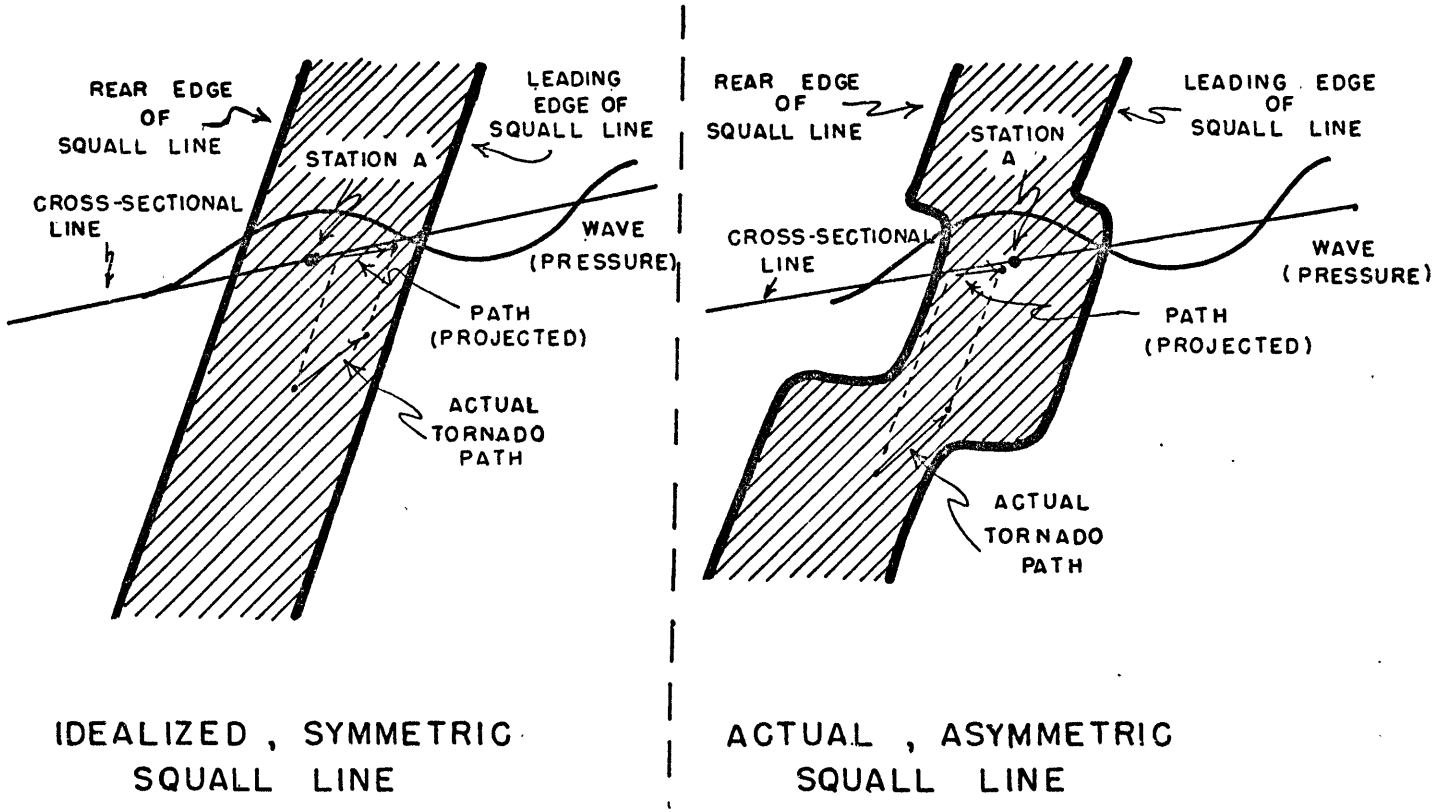

Fig. 2.7. Schematic representation of explanation for why a possibly existing relationship between mesoscale pressure tendency and tornado locations may not have been revealed with analysis technique employed. Wave depicts mesoscale pressure perturbation (p') from synoptic mean; shaded region corresponds to radar echo, in a quite idealized view.

Figs. 3.1-3.4: Life histories of major mesoscale pressure waves. Solid lines show hourly positions of troughs. Dots correspond to stations which experienced each wave (i.e. recorded a pressure oscillation). Numbers above and to right of dots denote the amplitude of each wave (as defined in text), in hundredths of inches of mercury; letters below dots indicate weather recorded at station with wave passage, as explained in legend for Figs. 2.2b-2.4b. 'N' indicates no rain, thunder, etc. reported.

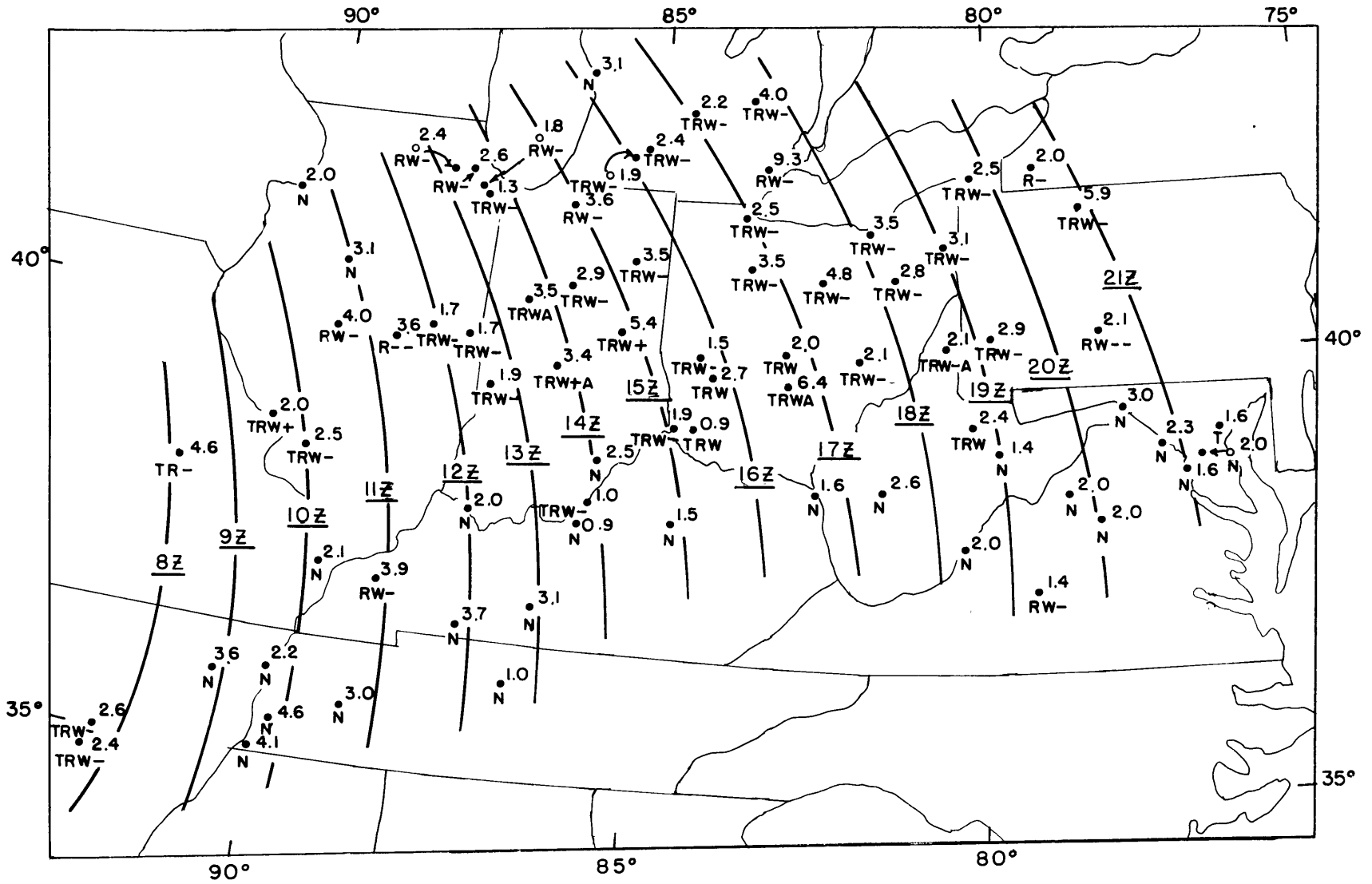

Fig. 3,1: Life history of "Wave No. 1". See opposite page.

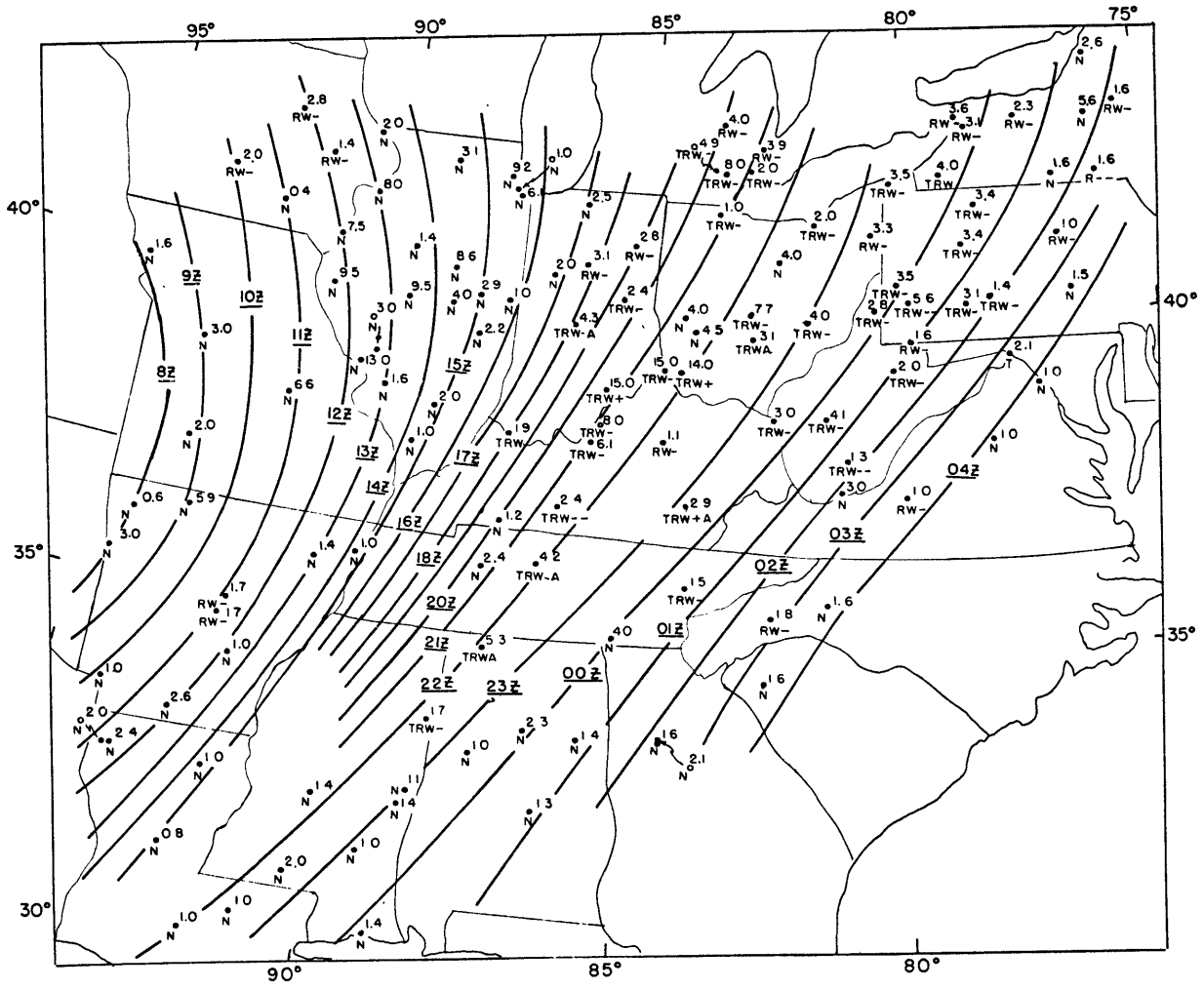

Fig. 3.2. Life history of "Wave No. 2". See explanation opposite Fig. 3.1. Note: position of trough at 2200Z denotes approximate position of a stationary squall line from 2200Z April 3 to 0400Z April 4.

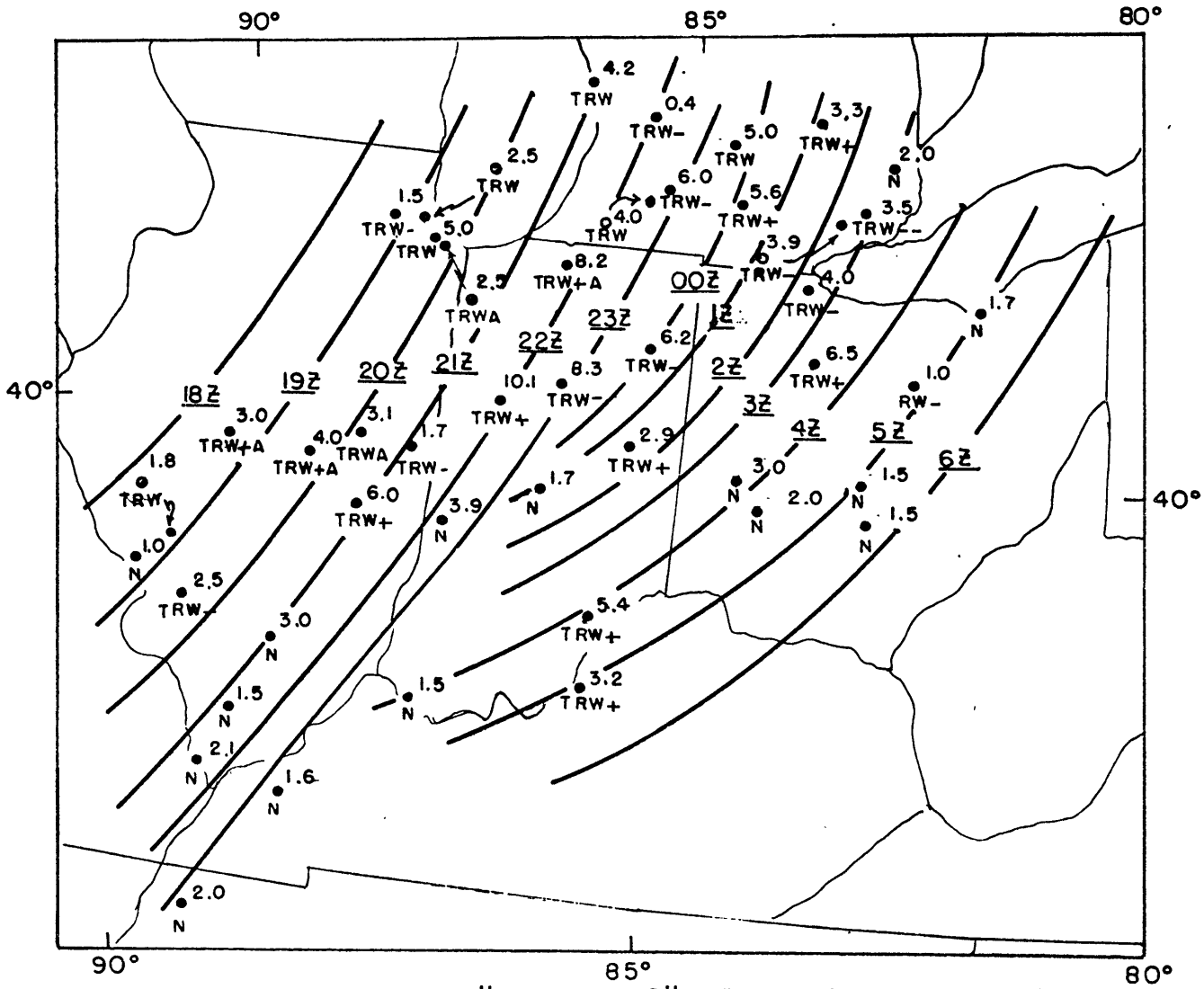

Fig. 3.3. Life history of "Wave No. 3". See explanation opposite Fig. 3.1

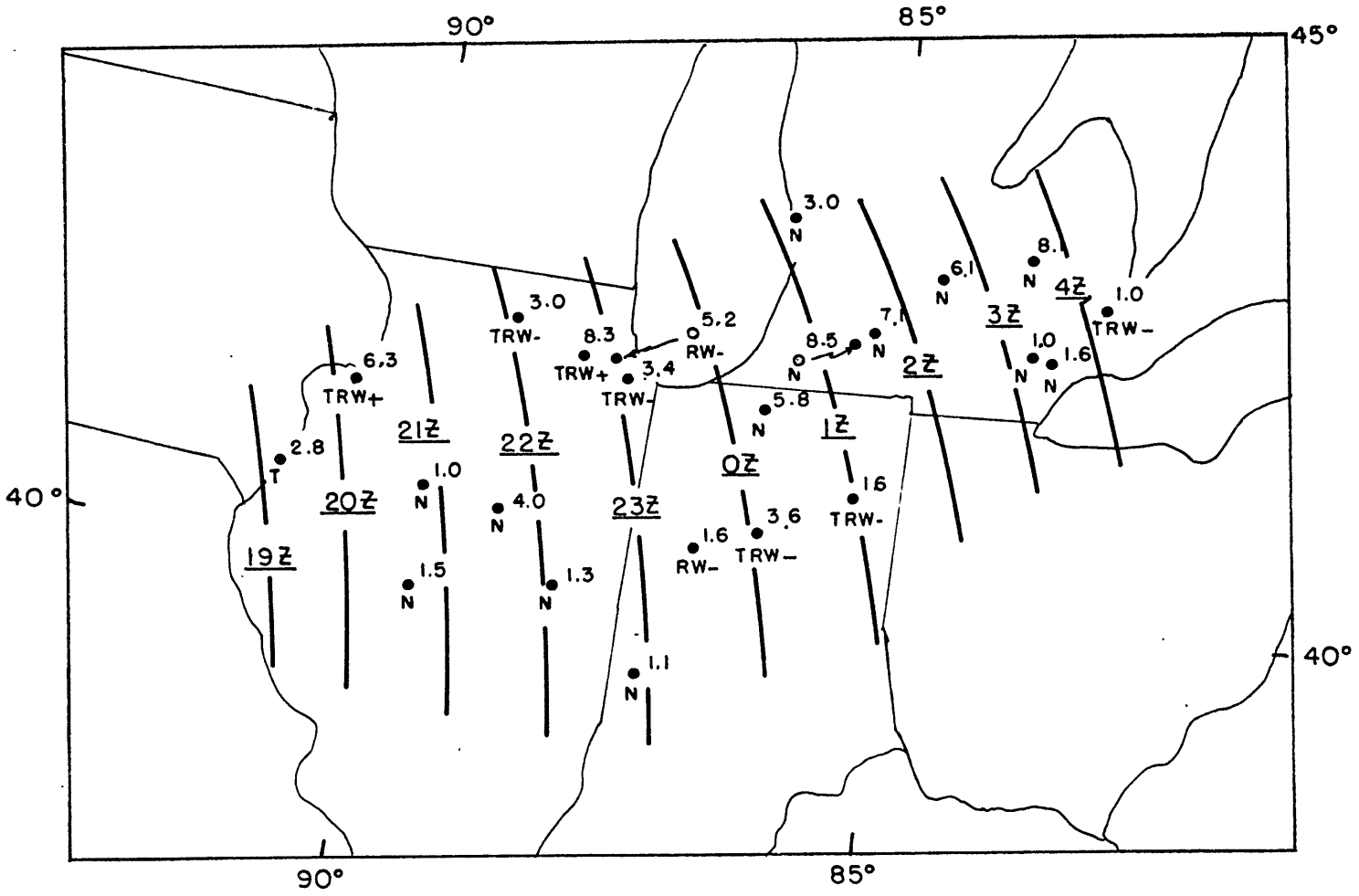

Fig. 3.4 Life history of "Wave No, 4". See explanation opposite Fig. 3.1

Figs. 3.5a -f: Transformation of squall line (associated with "Wave No. 2") into two major bands of convection, as seen from radar at Nashville, Tennessee (BNA). Those convective cells (dark regions) which constitute the trailing "squall line" are marked by an "x" to their north. Each ring denotes a 25 n.mile (46km) radius. Total radius is 125 n. miles (230km)

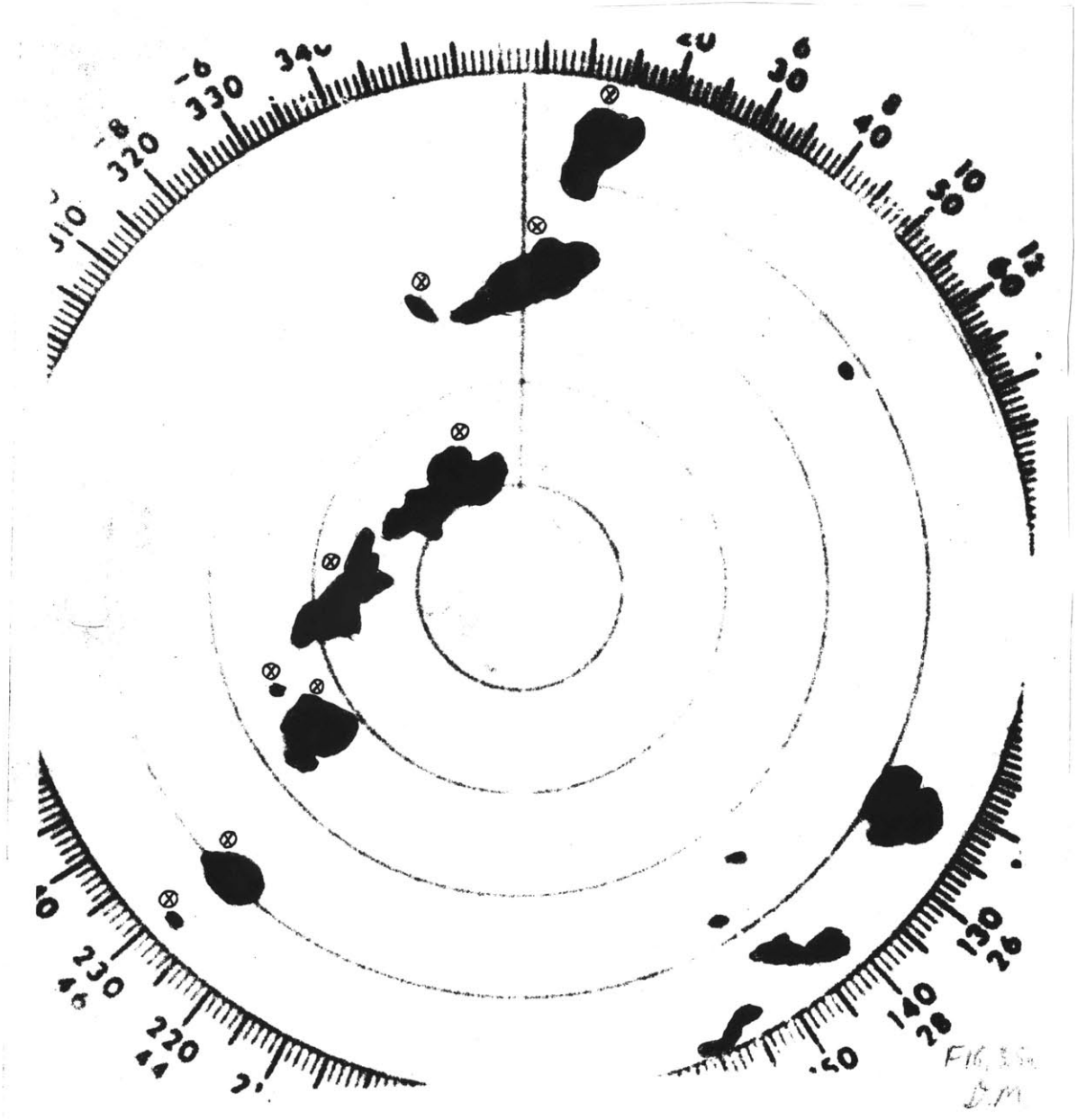

Fig. 3.5a. BNA echoes at 2100Z April 3, 1974. See opposite page.

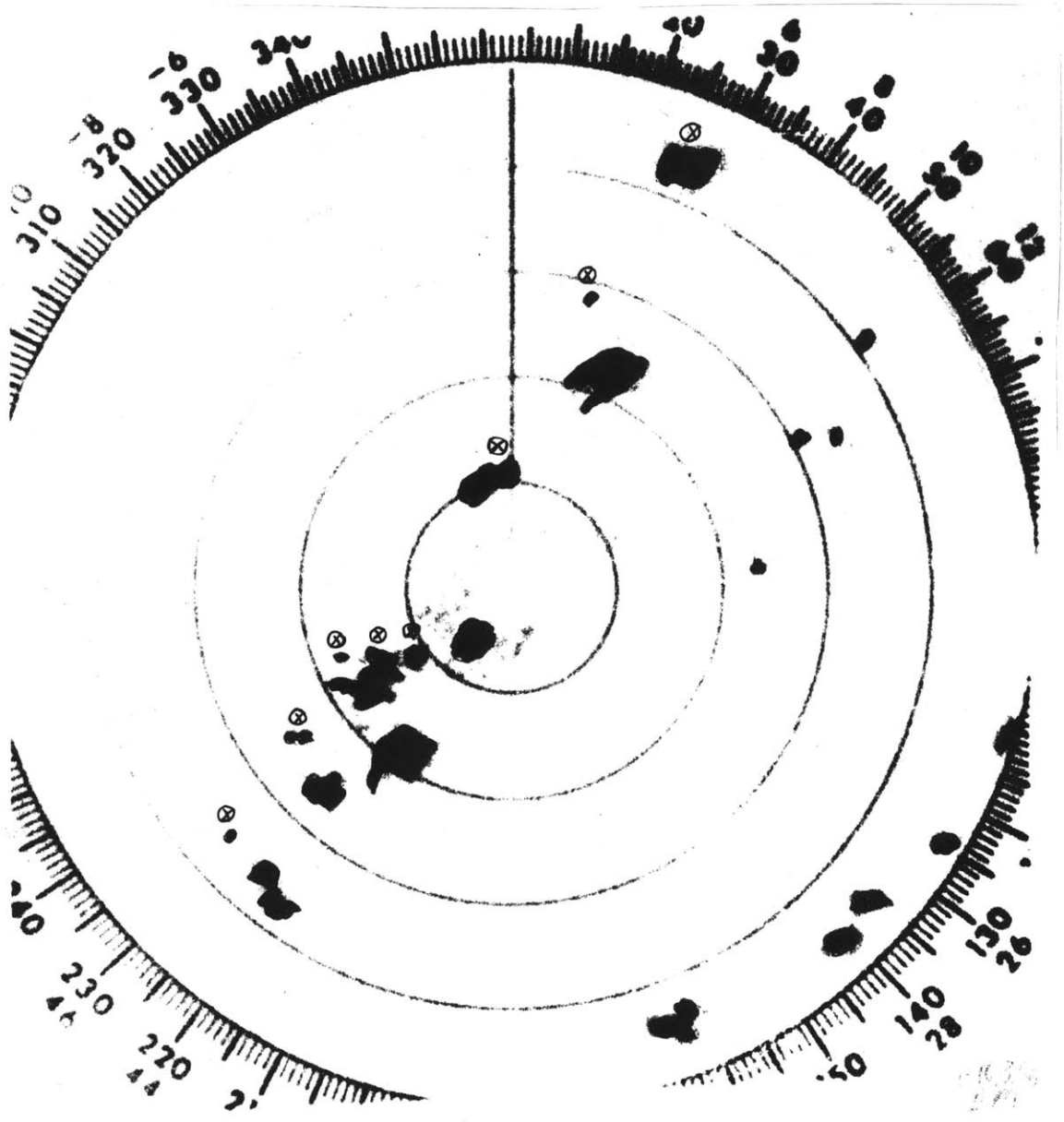

Fig. 3.5b. BNA radar echoes at 2200Z April 3, 1974.
See explanation opposite Fig. 3.5a.

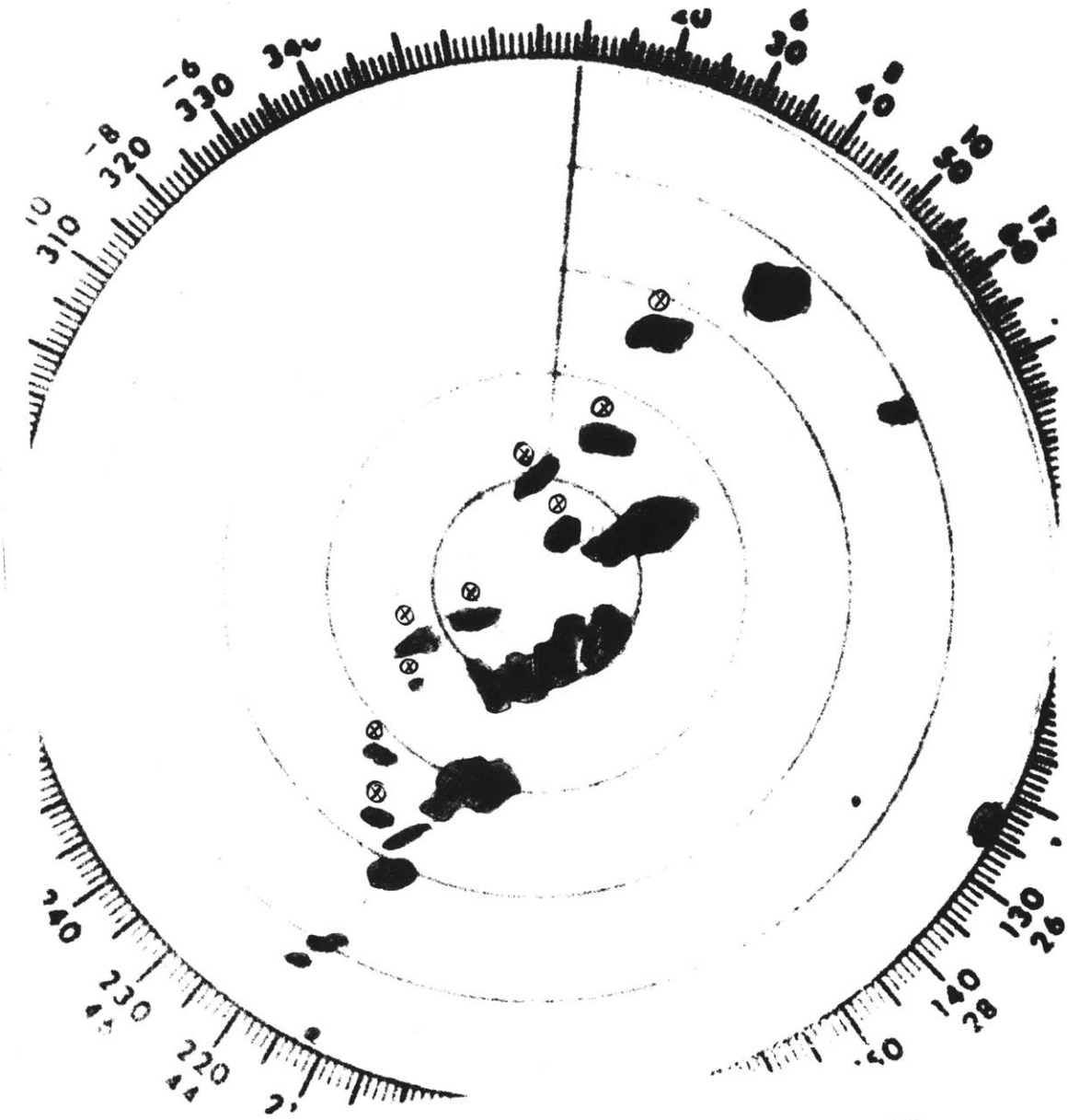

Fig. 3.5c. BNA radar echoes at 2300Z April 3, 1974. See explanation opposite Fig. 3.5a.

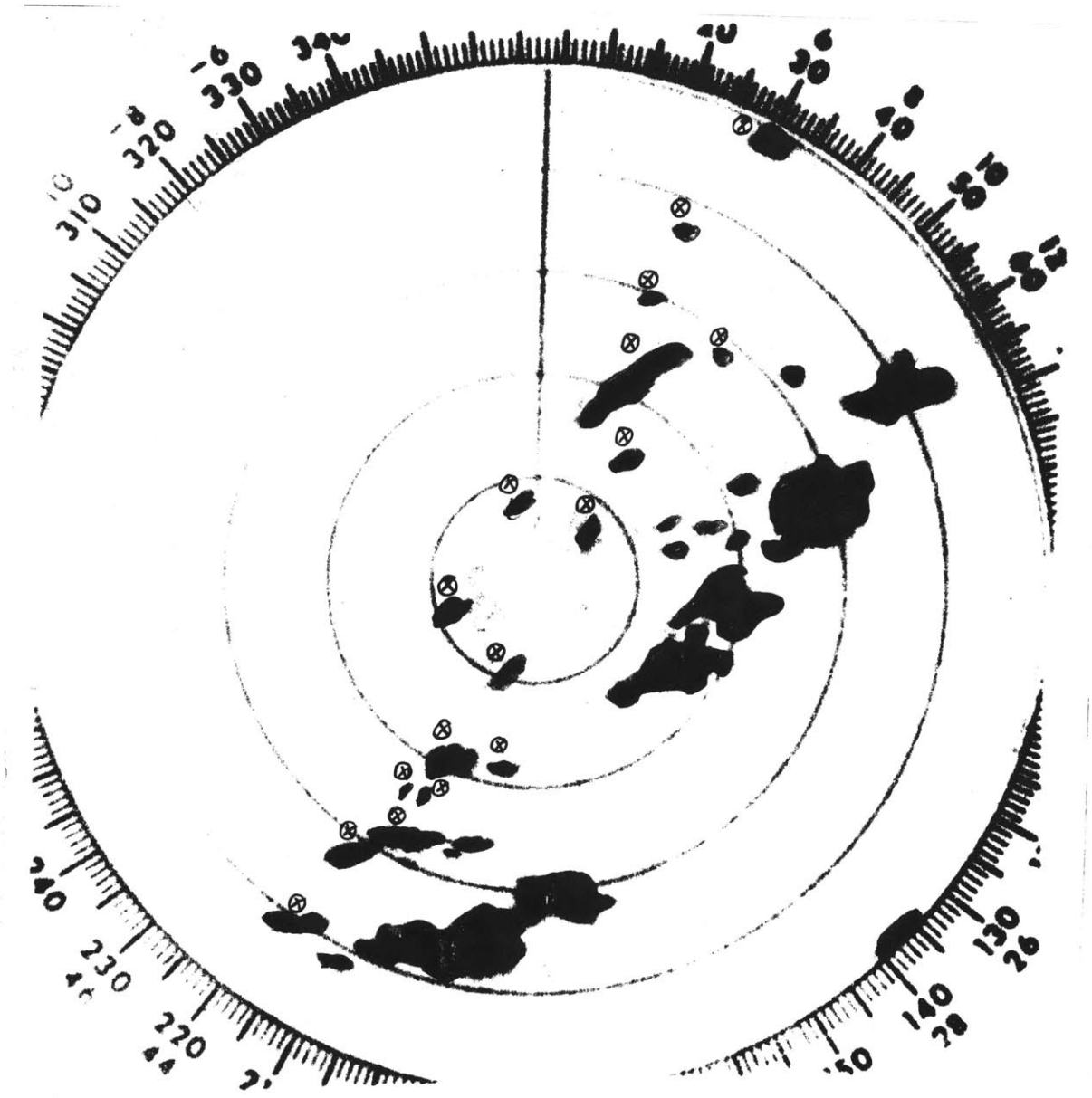

Fig. 3.5d. BNA radar echoes at 0000Z April 4, 1974. See explanation opposite Fig. 3.5a.

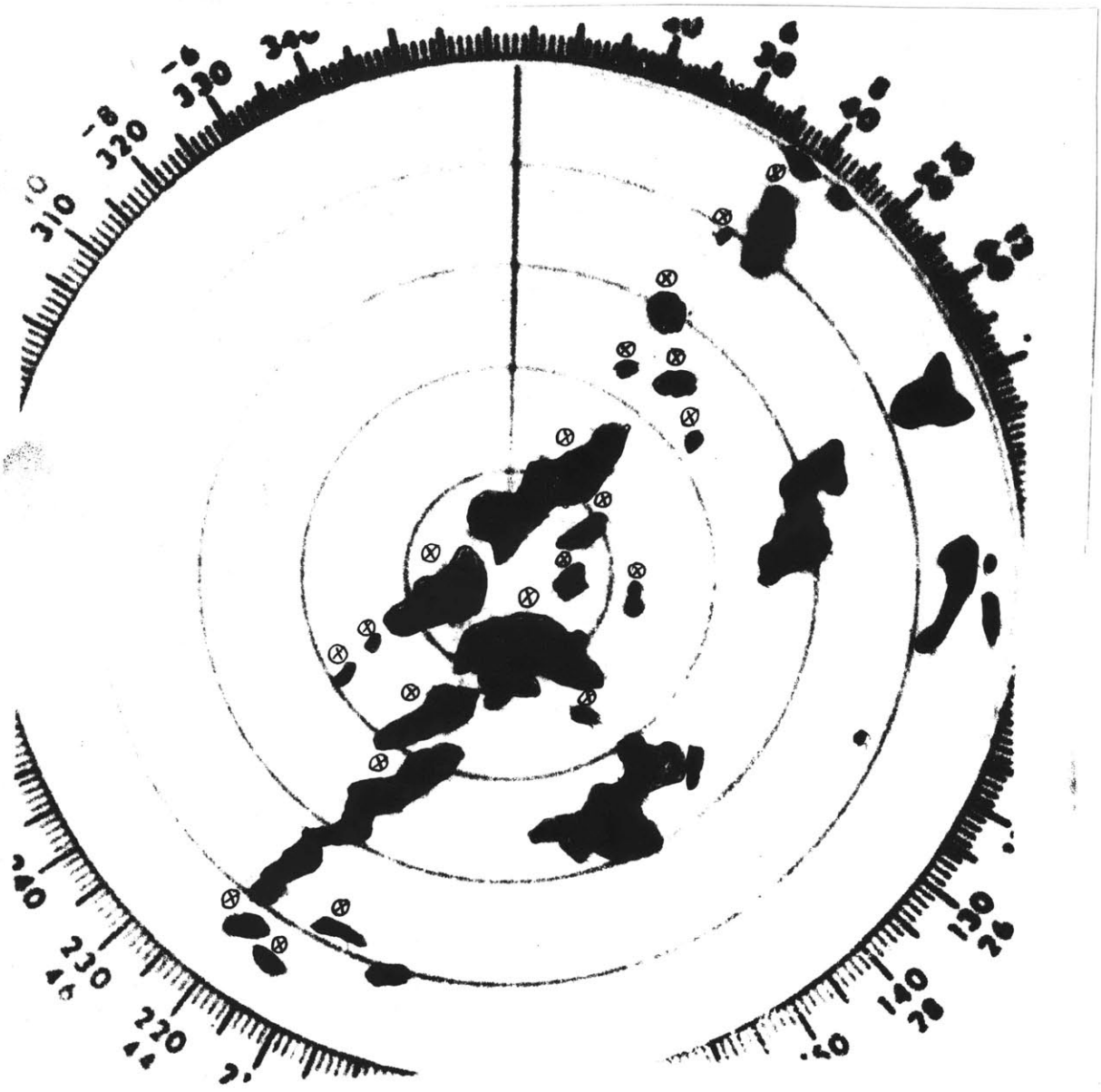

Fig. 3.5e. BNA radar echoes at 0130Z April 4, 1974. See explanation opposite Fig. 3.5a.

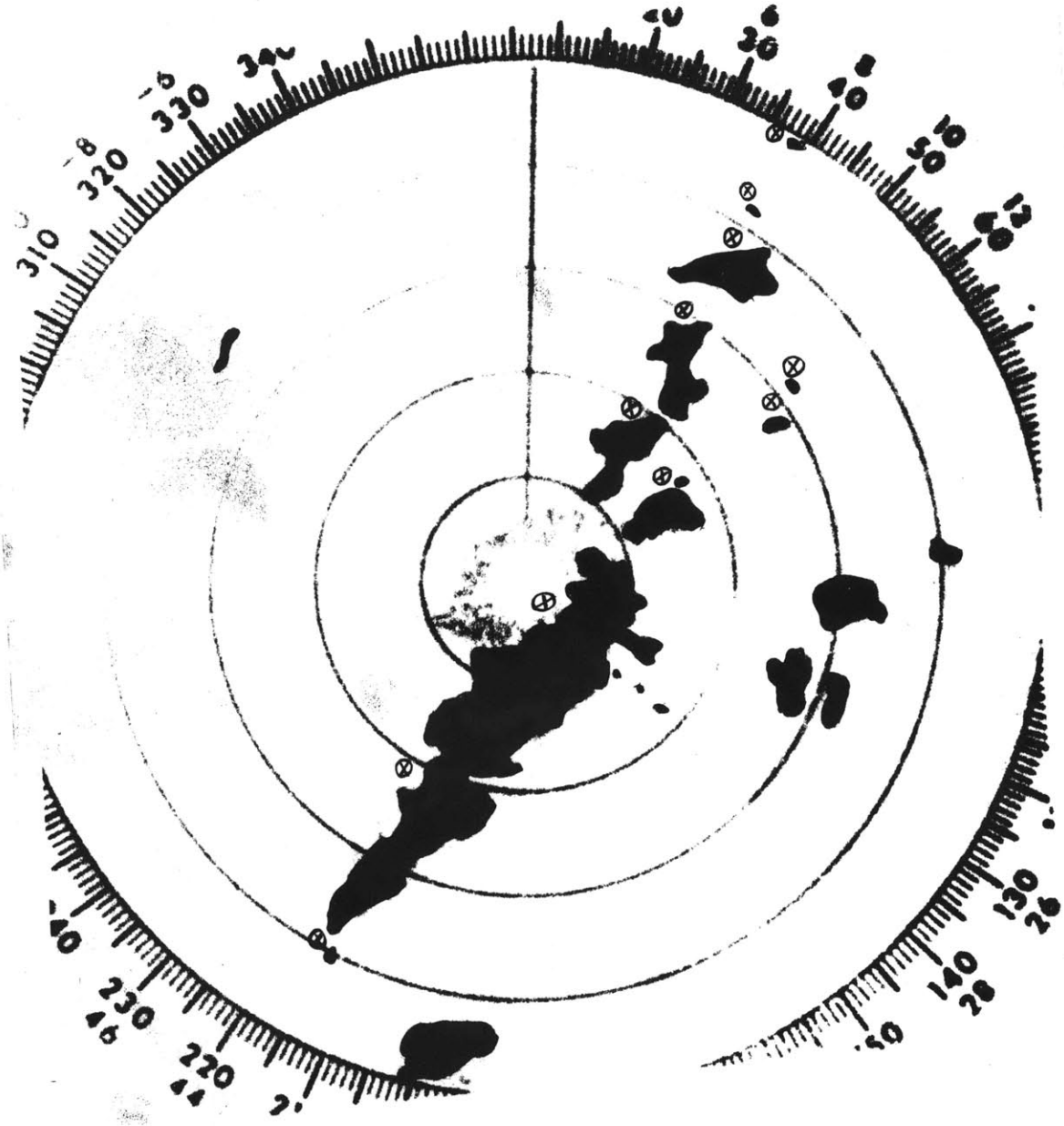

Fig. 3.5f. BNA radar echoes at 0300Z April 4, 1974. See explanation opposite Fig. 3.5a.

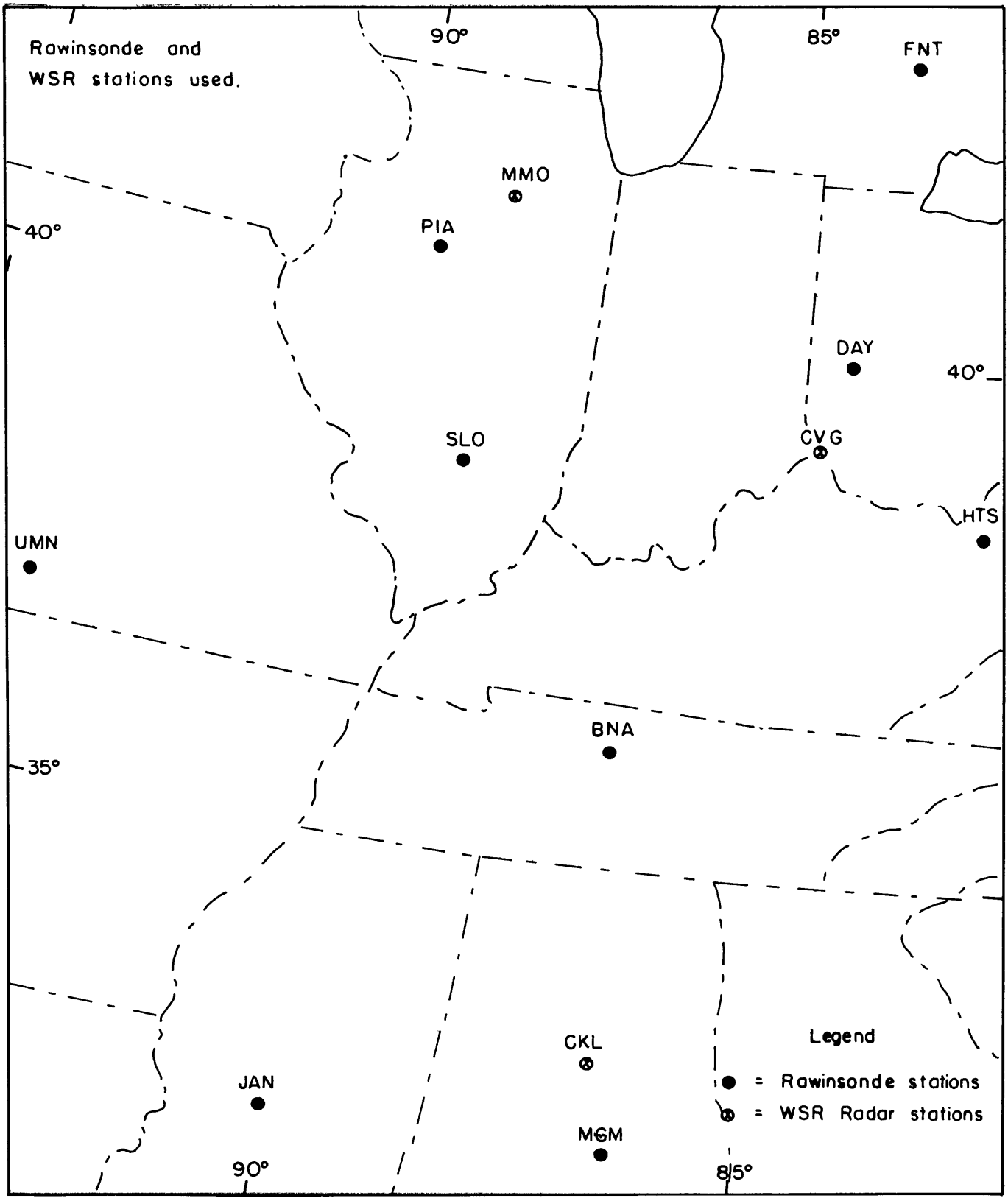

Fig. 4.1: Locations of stations for which soundings are depicted (colored dots) and for which radar photographs are displayed (circles enclosing x's).

Figs. 4.2-4.12: Atmospheric soundings, 1200Z April 3 and 0000Z April 4, 1974. Inset, lower left, is upper air sounding. Thin solid line is a dry adiabat (θ = 309°K); thin dashed line is a moist adiabat; Thick solid line is temperature; Thick dashed line is dewpoint temperature. On right (and on left in inset) is vertical profile of wind, with direction in degrees from north followed by speed in knots. (From pseudo-adiabatic diagram).

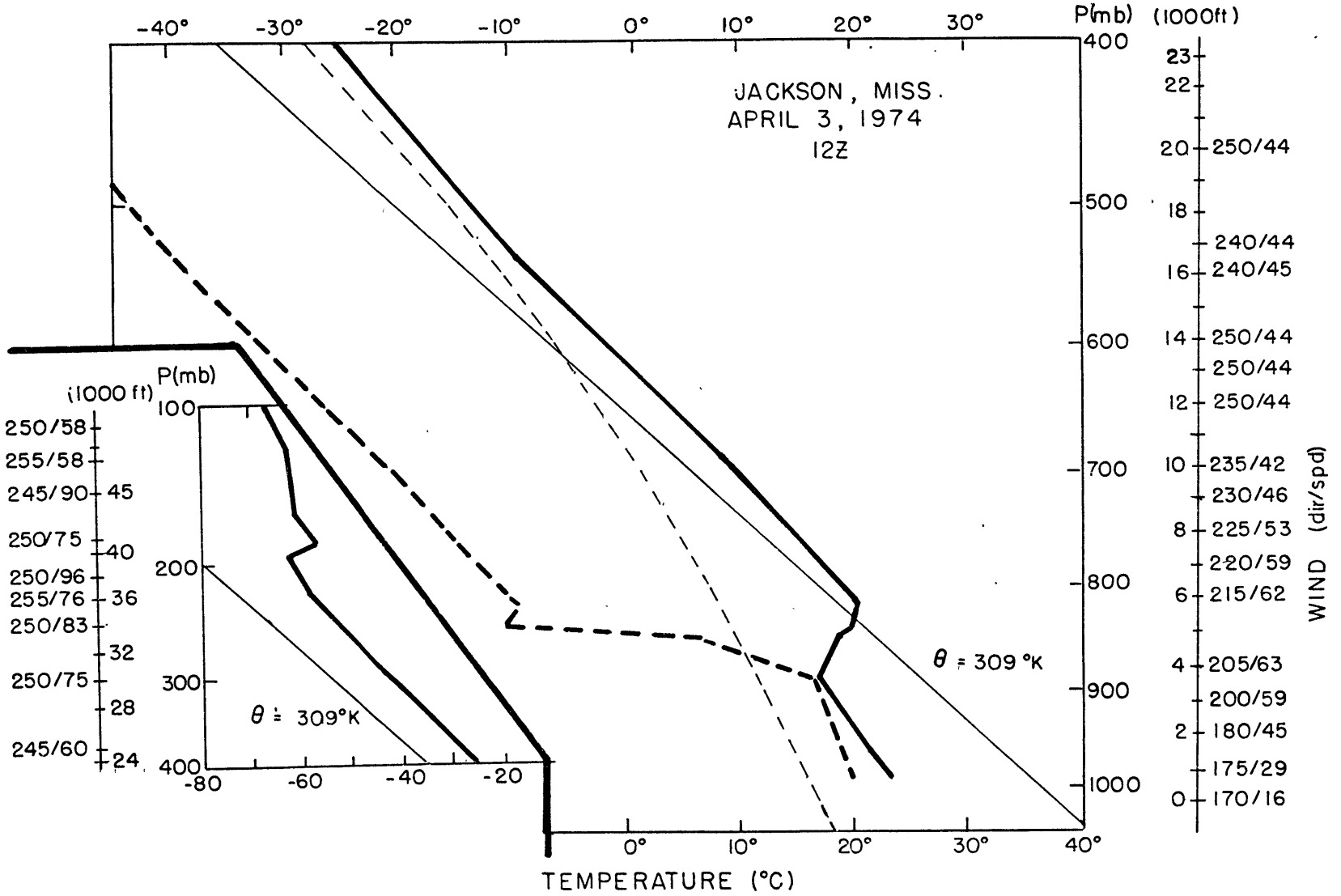

Fig. 4.2: Atmospheric sounding for Jackson, Mississippi (JAN), 1200Z April 3, 1974. See opposite page.

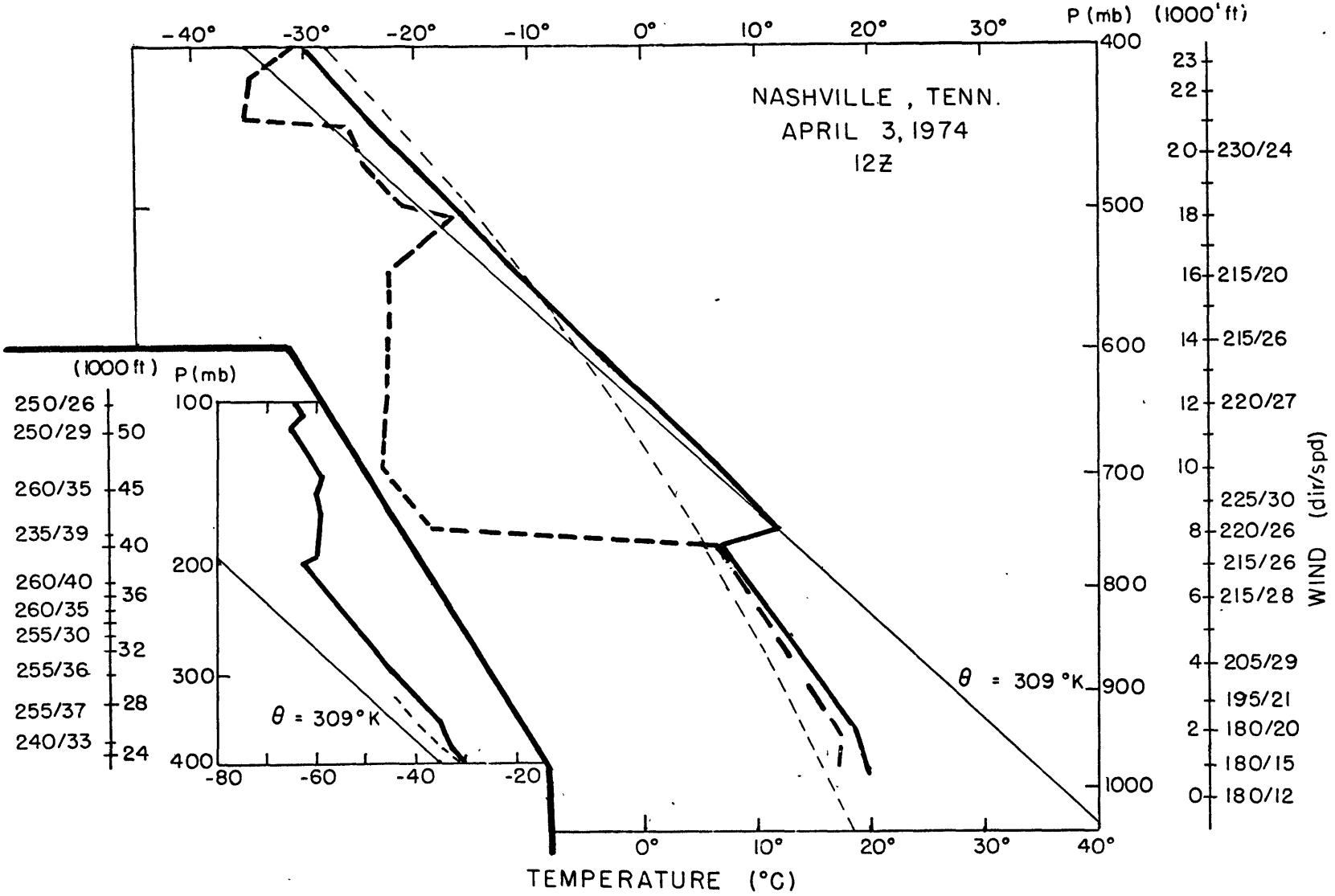

Fig. 4.3: Atmospheric sounding for Nashville, Tennessee (BNA), 1200Z April 3, 1974. See explanation opposite Fig. 4.2.

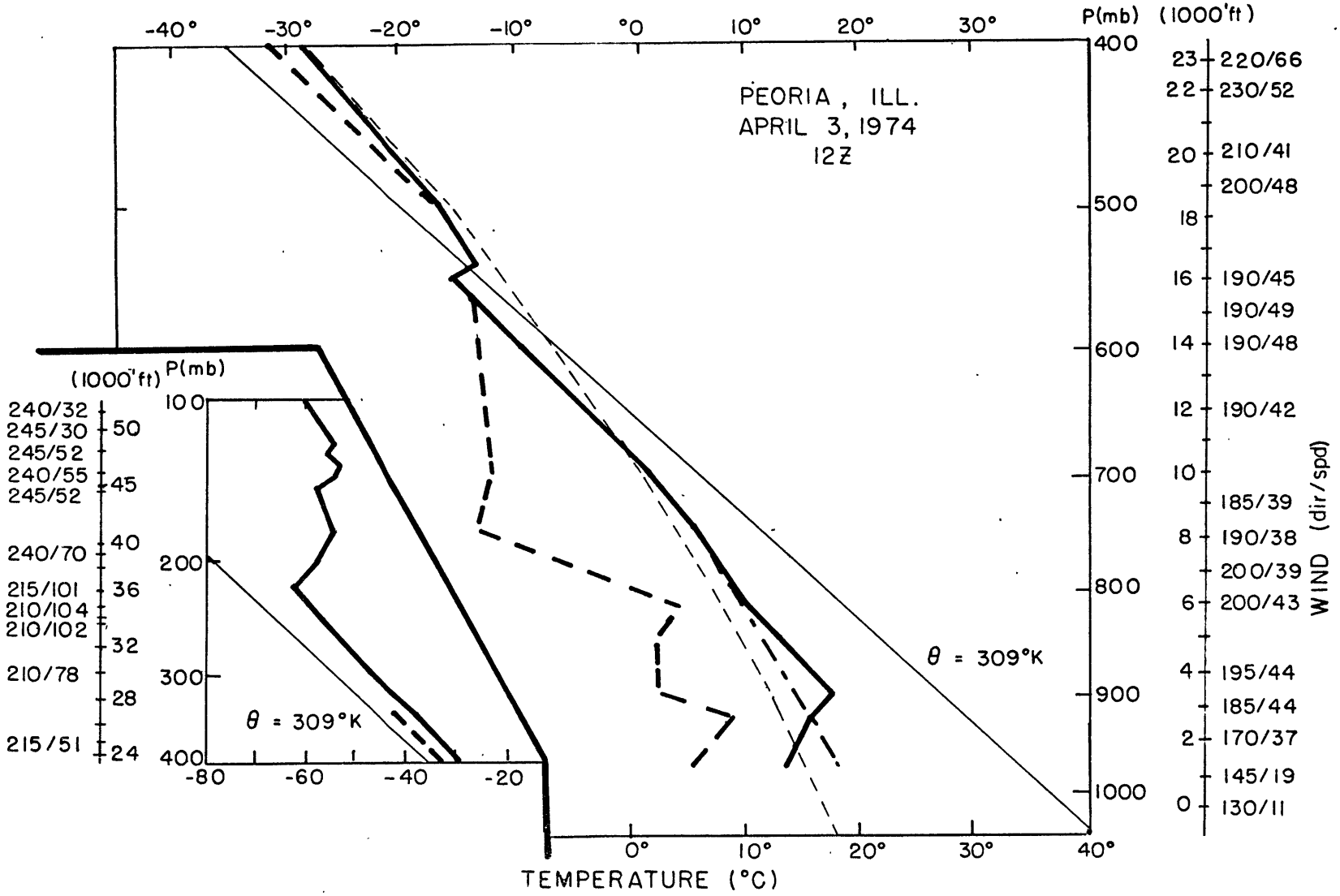

Fig. 4.4: Atmospheric sounding for Peoria, Illinois (PIA), 1200Z April 3, 1974. See explanation opposite Fig. 4.2.

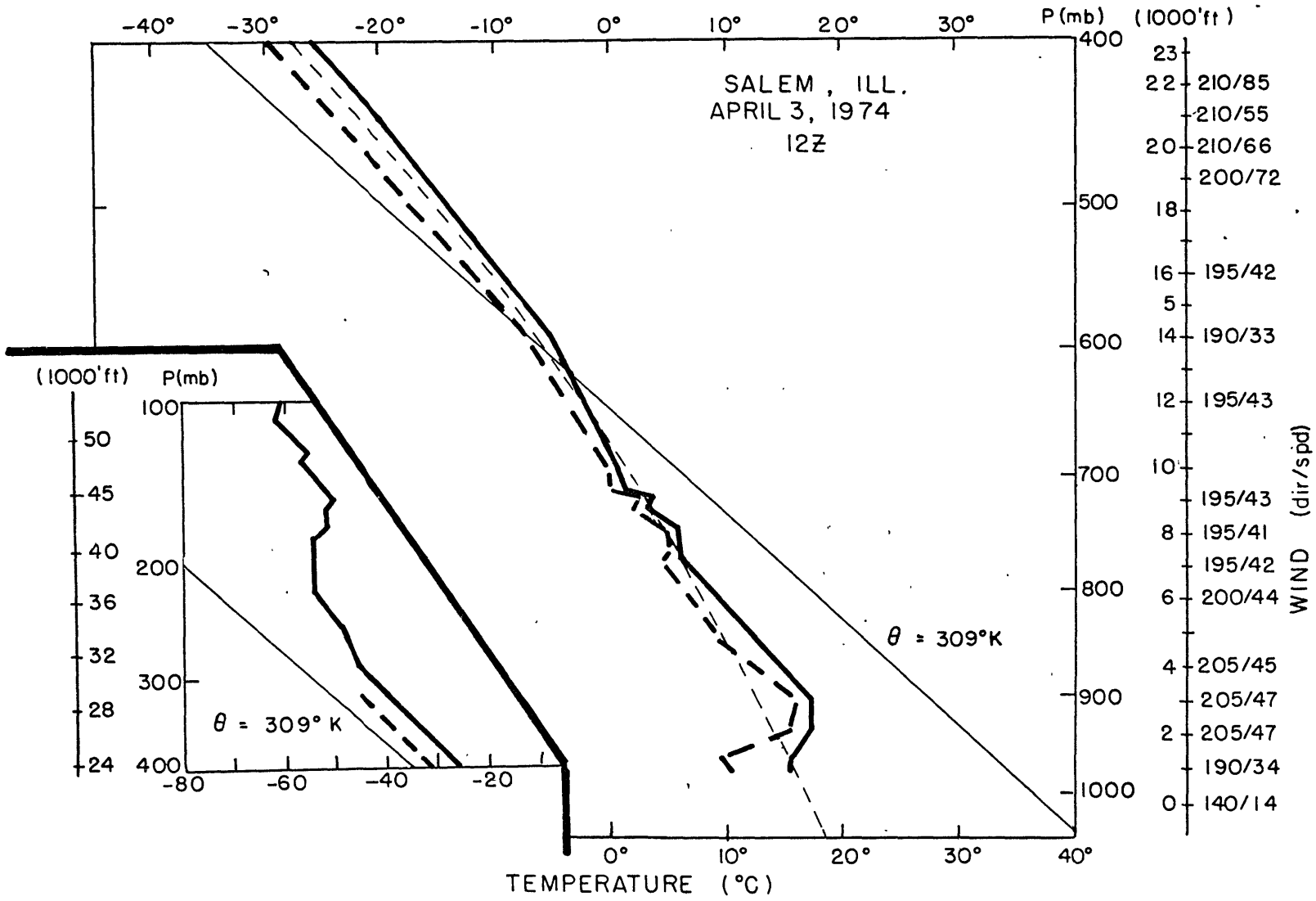

Fig. 4.5: Atmospheric sounding for Salem Illinois (SLO), 1200Z April 3, 1974. See explanation opposite Fig. 4.2.

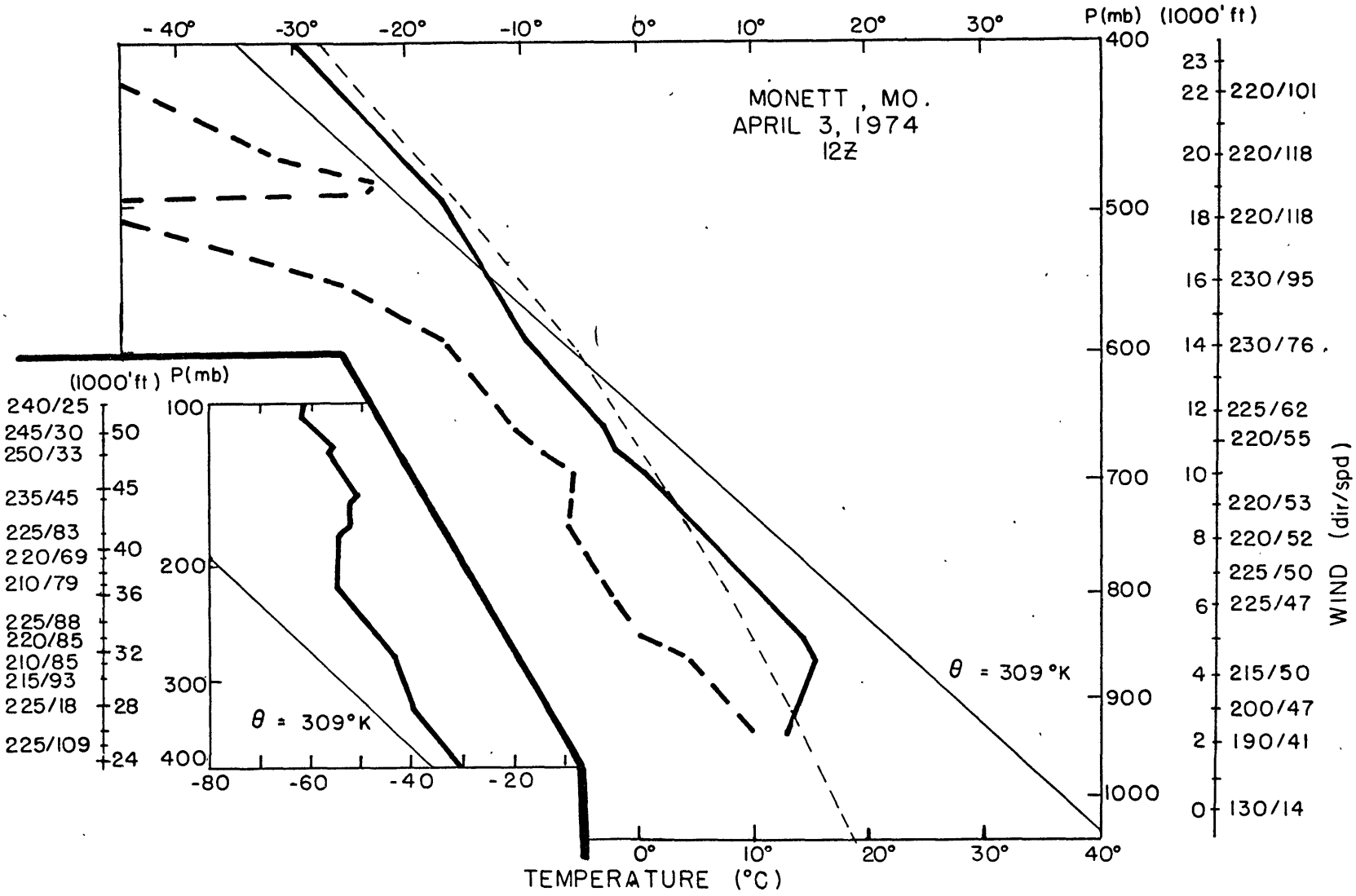

Fig. 4.6: Atmospheric sounding for Monett, Missouri (UMN), 1200Z April 3, 1974. See explanation opposite Fig. 4.2.

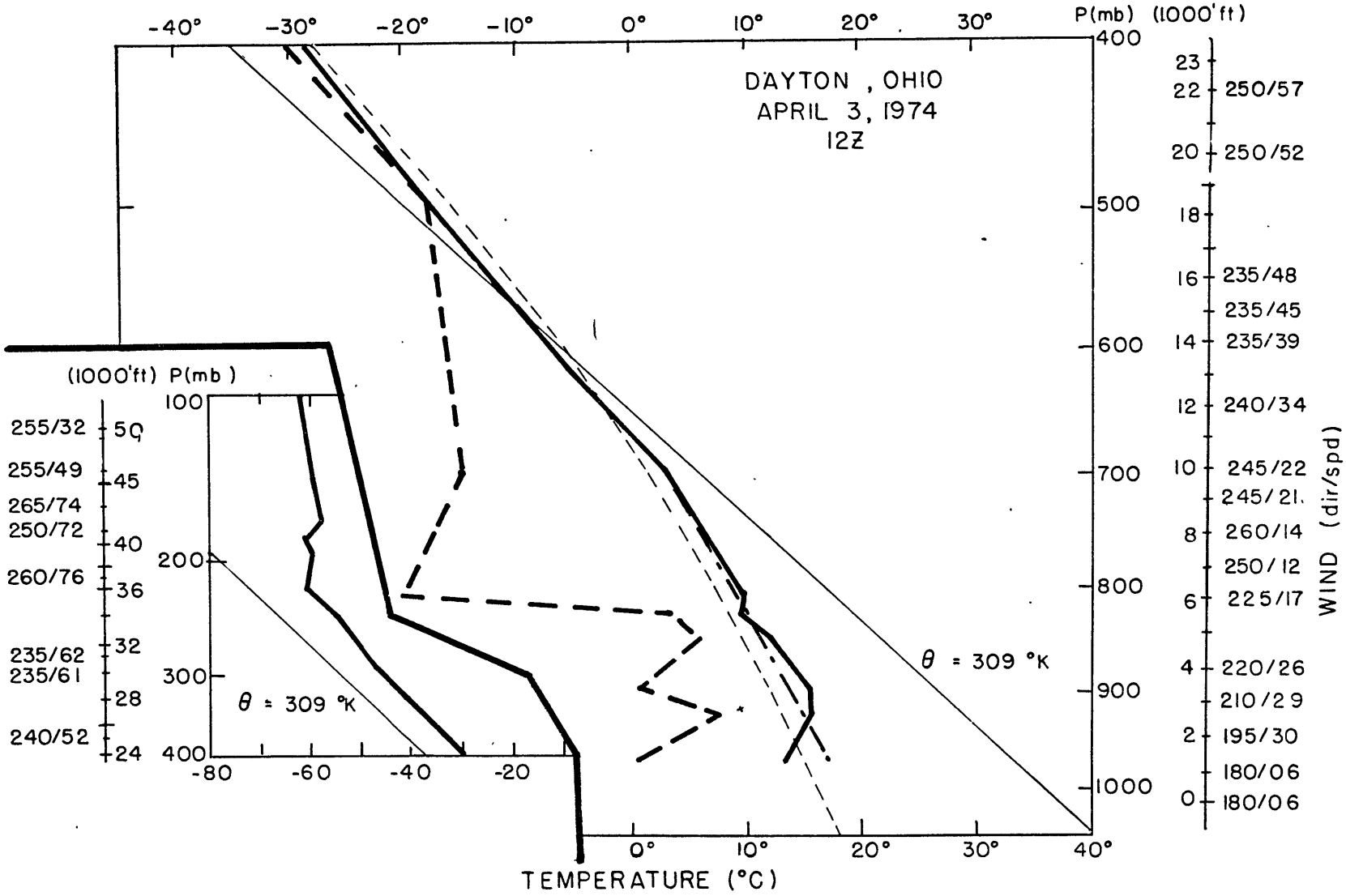

Fig. 4.7: Atmospheric sounding for Dayton, Ohio (DAY), 1200Z April 3, 1974. See explanation opposite Fig. 4.2.

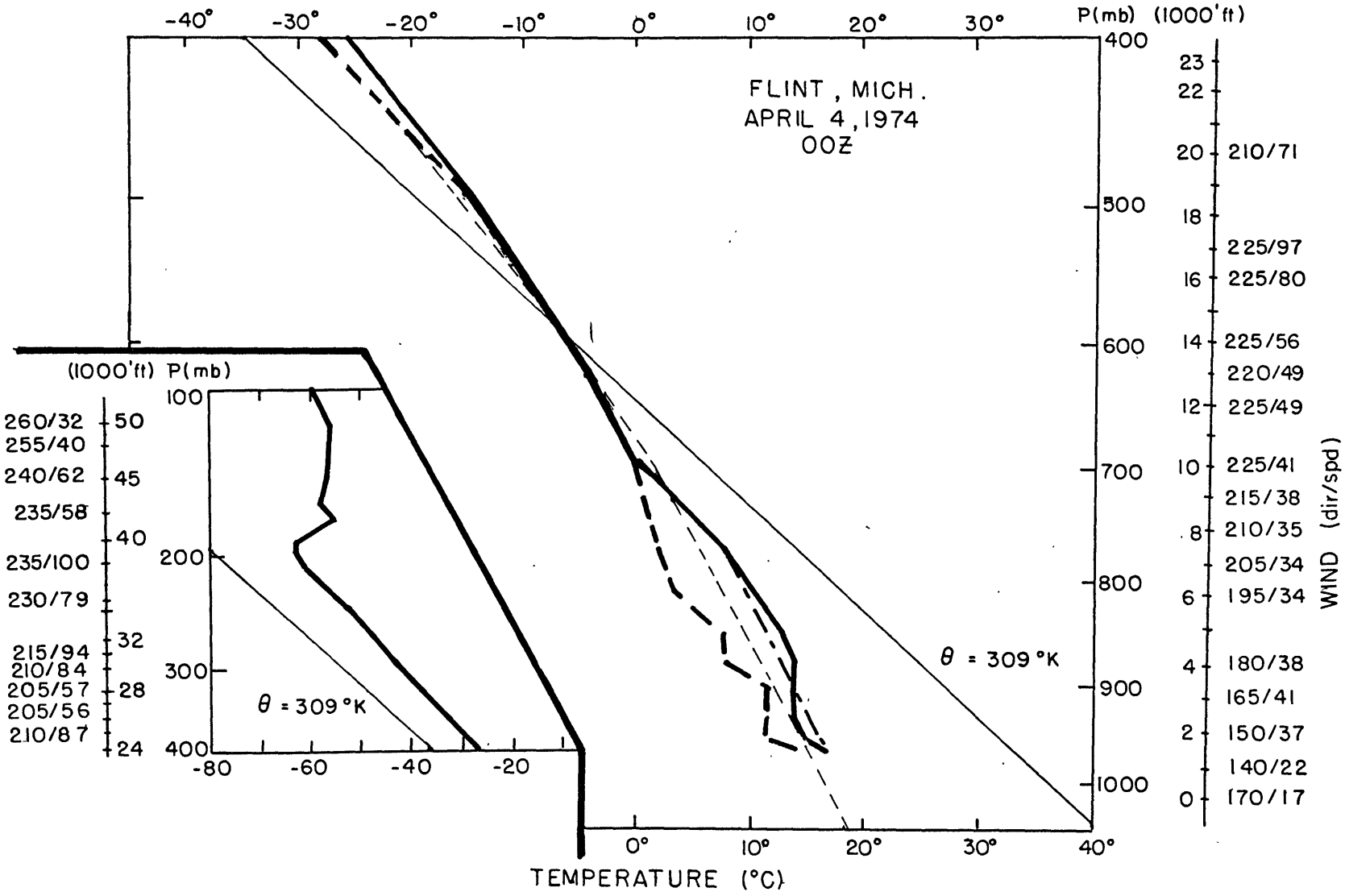

Fig. 4.8: Atmospheric sounding for Flint, Michigan (FNT), 0000Z April 4, 1974. See explanation opposite Fig. 4.2.

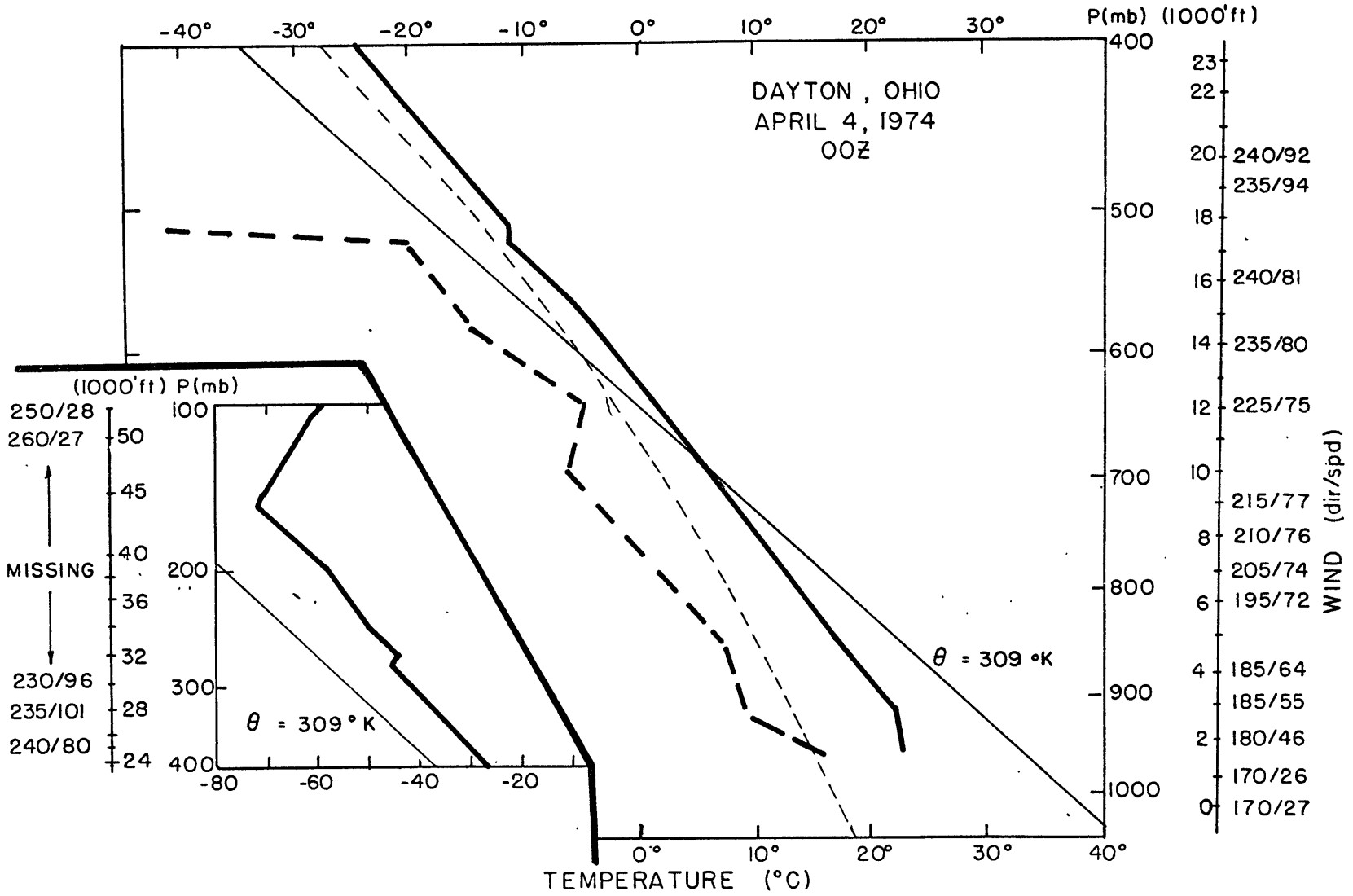

Fig. 4.9: Atmospheric sounding for Dayton, Ohio, (DAY), 0000Z April 4, 1974. See explanation opposite Fig. 4.2.

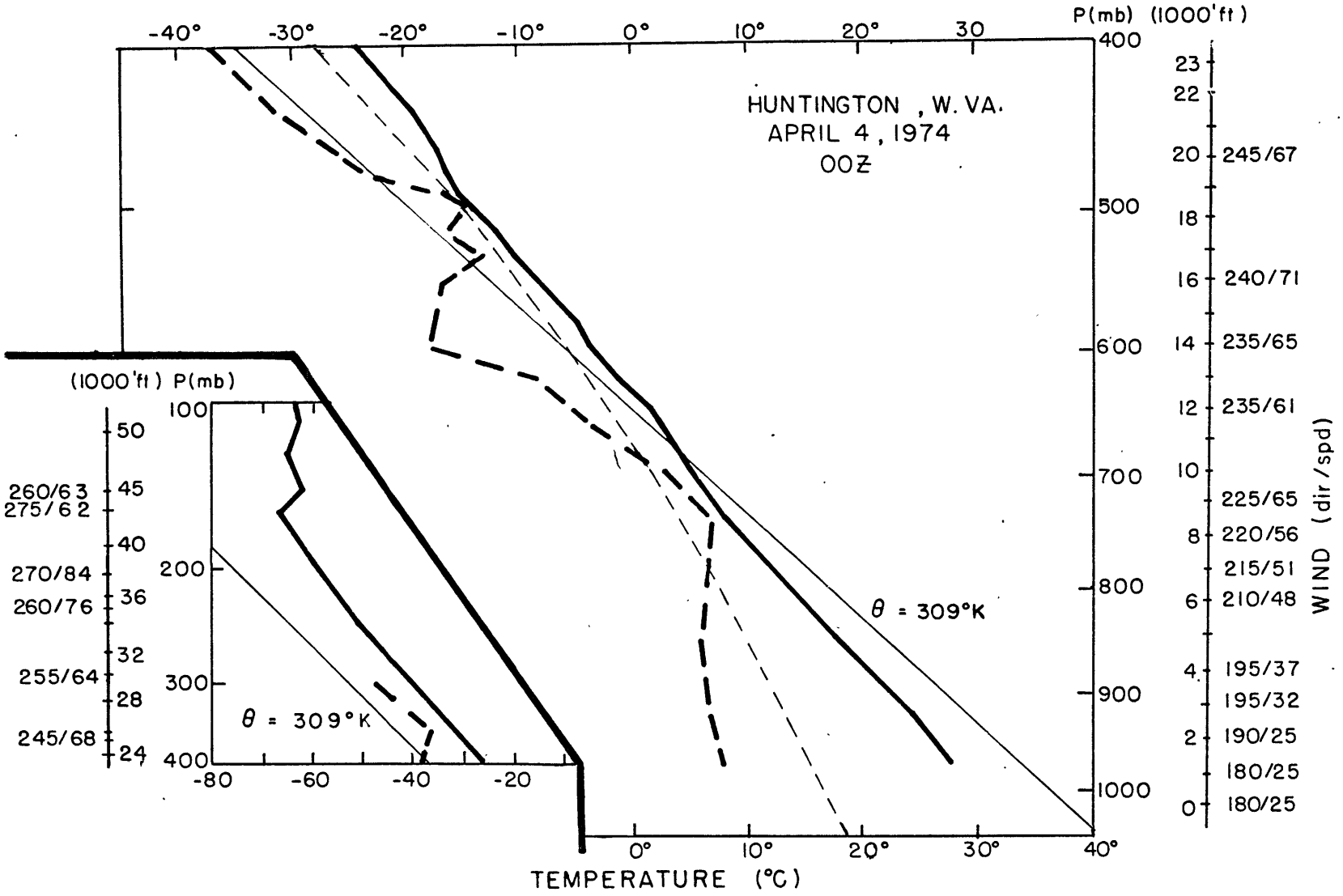

Fig. 4.10: Atmospheric sounding for Huntington, West Virginia (HTS), 0000Z April 4, 1974. See explanation opposite Fig. 4.2.

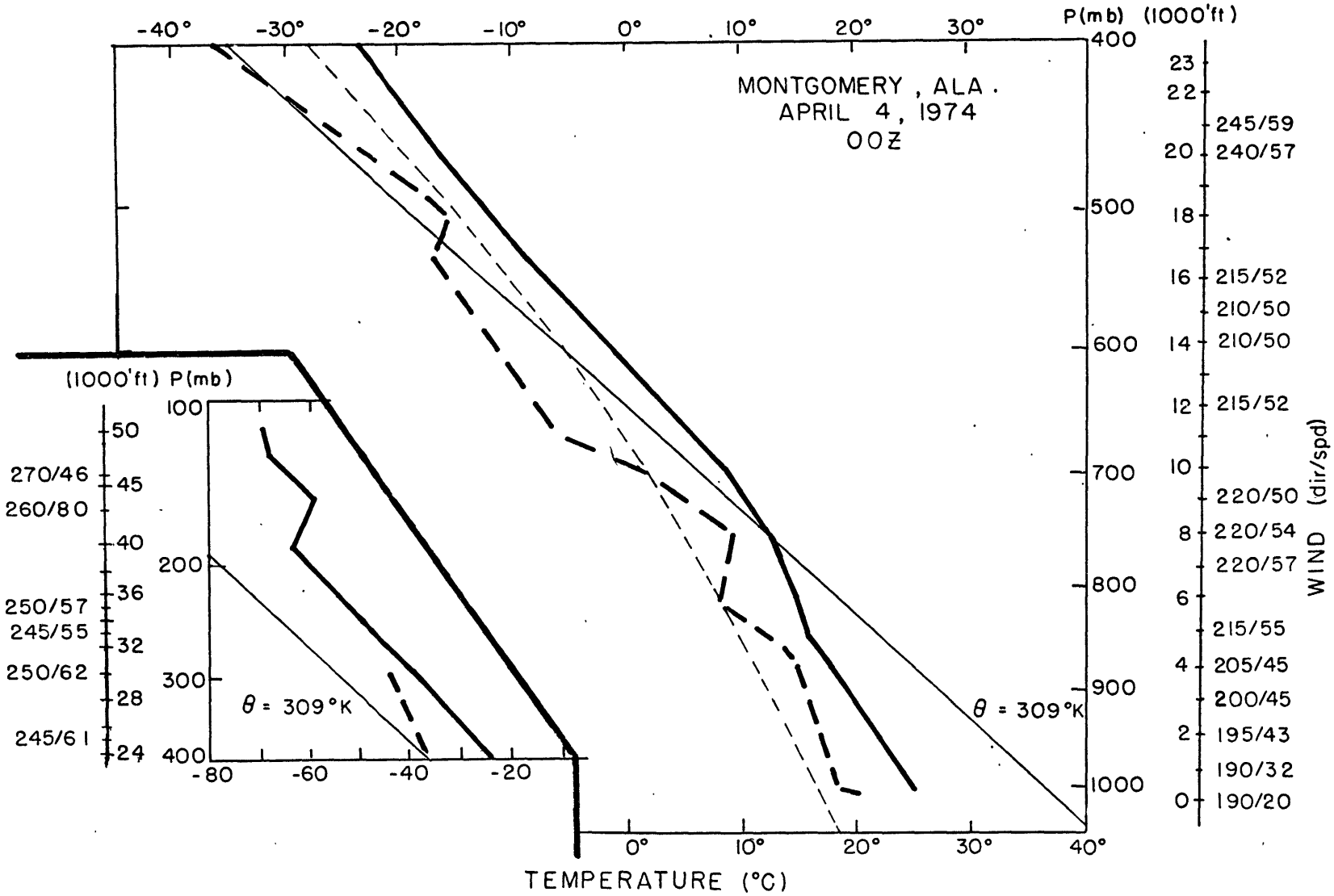

Fig. 4.11: Atmospheric sounding for Montgomery, Alabama (MGM), 0000Z April 4, 1974. See explanation opposite Fig. 4.2.

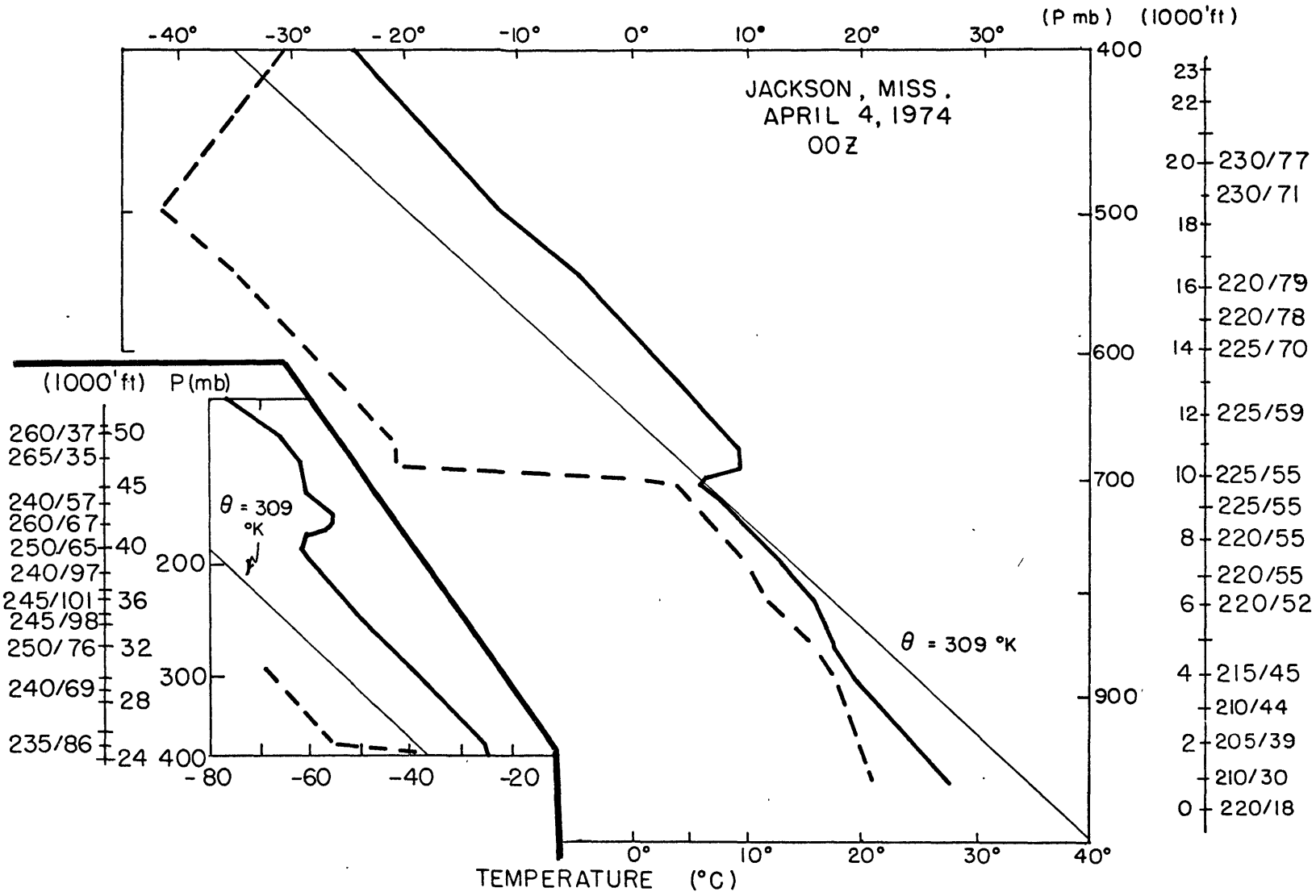

Fig. 4.12: Atmospheric sounding for Jackson, Mississippi (JAN), 0000Z April 4, 1974. See explanation opposite Fig. 4.2.

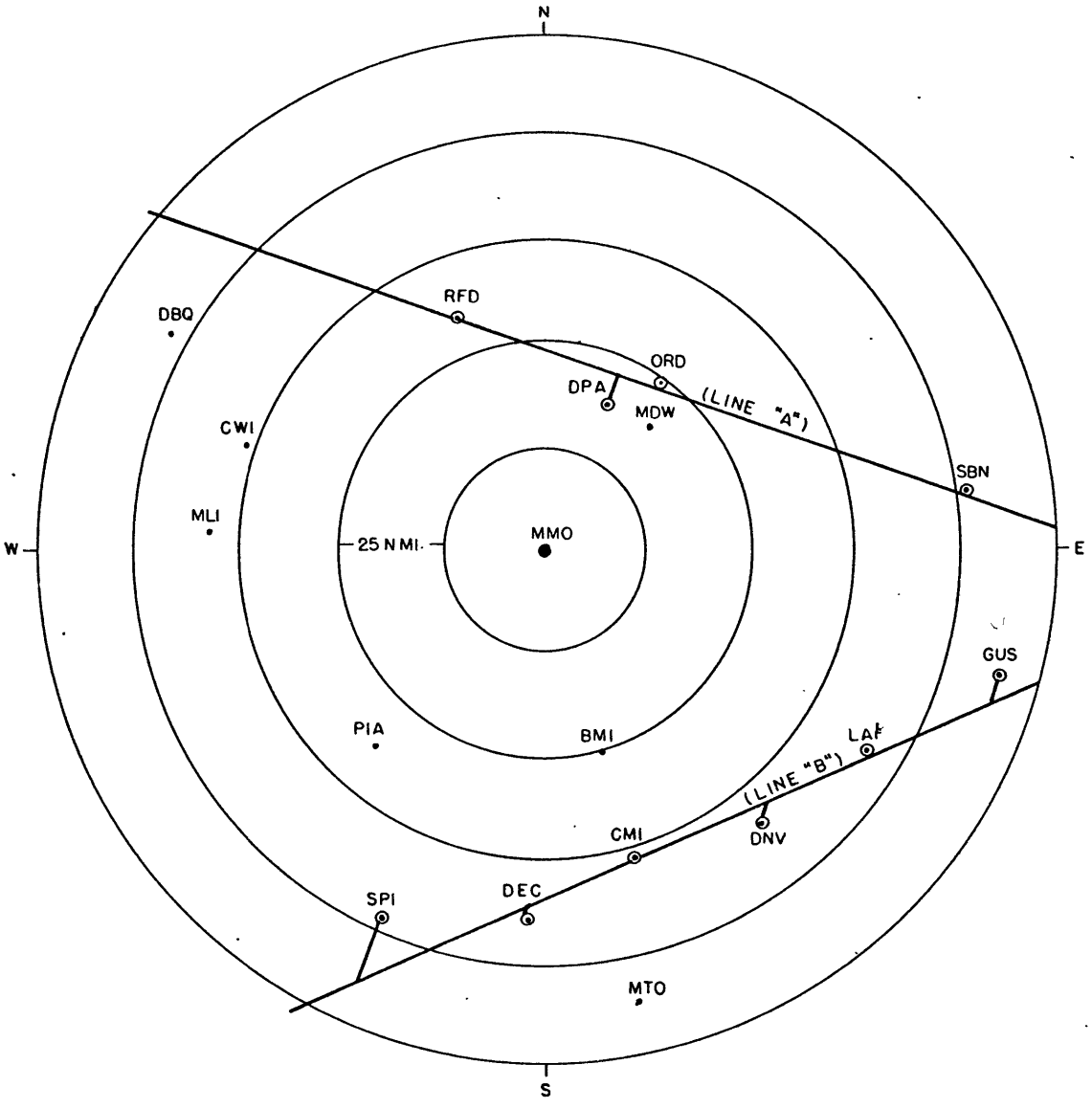

Fig. 6.1: Stations within range of Marseilles, Illinois (MMO) weather service radar, used for mesoscale pressure analyses. Long, straight, solid lines are those along which cross sections are constructed. Larger, hollow dots denote stations used in construction of cross sections. Concentric circles represent consecutive 25 nautical mile (46km) radius rings. Total range is 125 nautical miles (230km).

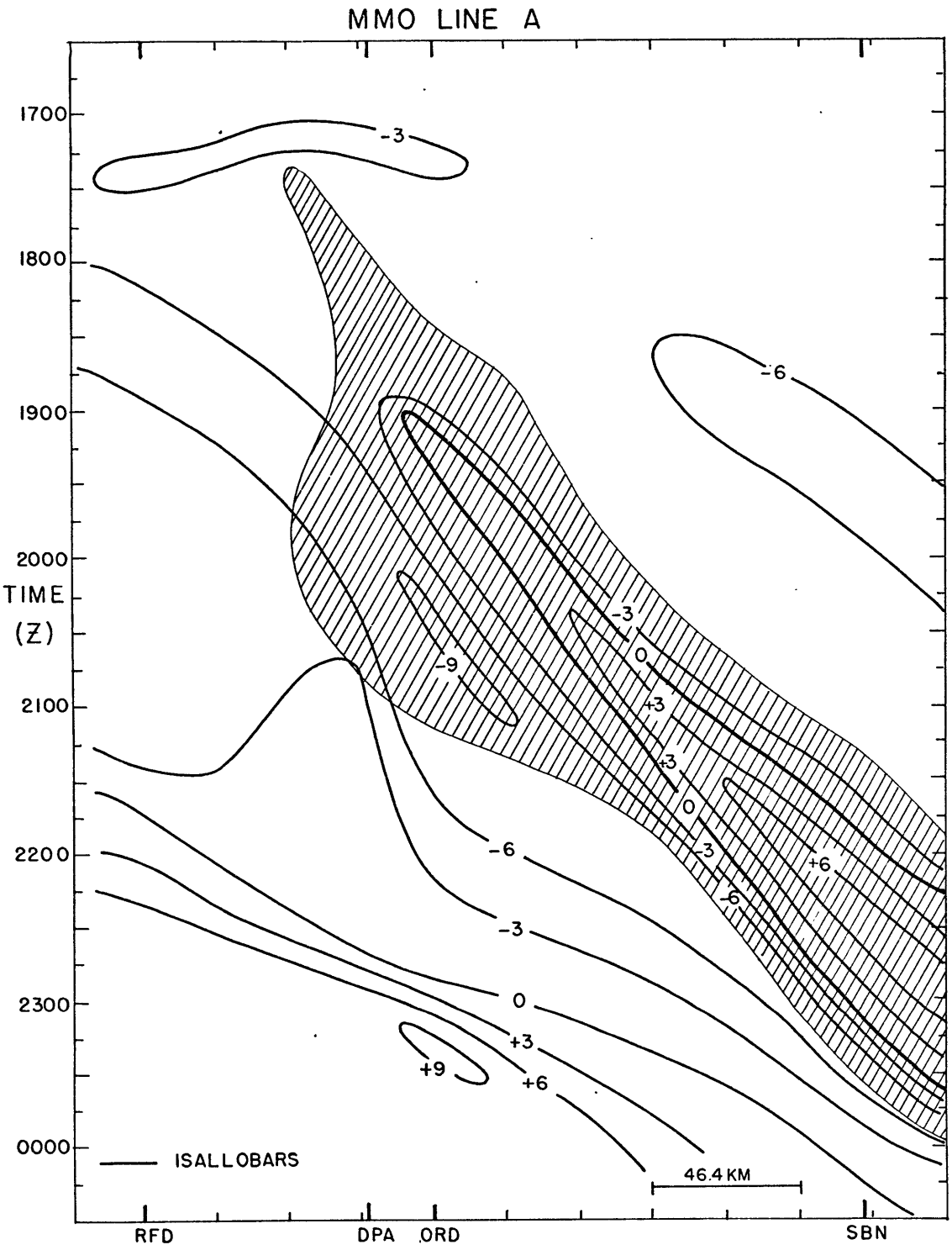

Fig. 6.2a: Time cross section MMO-A: hourly pressure tendency, 3-4 April, 1974. Solid lines: isallobars, in units of hundredths of inches of mercury per hour. Region shaded with hatching portrays radar echo.

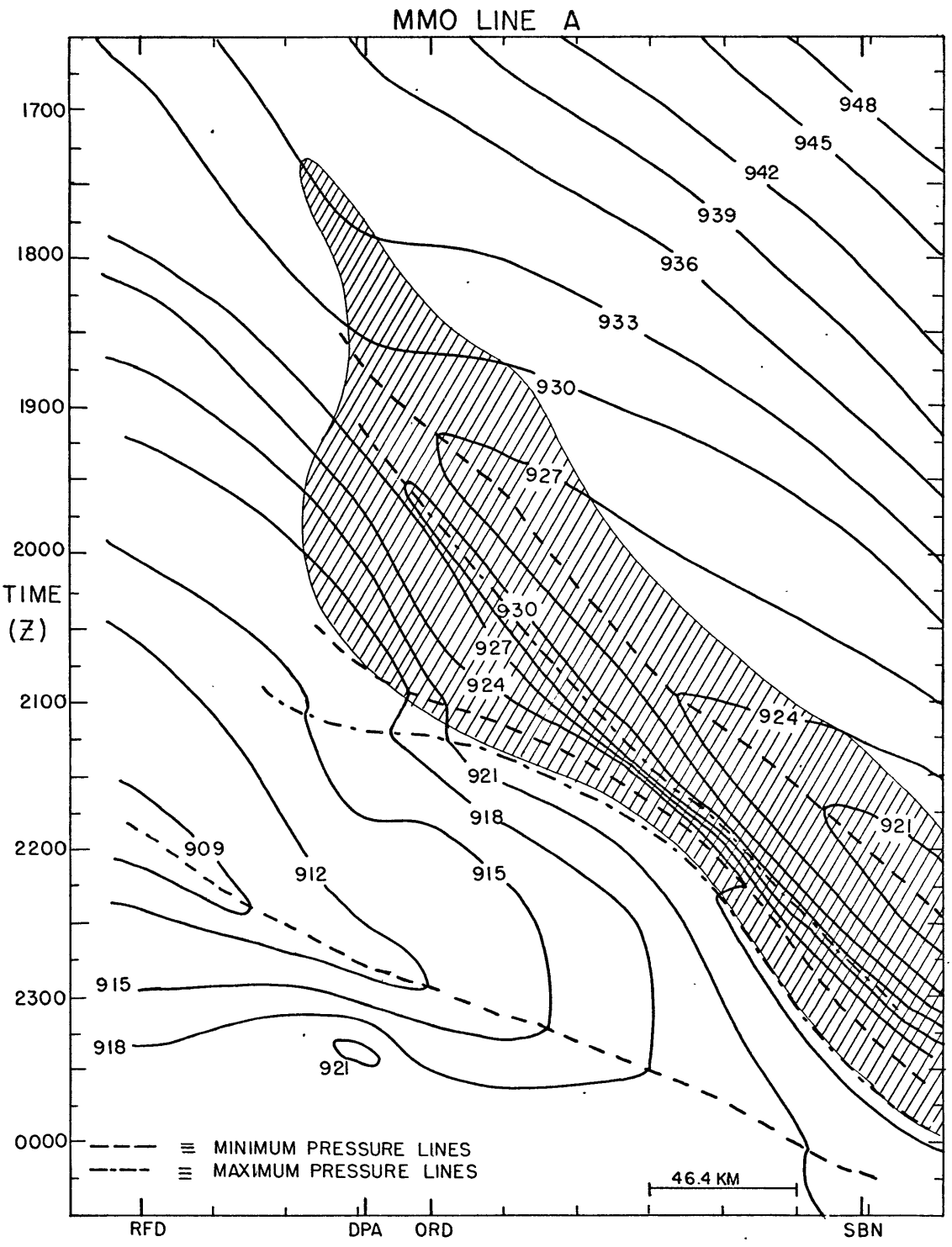

Fig. 6.2b: Time cross section MMO-A: pressure analysis, 3-4 April, 1974. Solid lines: surface pressure in hundredths of inches of mercury - in each instance, the preceding '2' has been deleted (i.e. '933' ≡ 29.33"hg). Dot-dashed lines denote pressure maxima; dashed lines denote pressure minima; hatch-shaded region portrays radar echo.

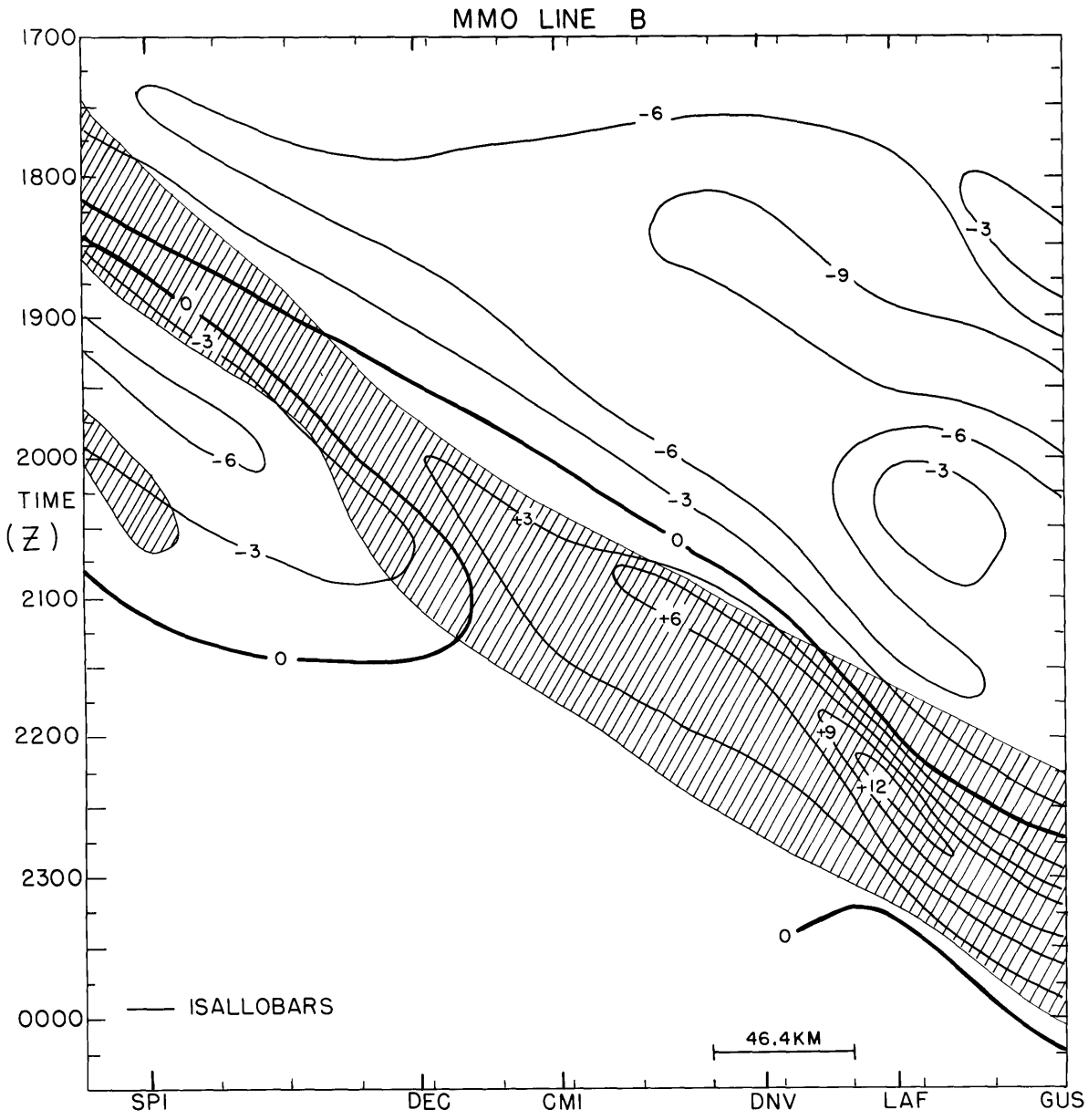

Fig. 6.3a: Time cross section MMO-B: hourly pressure tendency, 3-4 April, 1974. For details, see legend to Fig. 6.2a.

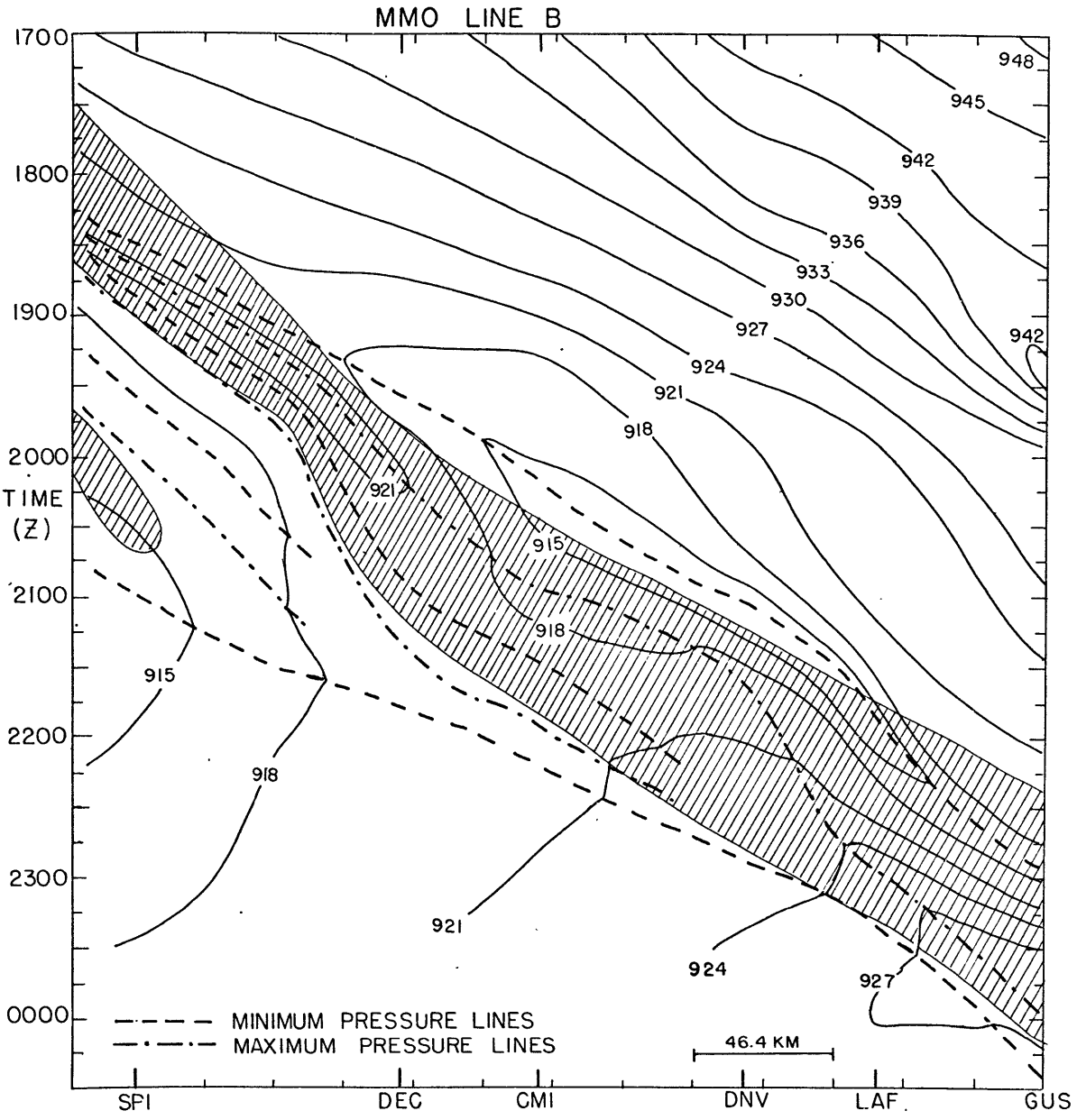

Fig. 6.3b: Time cross section MMO-B: pressure analysis, 3-4 April, 1974, For details, see legend to Fig. 6.2b.

Figs. 6.4-6.9: 1800Z-2300Z April 3, 1974 hourly mesoscale pressure analyses, super-imposed on MMO radar photographs. Solid lines are isobars, in hundredths of inches of mercury, with the preceding '2' deleted; dot-dashed lines denote ridges; dashed lines denote troughs. Dot shaded, hatch shaded, and cross-hatch shaded regions depict 1st, 2nd and 3rd relative levels of radar echo intensity, respectively, (in unspecified units). Very thick lines denote tornado tracks. Four digit, underlined numbers besides these thick lines indicate times of initiation of tornadoes. If more than one underlined number lies beside a tornado track, it indicates the time of termination of the tornado, or the time when it reaches a certain marked position.

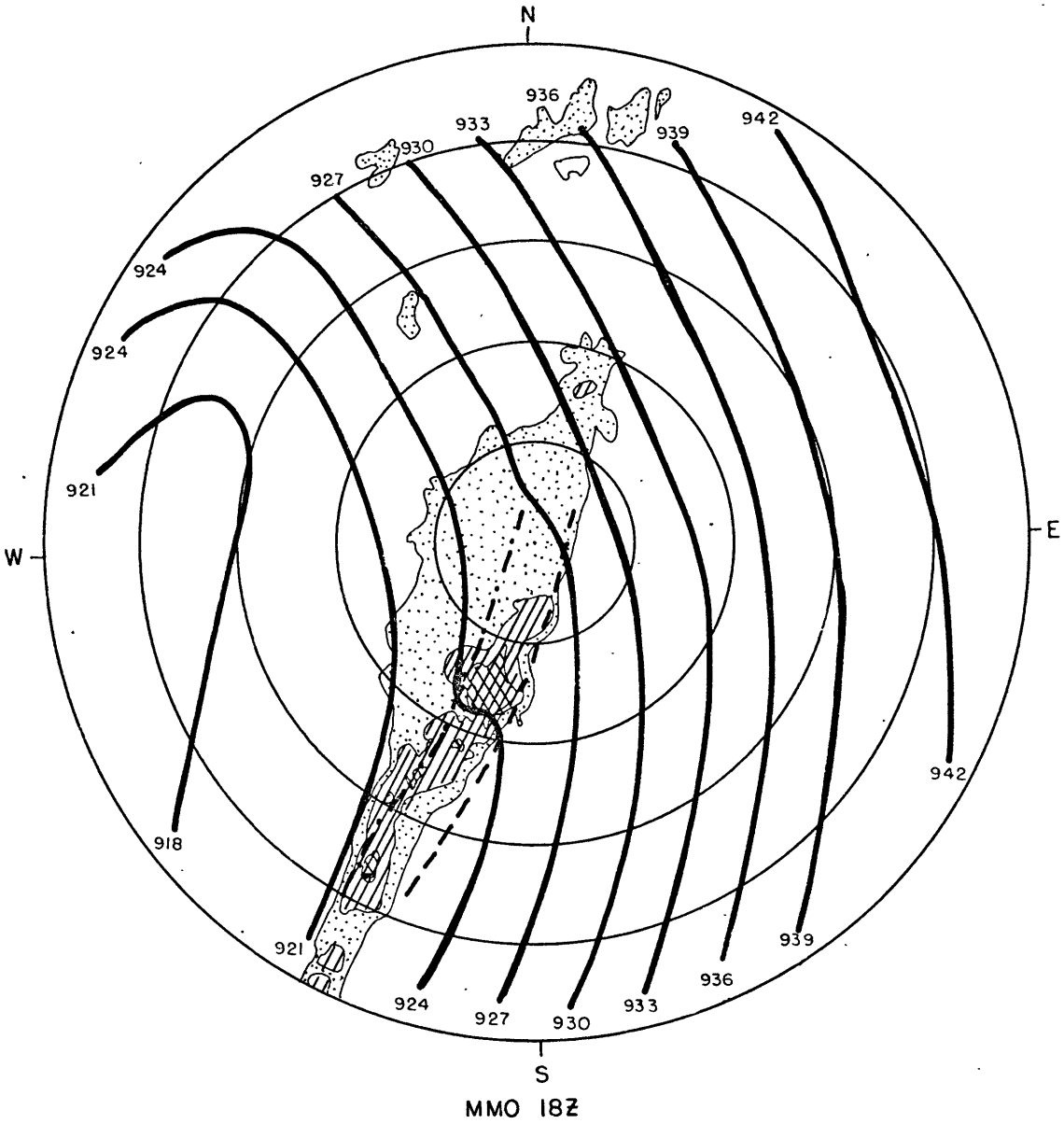

Fig. 6.4: 1800Z April 3, 1974 mesoscale pressure analysis, superimposed on MMO radar photograph. See opposite page.

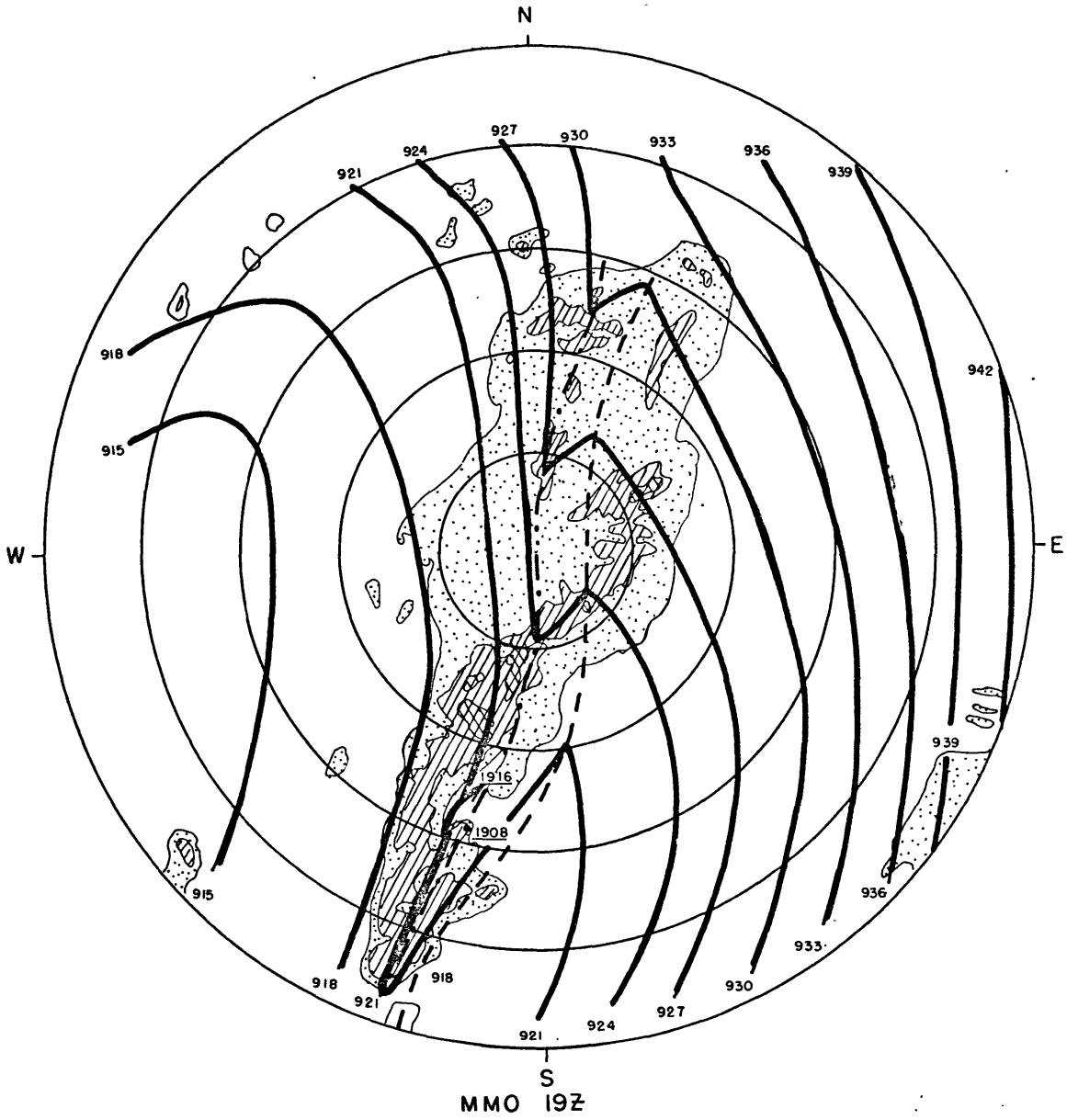

Fig. 6.5: 1900Z April 3, 1974 mesoscale pressure analysis, superimposed on MMO radar photograph. See explanation opposite Fig. 6.4.

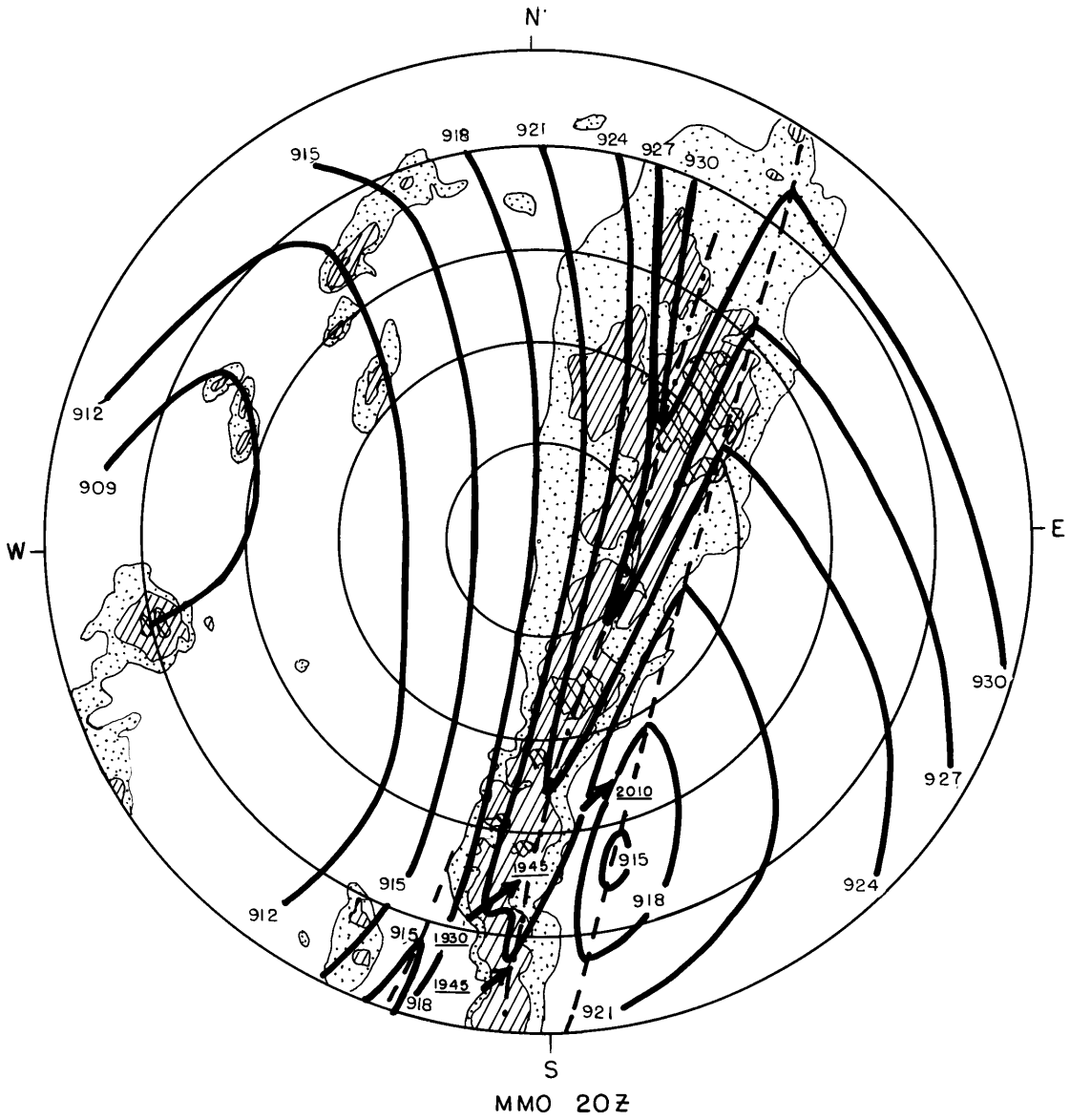

Fig. 6.6: 2000Z April 3, 1974 mesoscale pressure analysis, superimposed on MMO radar photograph. See explanation opposite Fig. 6.4.

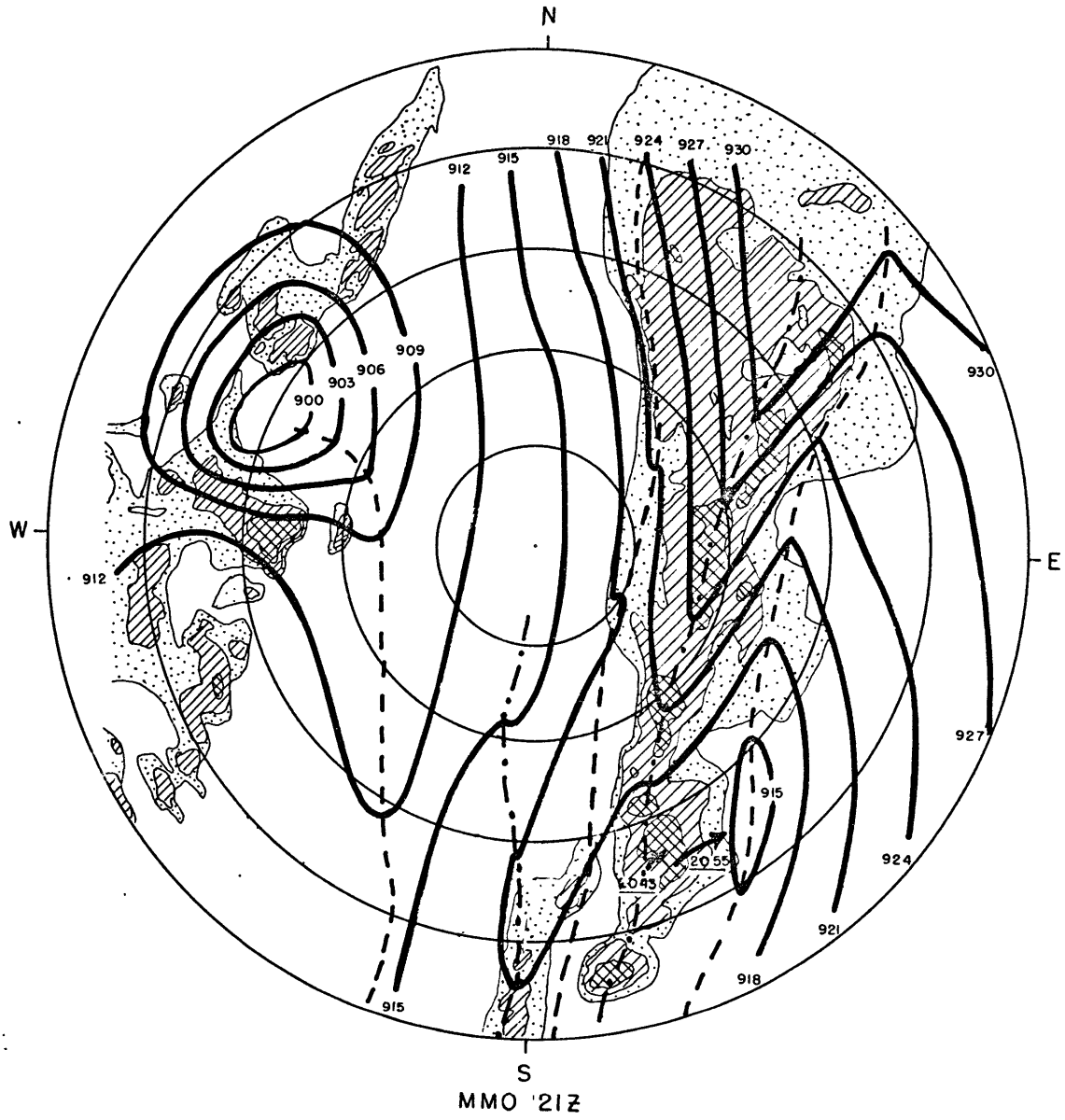

Fig. 6.7: 2100Z April 3, 1974 mesoscale pressure analysis, superimposed on MMO radar photograph. See explanation opposite Fig. 6.4.

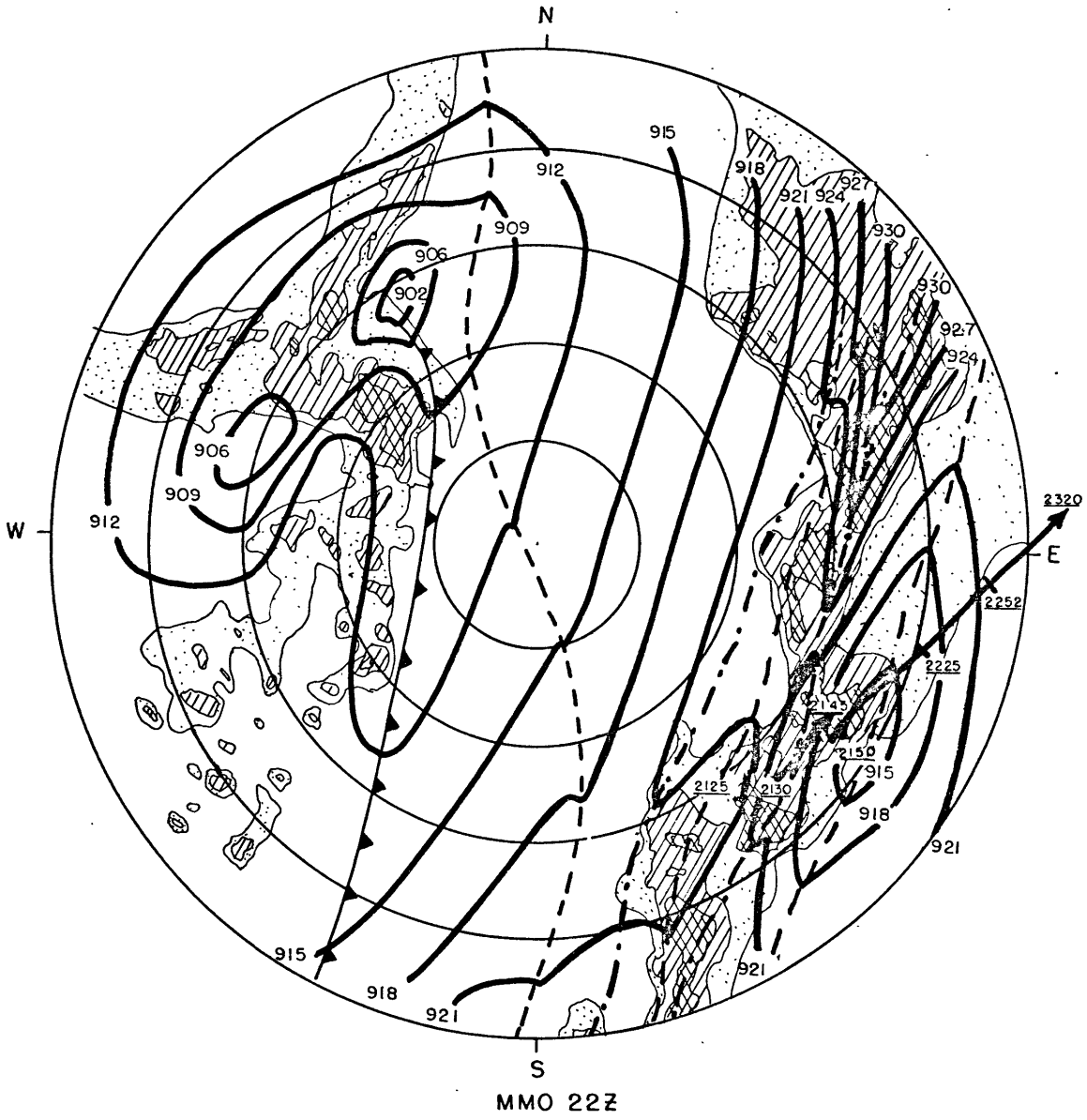

Fig. 6.8: 2200Z April 3, 1974 mesoscale pressure analysis, superimposod on MMO radar photograph. See explanation opposite 6.4.

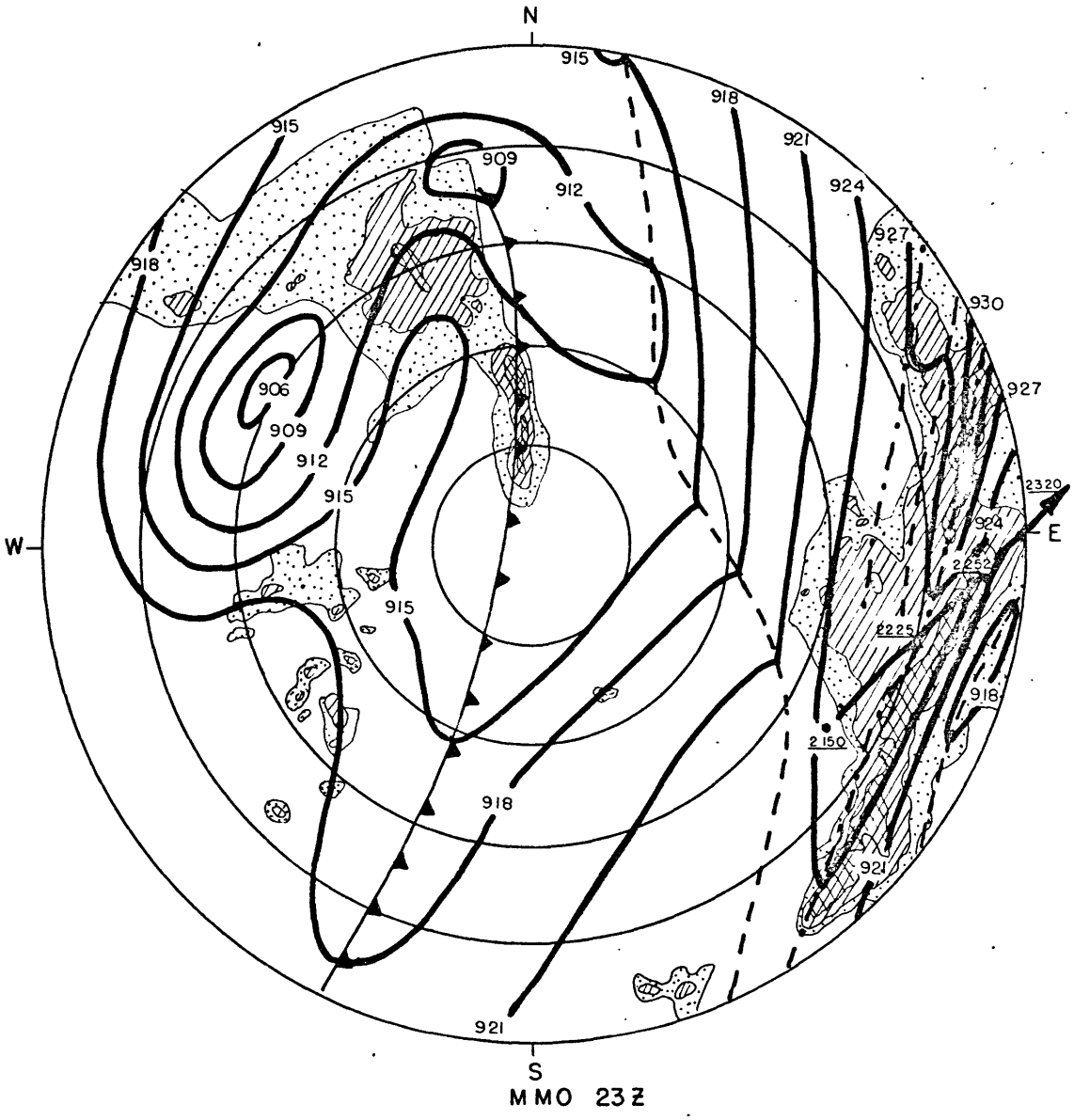

Fig. 6.9: 2300Z April 3, 1974 mesoscale pressure analysis, superimposed on MMO radar photograph. See explanation opposite Fig. 6.4.

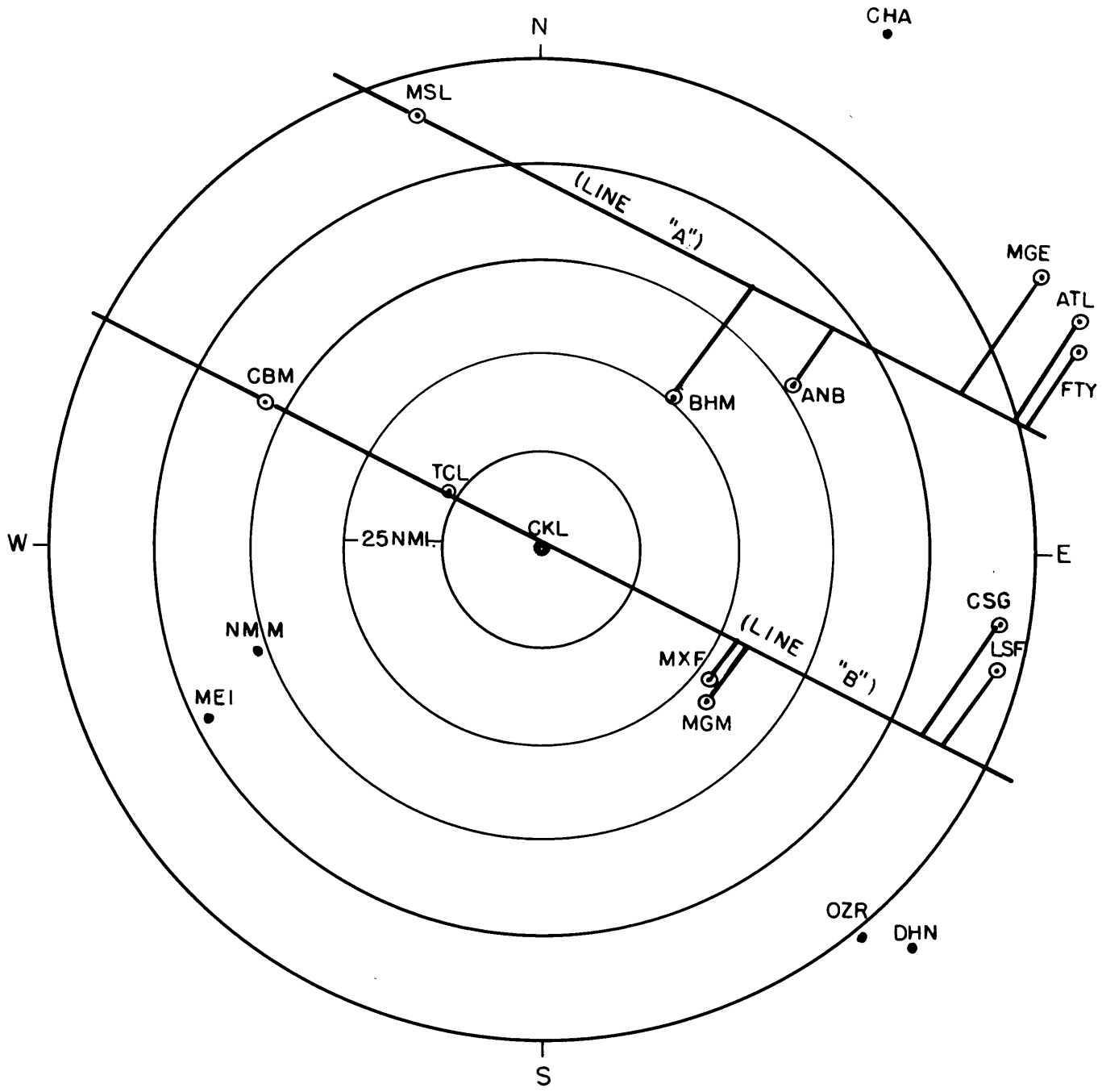

Fig. 7.1: Stations within range of Centreville, Alabama (CKL) weather service radar, used for mesoscale pressure analyses. For details, see legend to Fig. 6.1.

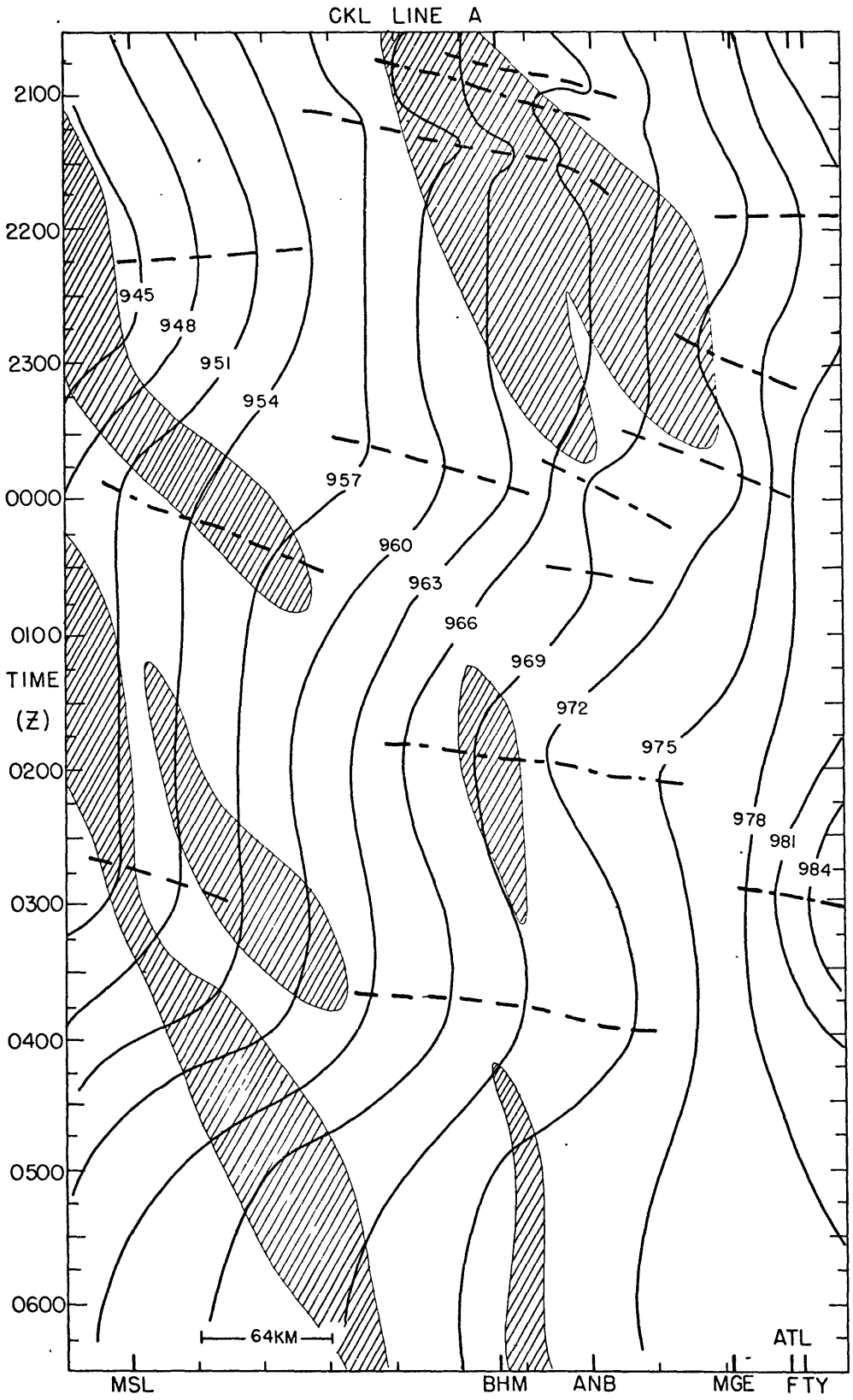

Fig. 7.2: Time cross-section CKL-A: pressure analysis, 3-4 April, 1974. For details, see legend to Fig. 6.2b.

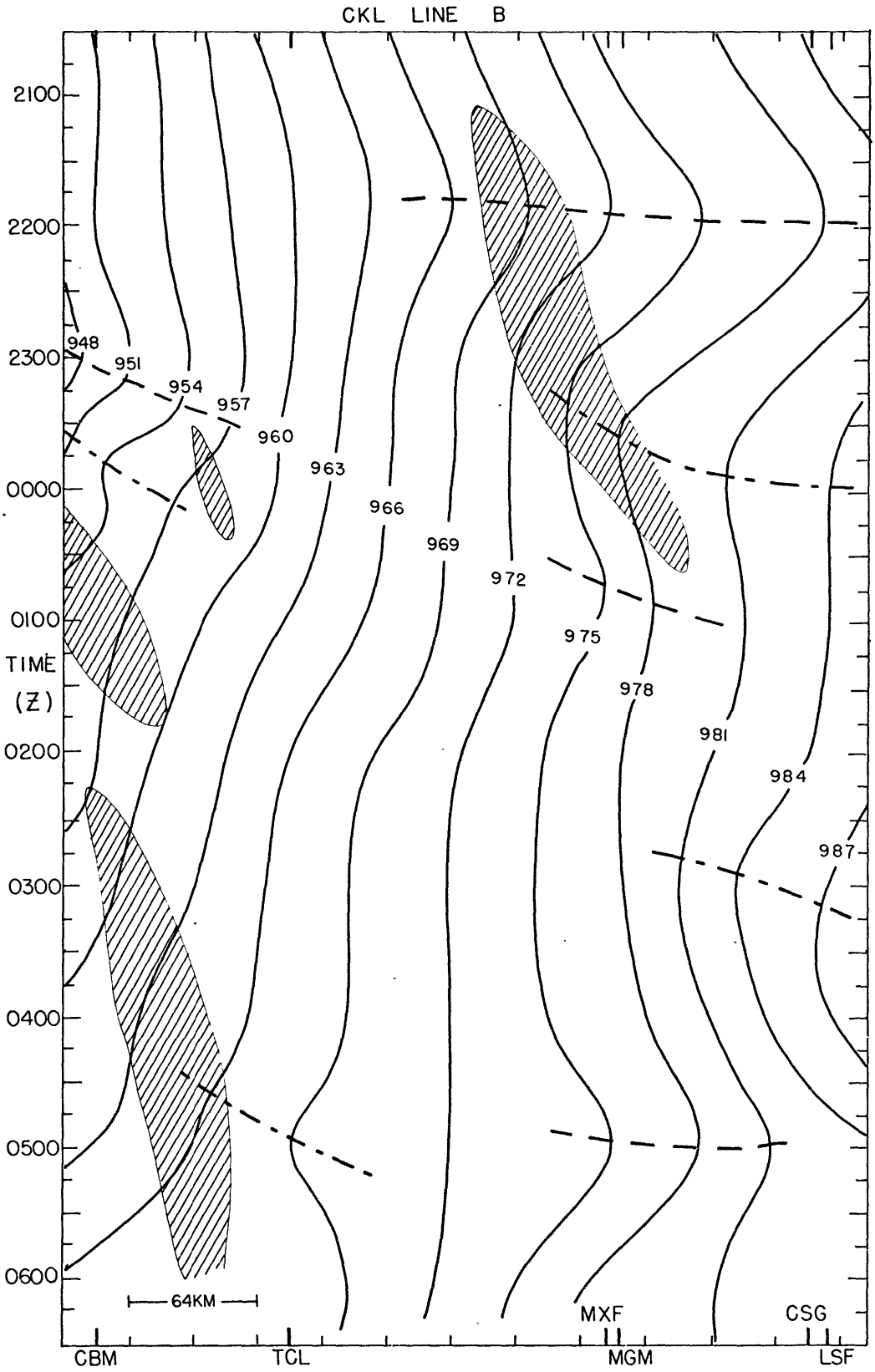

Fig. 7.3: Time cross-section CKL-B: pressure analysis, 3-4 April, 1974. For details, see legend to Fig. 6.2b.

Figs. 7.4-7.13: 2100Z April 3 - 0600Z April 4, 1974 hourly pressure analyses, superimposed on CKL radar photographs. Solid lines are isobars, in hundredths of inches of mercury, with the preceding '2' deleted. Hatch shaded, and dot shaded areas depict 1st and 2nd relative levels of radar echo intensity, respectively ,(in unspecified units). (Note: in some figures only the first level of echo intensity is depicted. In these instances the radar picture was taken without an intensity-graded display). Thick lines denote tornado tracks; four digit, underlined numbers besides these thick lines denote times of initiation, termination, or intermediate location of tornadoes.

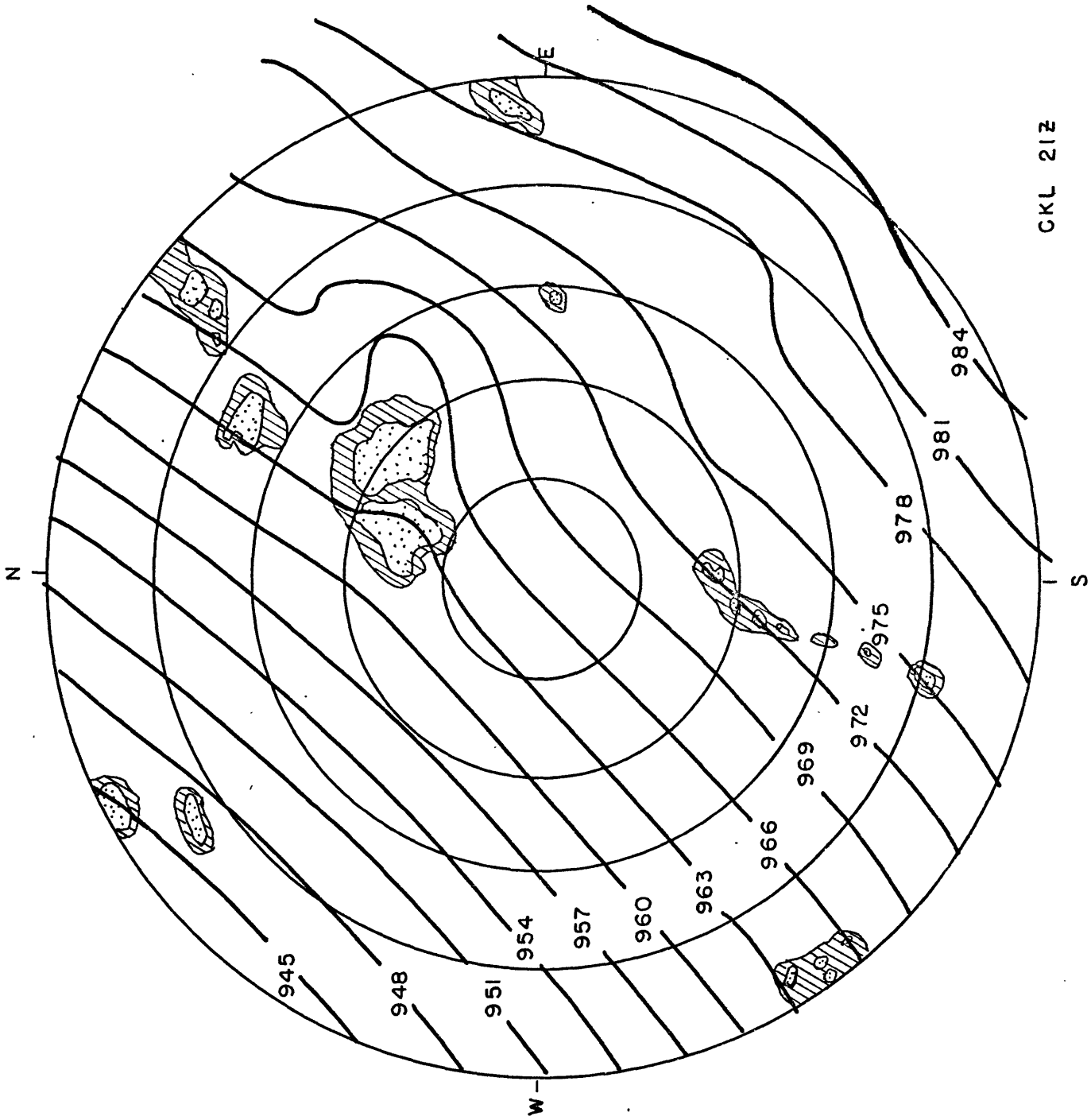

Fig. 7.4: 2100Z April 3, 1974 mesoscale pressure analysis, superimposed on CKL radar photograph. See opposite page.

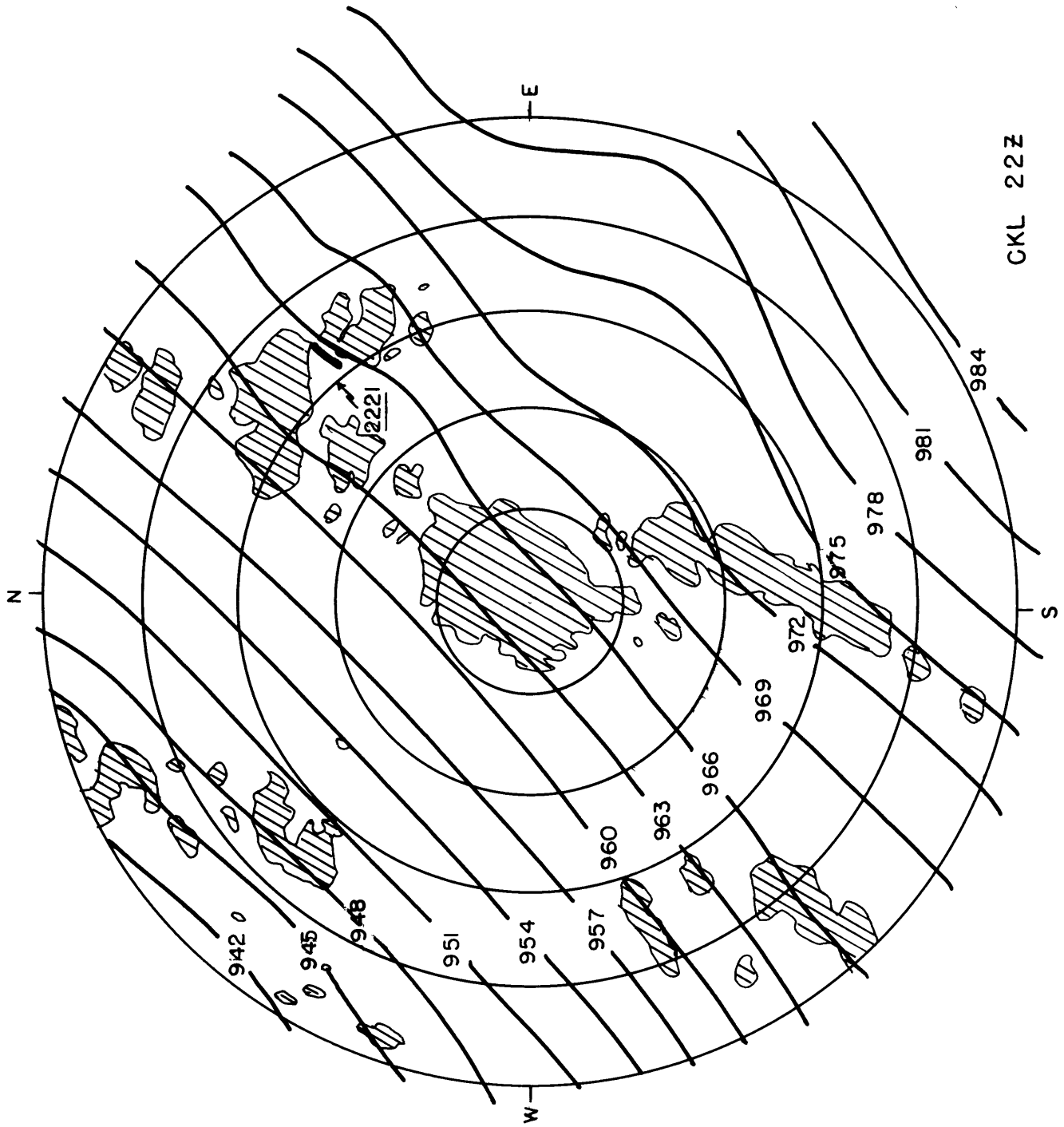

Fig. 7.5: 2200Z April 3, 1974 mesoscale pressure analysis, superimposed on CKL radar photograph. See explanation opposite Fig. 7.4.

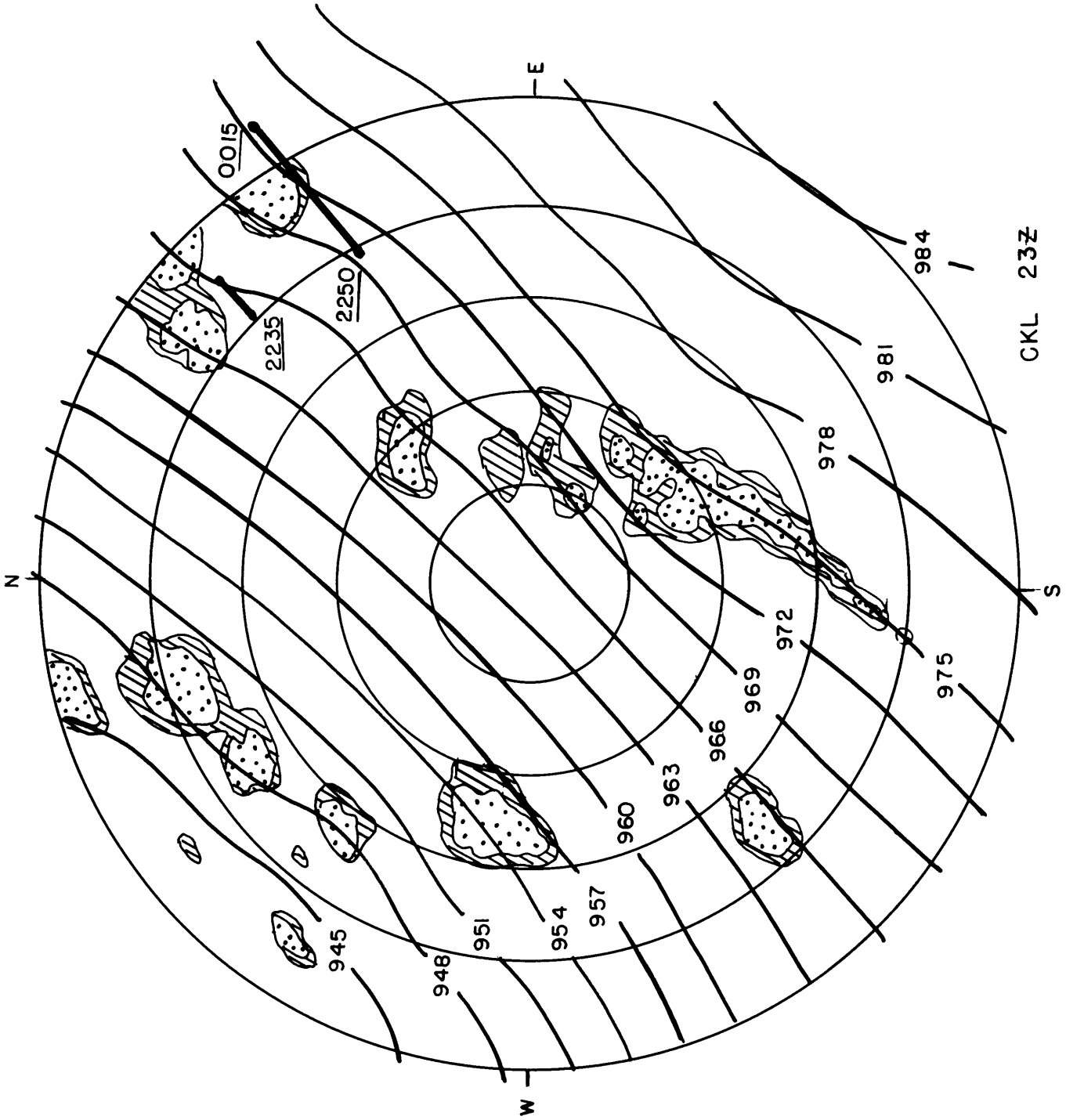

Fig. 7.6: 2300Z April 3, 1974 mesoscale pressure analysis, superimposed on CKL radar photograph. See explanation opposite Fig. 7.4.

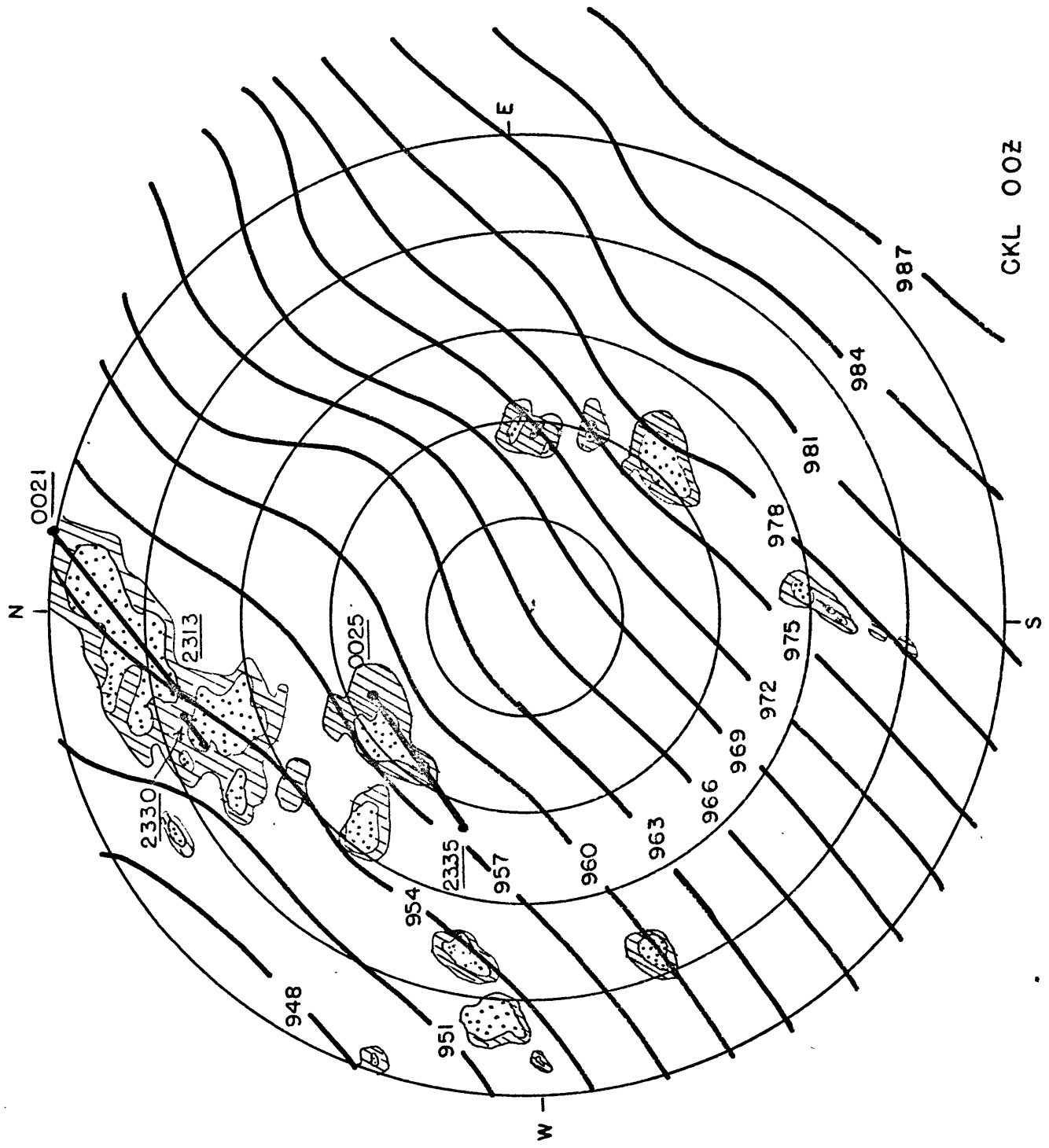

Fig. 7.7: 0000Z April 4, 1974 mesoscale pressure analysis, superimposed on CKL radar photograph. See explanation opposite Fig. 7.4.

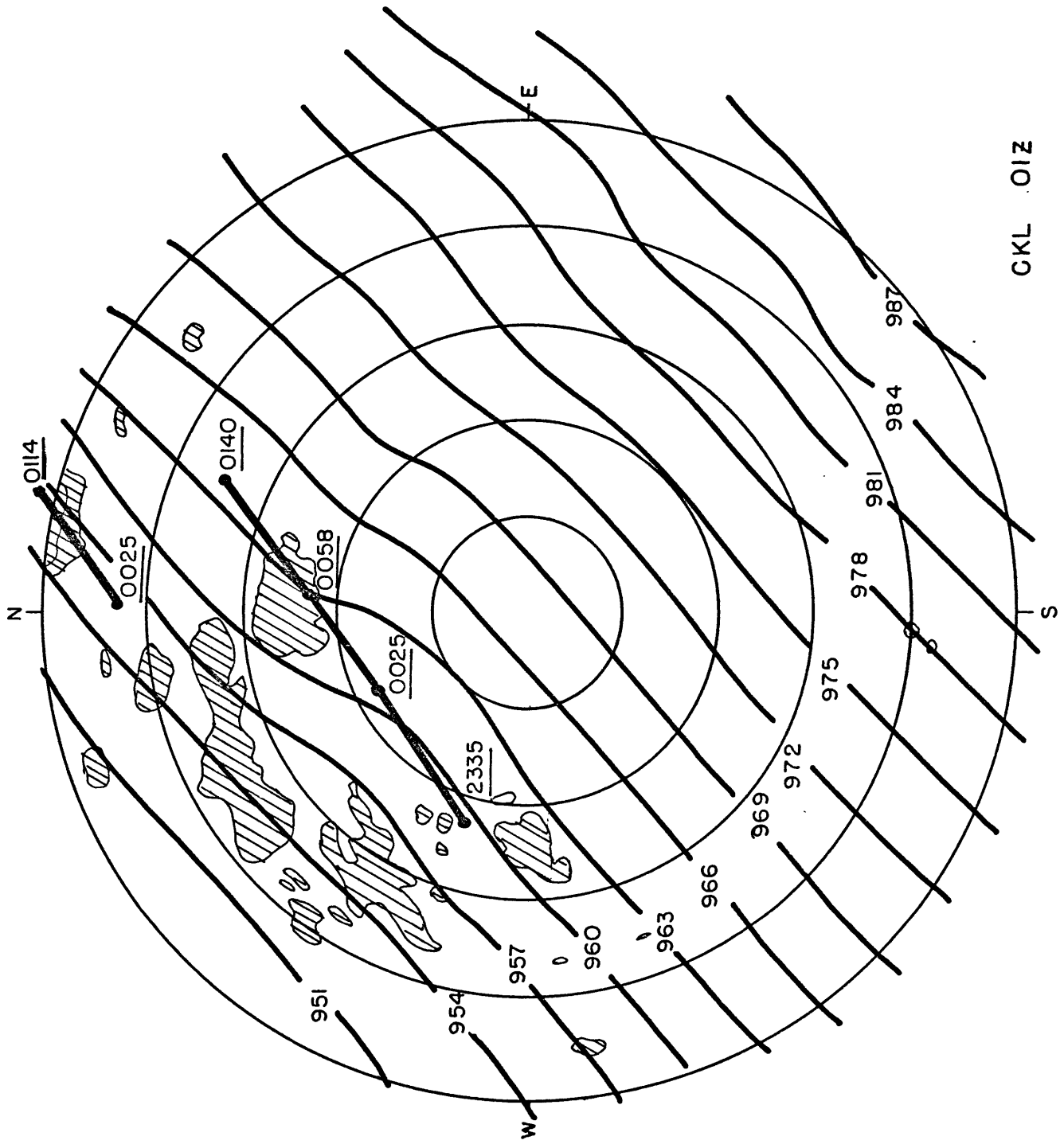

Fig. 7.8: 0100Z April 4, 1974 mesoscale pressure analysis, superimposed on CKL radar photograph. See explanation opposite Fig 7.4.

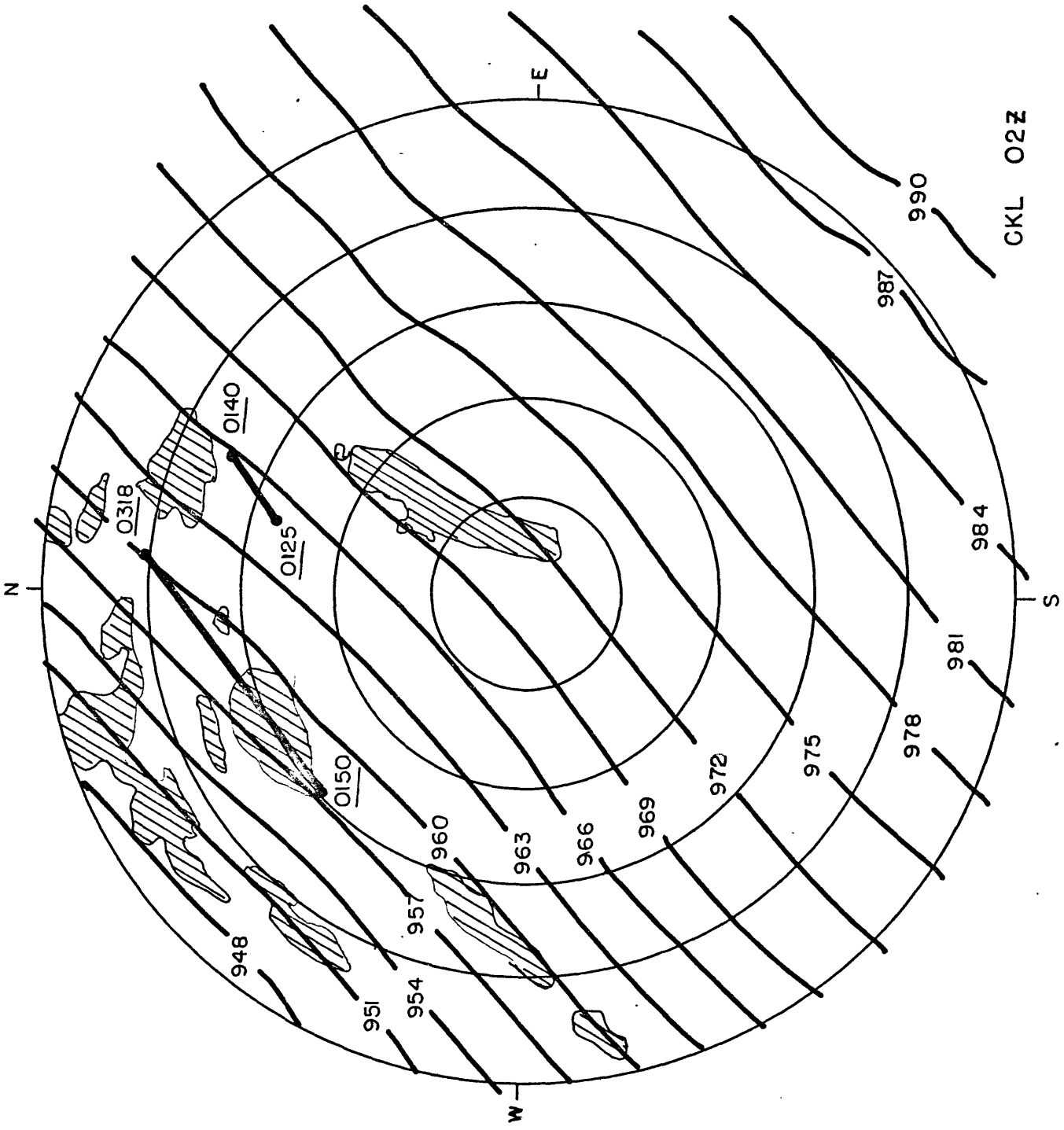

Fig. 7.9: 0200Z April 4, 1974 mesoscale pressure analysis, superimposed on CKL radar photograph. See explanation opposite Fig. 7.4.

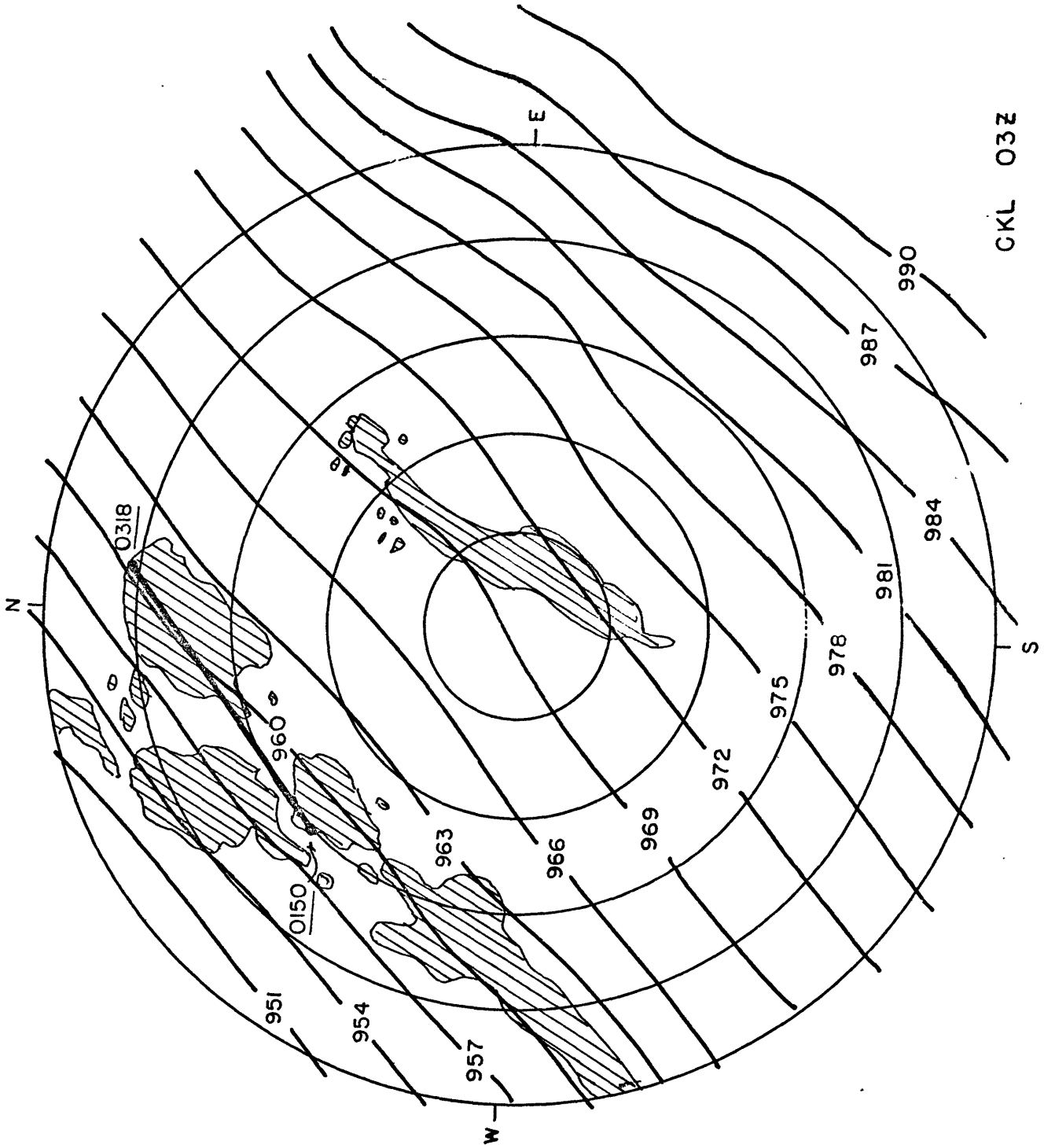

Fig. 7.10: 0300Z April 4, 1974 mesoscale pressure analysis, superimposed on CKL radar photograph. See explanation opposite Fig. 7.4.

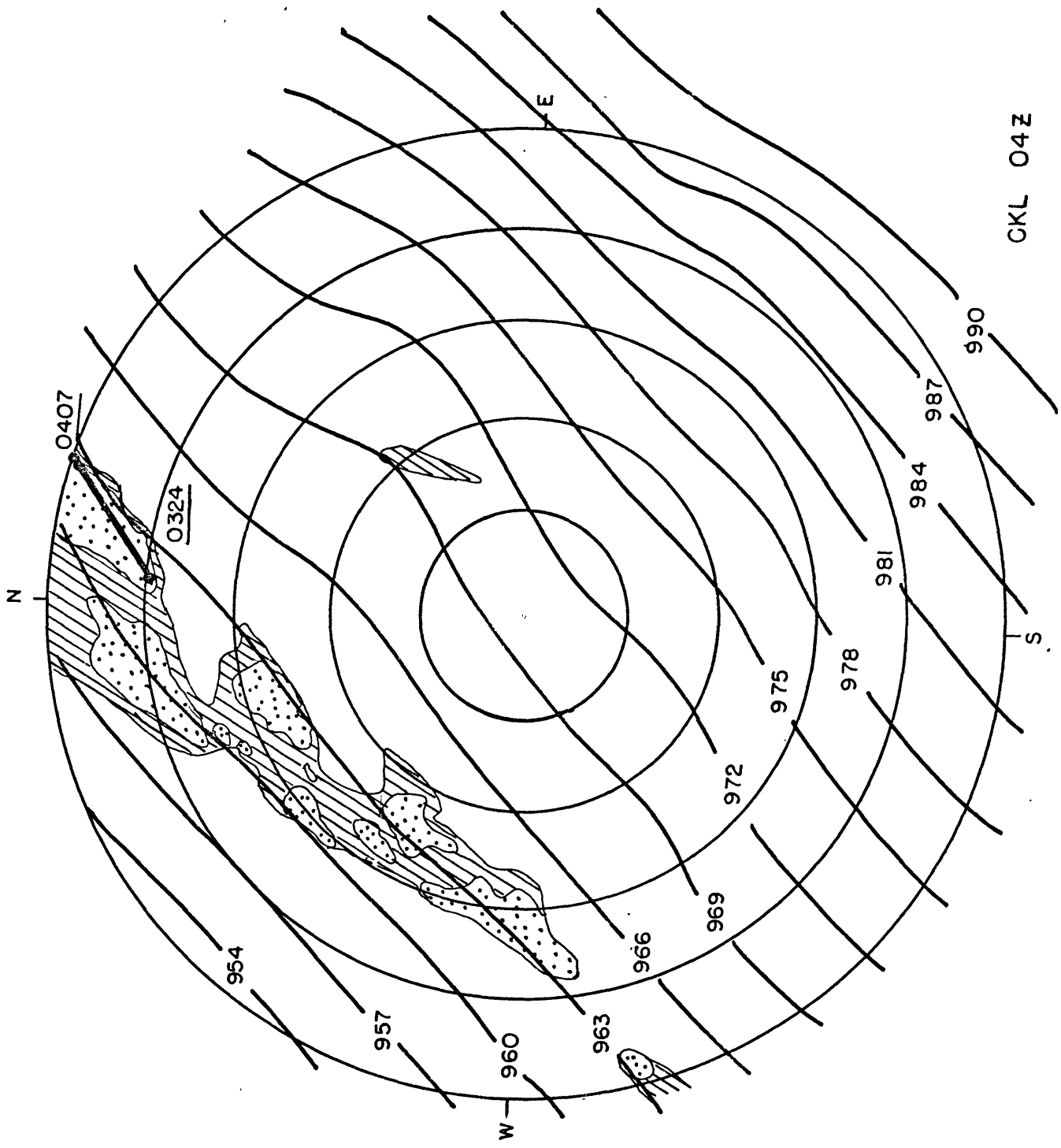

Fig. 7.11: 0400Z April 4, 1974 mesoscale pressure analysis, superimposed on CKL radar photograph. See explanation opposite Fig. 7.4.

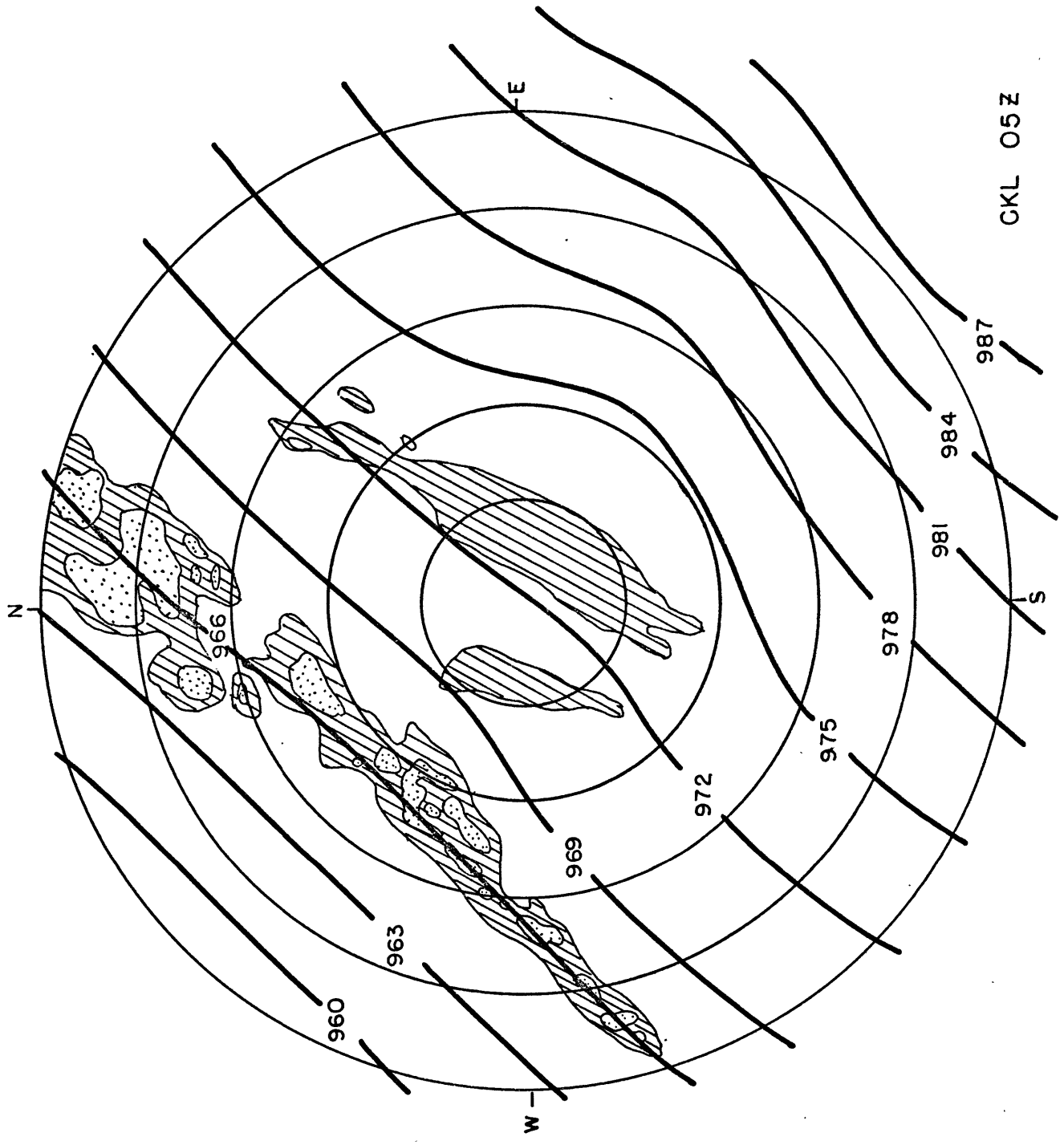

Fig. 7.12: 0500Z April 4, 1974 mesoscale pressure analysis, superimposed on CKL radar photograph. See explanation opposite Fig. 7.4.

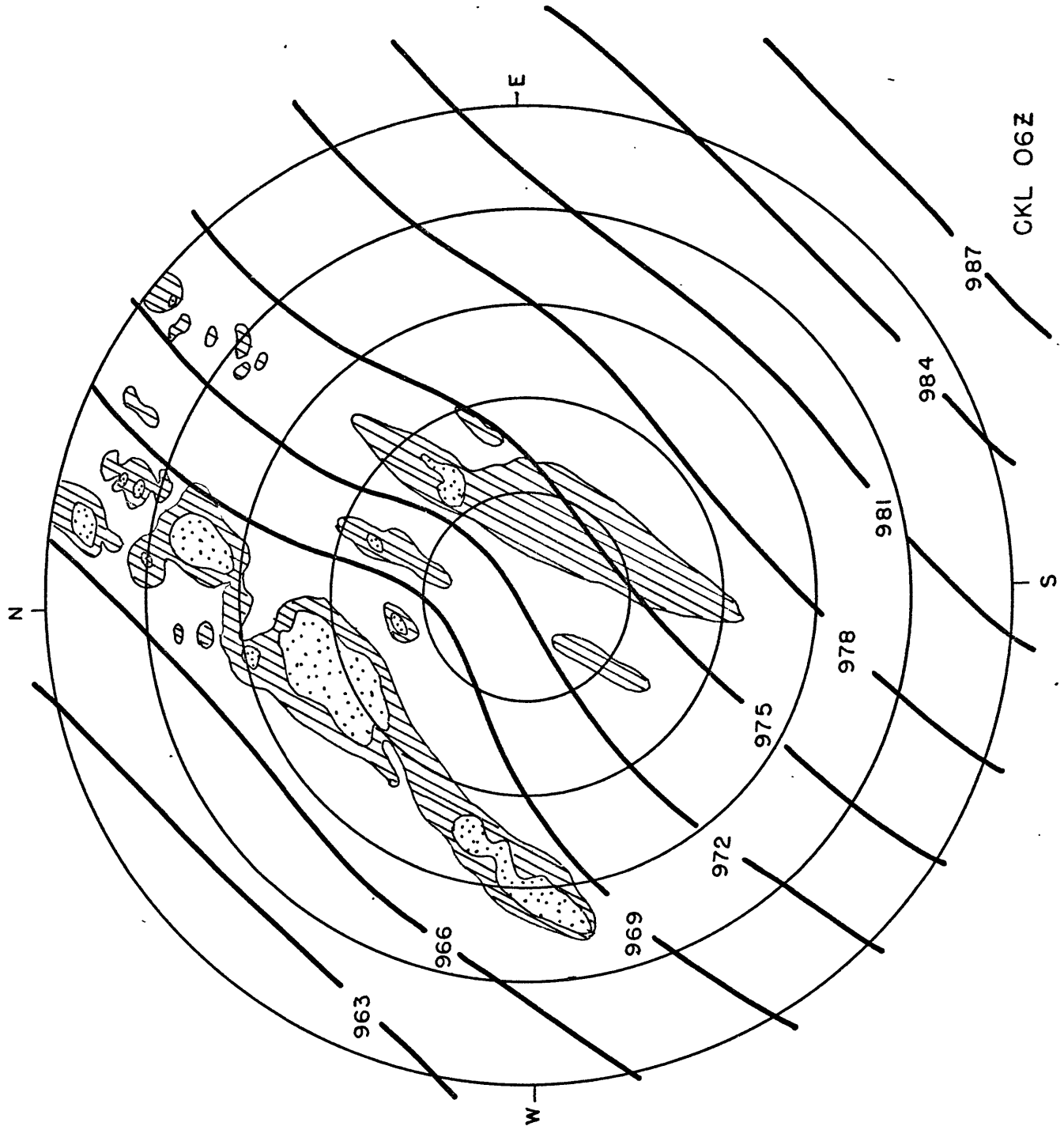

Fig. 7.13: 0600Z April 4, 1974 mesoscale pressure analysis, superimposed on CKL radar photograph. See explanation opposite Fig. 7.4.

Bibliography

Booker, J.R., and F.P. Bretherton, 1967: The critical layer for internal gravity waves in a shear flow. J. Fluid Mech., 27, 513-539.

Bosart, L.F., and J.P. Cussen, 1973: Gravity wave phenomena accompanying east coast cyclogenesis. Mon. Wea. Rev., 101, 446-454.

Einaudi, F., R.S. Lindzen, W.R. Peltier and W.H. Hooke, 1977: Gravity wave interactions with severe storms: workshop recommendations for Project SESAME. Report of the Gravity Wave Workshop, October 15-16, 1975. Planning Documentation Volume for Project SESAME (Severe Environmental Storms and Mesoscale Experiment), U.S. Department of Commerce, pp. 61-84.

Emanuel, K.A., 1978: Inertial stability and mesoscale convective systems. Ph.D. Thesis, Massachusetts Institute of Technology, Department of Meteorology, June, 1978.

Eom, J.K., 1975: Analysis of internal gravity wave occurrence of 19 April, 1970, in the Midwest. Mon. Wea. Rev., 103, 217-226.

Ferguson, H.L., 1967: Mathematical and synoptic aspects of a small-scale wave disturbance over the lower Great Lakes area. J. Appl. Meteor., 6, 523-529.

Foote, G.B., and J.C. Fankhauser, 1973: Airflow and moisture budget beneath a northeast Colorado hailstorm. J. Appl. Meteor., 12, 1330-1353.

Fujita, T., 1959: Precipitation and cold air production in mesoscale thunderstorm systems. J. Meteor., 16, 454-466.

_____, 1975: Super outbreak tornadoes of 3-4 April, 1974. University of Chicago Publication (Map with related statistics).

Hoxit, L.R., and C.F. Chappell, 1975: Tornado outbreak of 3-4 April, 1974; synoptic analysis. NOAA Technical Report, Boulder, Colorado. 48 pp.

_____, _____, and J.M. Fritsch, 1976: Formation of mesolows or pressure troughs in advance of cumulonimbus clouds. Mon. Wea. Rev., 104, 1419-1428.

Holton, J.R., 1972: An Introduction to Dynamic Meteorology, Academic Press, New York and London. 319 pp.

Ley, B.E., and W.R. Peltier, 1978: Wave generation and frontal collapse. J. Atmos. Sci., 35, 3-17.

Lindzen, R.S., and K.K. Tung, 1976: Banded convective activity and ducted gravity waves. Mon. Wea. Rev., 104, 1602-1617.

Raymond, D.J., 1975: A model for predicting the movement of continually propagating convective storms. J. Atmos. Sci., 32, 1308-1317.

Sanders, F., 1975: Fronts and Frontogenesis. Class notes. Department of Meteorology, Massachusetts Institute of Technology (unpublished), 56 pp.

_____, and K.A. Emanuel, 1977: The momentum budget and temporal evolution of a mesoscale convective system. J. Atmos. Sci., 34, 322-330.

_____, and R.J. Paine, 1975: The structure and thermodynamics of an intense mesoscale convective system in Oklahoma. J. Atmos. Sci., 32, 1563-1579.

Tepper, M., 1950: A proposed mechanism of squall lines: the pressure jump line. J. Meteor., 7, 21-29.

Uccellini, L.W., 1975: A case study of apparent gravity wave initiation of severe convective storms. Mon. Wea. Rev., 103, 497-513.

U.S. Dept. of Commerce, 1974: Storm data, 16, Nos. 4,6, and 12. U.S. Dept. of Commerce, NOAA, Asheville, N.C.

Wagner, A.J., 1962: Gravity waves over New England, April 12, 1961. Mon. Wea. Rev., 90, 431-436.